

**RRECOVERY OF LOW CONCENTRATION  
AMMONIACAL NITROGEN FROM AQUACULTURE  
WASTEWATER USING OIL PALM FIBER BIOCHAR**

**TANVEER AHMAD**

**MASTER OF ENGINEERING SCIENCE**

**FACULTY OF ENGINEERING AND GREEN  
TECHNOLOGY**

**UNIVERSITI TUNKU ABDUL RAHMAN**

**14 FEBRUARY 2023**

**RECOVERY OF LOW CONCENTRATION AMMONIACAL  
NITROGEN FROM AQUACULTURE WASTEWATER USING OIL  
PALM FIBER BIOCHAR**

By

**TANVEER AHMAD**

A dissertation submitted to the Department of Environmental Engineering,  
Faculty of Engineering and Green Technology,  
Universiti Tunku Abdul Rahman,  
In partial fulfilment of the requirements for the degree of  
Master of Engineering Sciences  
14 February 2023

## **ABSTRACT**

### **RECOVERY OF LOW CONCENTRATION AMMONIACAL NITROGEN FROM AQUACULTURE WASTEWATER USING OIL PALM FIBER BIOCHAR**

**TANVEER AHMAD**

The existence of ammonia-nitrogen ( $\text{NH}_3\text{-N}$ ) in water bodies has received much attention due to its toxicity and its impact on human health and the environment. Aquaculture wastewater (AQW) contains  $\text{NH}_3\text{-N}$ , and this can cause tissue damage or even death of fishes. Nevertheless,  $\text{NH}_3\text{-N}$  is also categorized as a nutrient and a source of nitrogen in fertilizer. Adsorption process is considered one of the promising techniques for the adsorption of  $\text{NH}_3\text{-N}$ . Recently, various sorbents have been used for  $\text{NH}_3\text{-N}$  treatment, however limited studies were reported on biochar as a sorbent for  $\text{NH}_3\text{-N}$  recovery in low concentration. Most the studies reported on synthetic wastewater and for the removal of high concentrations of  $\text{NH}_3\text{-N}$  ( $> 5\text{ppm}$ ). In this study, the feasibility of oil palm fiber (OPF) biochar on the recovery of  $\text{NH}_3\text{-N}$  was investigated. The OPF biochar was prepared in the presence of  $\text{N}_2$  (pyrolysis) or air (partial oxidation). The preparation was also tested for physically and chemically activated. Design of experiments (DOE) was used to optimize the biochar preparation process. Upon optimization, process study, thermodynamics, kinetics, and mechanism of the removal process was deduced using various parameters and models. Finally, a cost analysis was made to understand the economic viability of the product produced. The OPF biochar preparation was deduced as  $300\text{ }^\circ\text{C}$ , 150 min, and 100 ml air/min by

DOE. The best biochar prepared with air injection shows a removal efficiency of 71.6 % and capacity of 1.6 mg/g for NH<sub>3</sub>-N in synthetic wastewater. Further activation of biochar did not improve the removal efficiency. The process study was further optimized, and the following was achieved; contact time (180 min), shaking speed (150 rpm), dosage (2 g), pH 8~9, and temperature (25 °C). The best removal efficiency adsorption capacity achieved at above conditions are 72.6 % and 0.4 mg/g respectively in actual AQW. The isotherm data of NH<sub>3</sub>-N agreed well with Linear and non-Linear Freundlich model ( $R^2 = 0.9009, 0.9518$ ) compared to Langmuir model ( $R^2=0.8794, 0.9303$ ) respectively, show heterogenous nature of the OPF biochar. The Langmuir adsorption capacity is 6.42 mg/g for the OPF biochar using non-Linear model. In the kinetics study, the best  $R^2$  values were 0.9988, and 0.9950 for Linear and non-Linear pseudo second order as compared to pseudo first order ( $R^2 = 0.9861, \text{ and } 0.9843$ ), respectively, which indicates that chemisorption is the dominant mechanism. The results of the Intra-particle diffusion model indicate that the intraparticle diffusion is not the only rate-limiting step and shows strong initial adsorption as the  $R_i$  (0.47) is between  $0.5 > R_i > 0.1$ . Based on the temperature effect, the values of Gibbs free energy ( $\Delta G^\circ$ ) for OPF biochar were in the range of -13.83 to -15.38 kJ/mol. The negative value of  $\Delta G^\circ$  shows that adsorption is spontaneous. The entropy ( $\Delta S^\circ$ ) value (102.72 J/mol) suggests that randomness increases during the adsorption process. The positive value (16.90 kJ/mol) of the enthalpy change ( $\Delta H^\circ$ ) reveals that the process is endothermic and the adsorption efficiency of NH<sub>3</sub>-N increases with increasing temperature. In the AQW, OPF biochar exhibits selective

recovery of  $\text{NH}_3\text{-N}$ . The characterization of the OPF biochar shows that the ion exchange process occurs during  $\text{NH}_3\text{-N}$  recovery, however, oxygen surface functional groups also play a key role. The cost analysis of the OPF biochar was investigated using a pilot plant design. The optimized biochar is cost effective and the price is RM 2.17/kg comparable to the ones reported in literature and commercially available. Biochar is an environmentally friendly and biodegradable sorbent. It is suggested in future, the spent OPF biochar can be further utilized as a soil conditioner or fertilizer.

## **ACKNOWLEDGEMENT**

I would like to express my sincere gratitude to my research supervisor Professor Sumathi Sethupathi for the continuous support of my Master study and research, for her patience, motivation, enthusiasm, and immense knowledge. Her guidance helped me in all the time of research and writing of this thesis. I could not have imagined having a better advisor and mentor than her.

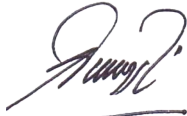
Besides my advisor, I would like to thank my co-supervisor Professor Dr. Mohammed J.K. Bashir, for his encouragement and insightful comments. I would like to thank all the lab-staff for their support in completing this project. I would also like to thank UTAR as a whole for accepting me, financing my research project under the scheme Long Term Research Grant Scheme (LRGS/1/2018/USM/01/1/2) - (UTAR/4411/S01) provided by Ministry of Higher Education Malaysia, and making me a better individual.

I would also like to dedicate this work to every single person, who in their own capacity, tries to protect our planet and environment. Lastly, I would like to dedicate this work to my parents, whose unconditional love has been the inspiration behind all the success in my life.

## APPROVAL SHEET

This dissertation entitled **“RECOVERY OF LOW CONCENTRATION AMMONIACAL NITROGEN FROM AQUACULTURE WASTEWATER USING OIL PALM FIBER BIOCHAR”** was prepared by TANVEER AHMAD and submitted as partial fulfillment of the requirements for the degree of Master of Science in Engineering at Universiti Tunku Abdul Rahman.

Approved by:



(Professor Dr. Sumathi Sethupathi)

Date...14/02/2023.....

Supervisor

Department of Environmental Engineering  
Faculty of Engineering and Green Technology  
Universiti Tunku Abdul Rahman



(Professor Dr. Mohamed J.K. Bashir)

Date..14/02/2023.....

Co-supervisor

Department of Environmental Engineering  
Faculty of Engineering and Green Technology  
Universiti Tunku Abdul Rahman

**FACULTY OF ENGINEERING AND GREEN TECHNOLOGY**

**UNIVERSITI TUNKU ABDUL RAHMAN**

Date: 14/02/2023

**SUBMISSION OF DISSERTATION**

It is hereby certified that **Tanveer Ahmad** (ID No: **19AGM05256**) has completed this dissertation\* entitled “ **RECOVERY OF LOW CONCENTRATION AMMONIACAL NITROGEN FROM AQUACULTURE WASTEWATER USING OIL PALM FIBER BIOCHAR**” under the supervision of Prof. Dr. Sumathi Sethupathi (Supervisor) from the Department of Environmental Engineering, Faculty of Engineering and Green Technology, and Prof. Dr. Mohamed J.K. Bashir (Co-Supervisor) from the Department of Environmental Engineering, Faculty of Engineering and Green Technology.

I understand that University will upload softcopy of my dissertation in pdf format into UTAR Institutional Repository, which may be made accessible to UTAR community and public.

Your truly,




(Tanveer Ahmad)



## DECLARATION

I TANVEER AHMAD hereby declare that the dissertation is based on my original work except for quotations and citations which have been duly acknowledged. I also declare that it has not been previously or concurrently submitted for any other degree at UTAR or other institutions.

Signature: 

Name: Tanveer Ahmad

ID No: 19AGM05256

Date: 14/02/2023

## TABLE OF CONTENT

<b>ABSTRACT .....</b>	<b>II</b>
<b>ACKNOWLEDGEMENT .....</b>	<b>V</b>
<b>APPROVAL SHEET.....</b>	<b>VI</b>
<b>DECLARATION .....</b>	<b>VIII</b>
<b>LIST OF TABLES.....</b>	<b>XI</b>
<b>LIST OF FIGURES.....</b>	<b>XIII</b>
<b>LIST OF ABBREVIATION .....</b>	<b>XVI</b>
<b>CHAPTER 1.....</b>	<b>1</b>
<b>INTRODUCTION .....</b>	<b>1</b>
<b>1.1. Background of the study (Aquaculture).....</b>	<b>1</b>
<b>1.2. Aquaculture wastewater .....</b>	<b>3</b>
<b>1.3. Oil palm industry waste .....</b>	<b>4</b>
<b>1.4. Problem statement .....</b>	<b>6</b>
<b>1.5. Objectives of the study .....</b>	<b>8</b>
<b>1.6. Novelty .....</b>	<b>8</b>
<b>1.7. Scope of study.....</b>	<b>9</b>
<b>1.8. Organization of dissertation .....</b>	<b>10</b>
<b>CHAPTER 2.....</b>	<b>12</b>
<b>LITERATURE REVIEW .....</b>	<b>12</b>
<b>2.1. Characteristics of AQW.....</b>	<b>12</b>
<b>2.2. Treatment technologies for AQW pollutants .....</b>	<b>16</b>
<b>2.3. Advantages and disadvantages of current treatment methods .....</b>	<b>27</b>
<b>2.4. Nitrogen compound removal or recovery from AQW by adsorption....</b>	<b>29</b>
<b>2.5. Biochar.....</b>	<b>33</b>
<b>2.5.1. Preparation of biochar .....</b>	<b>34</b>
<b>2.5.2 Nutrients removal/recovery by biochar .....</b>	<b>37</b>
<b>2.6. OPF biochar .....</b>	<b>45</b>
<b>2.7. Cost analysis of biochar .....</b>	<b>47</b>
<b>CHAPTER 3.....</b>	<b>49</b>
<b>RESEARCH METHODOLOGY .....</b>	<b>49</b>
<b>3.1. Introduction .....</b>	<b>49</b>
<b>3.2. Materials.....</b>	<b>51</b>
<b>3.3. Apparatus.....</b>	<b>52</b>
<b>3.4. Preparation of OPF .....</b>	<b>52</b>
<b>3.4.1. Preliminary preparation of biochar with and without Air .....</b>	<b>53</b>
<b>3.4.2. Preliminary preparation of activated biochar .....</b>	<b>54</b>
<b>3.4.3. Optimization via DOE.....</b>	<b>55</b>
<b>3.5. Synthetic NH<sub>3</sub>-N solution preparation.....</b>	<b>57</b>
<b>3.6. Collection and characterization of actual AQW .....</b>	<b>58</b>
<b>3.7. NH<sub>3</sub>-N adsorption .....</b>	<b>59</b>
<b>3.7.1. Process study .....</b>	<b>60</b>
<b>3.7.2. Adsorption kinetics, isotherms, and thermodynamics study .....</b>	<b>61</b>
<b>3.8. Characterization .....</b>	<b>64</b>
<b>3.8.1. Attenuated Total Reflectance (ATR-FTIR).....</b>	<b>65</b>

3.8.2. Field Emission Electron Microscopy (FESEM) .....	66
3.8.3. Energy Dispersion X-ray (EDX).....	66
3.8.4. Brunauer-Emmett-Teller (BET) .....	66
3.8.5. Cation Exchange Capacity (CEC).....	67
3.8.6. Point Zero charge (PHzc) and Zeta Potential .....	68
3.8.7. Thermogravimetric analysis (TGA).....	68
3.8.8. Ultimate analysis .....	69
3.9. Cost analysis .....	69
<b>CHAPTER 4.....</b>	<b>73</b>
<b>RESULTS AND DISCUSSION .....</b>	<b>73</b>
4.1. Preliminary carbonization .....	73
4.1.1. N <sub>2</sub> and air carbonization of OPF .....	73
4.1.2. Activation of carbonized OPF .....	74
4.2. Design of experiments for OPF biochar .....	81
4.2.1. The design.....	82
4.2.2. ANOVA analysis .....	84
4.2.3. Effect of variables on NH <sub>3</sub> -N adsorption .....	87
4.2.4. Validation of the model and optimization .....	90
4.3. Effect of initial concentration of NH <sub>3</sub> -N .....	92
4.4. Characterization of OPF biochar.....	93
4.5. Adsorption process study on actual AQW .....	107
4.5.1. Contact time .....	107
4.5.2. Effect of shaking .....	109
4.5.3. Effect of OPF biochar dosage .....	110
4.5.4. Effect of pH .....	112
4.5.5. Effect of temperature.....	113
4.6. Thermodynamics analysis.....	114
4.7. Adsorption equilibrium and kinetics .....	116
4.8. Nutrient recovery from actual AQW .....	124
4.9. Comparison of OPF biochar with different adsorbents.....	128
4.10. OPF biochar production cost analysis .....	131
4.10.1. Process flow design .....	131
4.10.2. Manufacturing of OPF biochar at 300 °C .....	135
4.10.3. Cost analysis .....	136
<b>CHAPTER 5.....</b>	<b>143</b>
<b>CONCLUSION AND RECOMMENDATION .....</b>	<b>143</b>
5.1. Conclusion .....	143
5.2. Future recommendation.....	146
<b>LIST OF REFERENCES.....</b>	<b>148</b>
<b>LIST OF PUBLICATIONS .....</b>	<b>199</b>
<b>APPENDIX .....</b>	<b>200</b>

## List of Tables

<b>Tables</b>		<b>Pages</b>
2.1	Characteristics of AQW	14
2.2	Particles removal efficiency of various techniques for AQW treatment	18
2.3	Nutrient recovery from AQW using different treatment methods	20
2.4	Advantage and disadvantages AQW treatment methods	28
2.5	Adsorption capacity / efficiency of adsorbents for AQW nitrogen compound removal	30
2.6	Nutrient removal by biochar from wastewater	39
2.7	OPF based adsorbent for removal of different pollutants from wastewater	46
3.1	List of materials and chemicals	51
3.2	List of apparatus	52
3.3	Input parameter range for DOE design	56
3.4	Design of experiments	57
3.5	AQW parameters and its measurement methods	59
3.6	Estimated cost measurement method for pilot plant based on the percentage in Peters and Timmerhaus, (1991).	71
4.1	EDX elemental analysis of the adsorbent samples	81
4.2	Design of experiments generated from Design-Expert® software	83

4.3	ANOVA results for response surface quadratic model for NH <sub>3</sub> -N	86
4.4	Model Validation of the predicted and experimental results	91
4.5	Physical characteristics of raw fiber and OPF and spent OPF biochar	99
4.6	Thermodynamic parameters for adsorption of NH <sub>3</sub> -N onto OPF biochar	115
4.7	Isotherm parameters for NH <sub>3</sub> -N adsorption onto OPF biochar	119
4.8	Kinetic parameters for adsorption of NH <sub>3</sub> -N onto OPF biochar	121
4.9	Composition of aquaculture wastewater before and after treatment	125
4.10	Comparison of different adsorbents with OPF biochar for NH <sub>3</sub> -N in AQW	130
4.11	Electricity consumption for OPF biochar	134
4.12	Estimated equipment capital cost for OPF biochar	137
4.13	Estimated annual operating cost for OPF biochar	138
4.14	Summary of the cost	139
4.15	Comparative cost of biochar and activated carbon production	140

## List of Figures

Figures		Pages
1.1	World fisheries and aquaculture production	1
1.2	Aquaculture production in Malaysia	2
2.1	AQW treatment methods	16
3.1	Schematic flow chart of the research study	50
3.2	Raw (a) and Cut (b) OPF	53
3.3	Sampling of AQW from fishpond	58
4.1	Adsorption efficiency/capacity of NH <sub>3</sub> -N onto carbonized biochar	74
4.2	Adsorption efficiency/capacity of NH <sub>3</sub> -N onto CO <sub>2</sub> activated biochar	75
4.3	NH <sub>3</sub> -N adsorption efficiency/capacity onto modified biochar, A=BC-HNO <sub>3</sub> , B=BC-CH <sub>3</sub> COOH, C=BC-HCl, D=BC-H <sub>2</sub> O <sub>2</sub> , E=BC-H <sub>2</sub> SO <sub>4</sub> , F=BC-H <sub>3</sub> PO <sub>4</sub>	76
4.4	NH <sub>3</sub> -N adsorption efficiency/capacity on HNO <sub>3</sub> activated biochar at different temperature	77
4.5	NH <sub>3</sub> -N removal efficiency/capacity onto HNO <sub>3</sub> modified biochar at different molarity	78
4.6	ATR-IR results of adsorbent samples	80
4.7	Predicted versus actual adsorption efficiency of NH <sub>3</sub> -N	87
4.8	Response surface plot of (a) pyrolysis temperature versus holding time (b) pyrolysis temperature versus air flow rate, and (c) holding time versus air flow rate for NH <sub>3</sub> -N adsorption	89

4.9	Effect of initial concentration of solution on adsorption efficiency of OPF biochar for NH <sub>3</sub> -N recovery	92
4.10	FESEM image of raw fiber at different magnification (a) 1000X, and (b) 2000X	94
4.11	FESEM image of OPF biochar at different magnification (a) 1000X, and (b) 2000X	96
4.12	FESEM image of spent OPF biochar at different magnification (a) 1000X, and (b) 2000X	97
4.13	CEC of OPF biochar prepared at different carbonization temperature	101
4.14	Effect of CEC of OPF biochar versus NH <sub>3</sub> -N adsorption efficiency	102
4.15	ATR-IR results of the OPF biochar	104
4.16	(a) Zeta potential and (b) pH <sub>Zc</sub> of the OPF biochar samples	106
4.17	Effect of contact time of adsorption efficiency/capacity onto OPF biochar	108
4.18	Effect of various shaking speed on the adsorption efficiency/capacity of NH <sub>3</sub> -N onto OPF biochar	109
4.19	Effect of the OPF biochar dosage on the adsorption efficiency/capacity of NH <sub>3</sub> -N	111
4.20	Effect of initial pH on the adsorption efficiency/capacity of NH <sub>3</sub> -N onto OPF biochar	113
4.21	Effect of temperature on the adsorption efficiency/capacity of NH <sub>3</sub> -N onto OPF biochar	114
4.22	Linear plot of lnK <sub>c</sub> vs 1/T	115

4.23	Adsorption isotherm (a) Linear Langmuir (b) Linear Freundlich (c) Linear and non-Linear	118
4.24	Plot for (a) Linear model of pseudo first order model (b) Linear model of pseudo second order (c) Linear model of intra-particle diffusion model (d) Non-Linear kinetics models	122
4.25	Process flow diagram for the production of OPF biochar	132



## List of abbreviation

AQW	Aquaculture wastewater
OPF	Oil palm fiber
FAO	Food and Agriculture Organization of the United Nations
DOF	Department of fisheries
GDP	Gross domestic product
SS	Suspended solid
NH <sub>3</sub>	Ammonia
NH <sub>3</sub> -N	Ammoniacal-nitrogen
NO <sub>2</sub> <sup>-</sup>	Nitrite
NO <sub>2</sub> <sup>-</sup> -N	Nitrite-nitrogen
NO <sub>3</sub> <sup>-</sup>	Nitrate
NO <sub>3</sub> <sup>-</sup> -N	Nitrate-nitrogen
TN	Total nitrogen
PO <sub>4</sub> <sup>3-</sup> -P	Reactive phosphorus
TP	Total phosphorus
BOD	Biological oxygen demand
COD	Chemical oxygen demand
TDS	Total dissolved solid
TSS	Total suspended solid
DO	Dissolved oxygen
Cl <sup>-</sup>	Chloride
SO <sub>4</sub> <sup>2-</sup>	Sulphate
CaCO <sub>3</sub>	Calcium carbonate
EFB	Empty fruit bunches
PKS	Palm kernel shell
POME	Palm oil effluent
RAS	Recirculating aquaculture system
IMTA	Integrated multi-tropic aquaculture
BFT	Biofloc technology
CGS	Calcined gastropod shell
PCFF	Pyrolyzed chicken feathers fiber

DS	Desulfurization slag
IBI	International Biochar Initiative
CO	Carbon monoxide
CO <sub>2</sub>	Carbon dioxide
CH <sub>4</sub>	Methane
H <sub>2</sub>	Hydrogen
HTC	Hydrothermal carbonization
Cu	Copper
Fe	Iron
Zn	Zinc
Mn	Manganese
Ca	Calcium
Mg	Magnesium
Na	Sodium
K	Potassium
NH <sub>4</sub> <sup>+</sup>	Ammonium
Pb	Lead
RT	Room temperature
CEC	Cation exchange capacity
NaOH	Sodium hydroxide
HNO <sub>3</sub>	Nitric acid
HCl	Hydrochloric acid
H <sub>2</sub> O <sub>2</sub>	Hydrogen peroxide
H <sub>3</sub> PO <sub>4</sub>	Phosphoric acid
CH <sub>3</sub> COOH	Acetic acid
H <sub>2</sub> SO <sub>4</sub>	Sulfuric acid
AgNO <sub>3</sub>	Silver nitrate
NaCl	Sodium chloride
N <sub>2</sub>	Nitrogen gas
BET	Brunauer-Emmett-Teller
FESEM	Field Emission Scanning Electron Microscope
EDX	Energy Dispersion X-ray
ATR	Attenuated Total Reflectance

RSM	Response surface methodology
CCD	Central composite design
ANOVA	Analysis of variance
F-value	Fisher variance ratio
p-value	Probability value
DOE	Design of experiments
$(\text{NH}_4)_2\text{SO}_4$	Ammonium sulfate
pH <sub>zc</sub>	Point zero charge
TGA	Thermogravimetric analysis
Al	Aluminum
Si	Silicon
C	Carbon
O	Oxygen
hr	Hour
min	Minute
PFO	Pseudo first order
PSO	Pseudo second order
E <sub>a</sub>	Activation energy
$\Delta S^\circ$	Change in entropy
$\Delta H^\circ$	Change in enthalpy
$\Delta G^\circ$	Change in Gibb's free energy
\$	US dollar
RM	Malaysian ringgit

# CHAPTER 1

## INTRODUCTION

### 1.1. Background of the study (Aquaculture)

Aquaculture and sea capturing represent 46 % and 54 % of the total fish production (178.5 million tonnes in 2018) respectively. But sea capture has been almost the same since the 1990s, as shown in **Figure 1.1**. The increase in fish consumption increased at a rate of 3.1 % annually from 1961 to 2017.

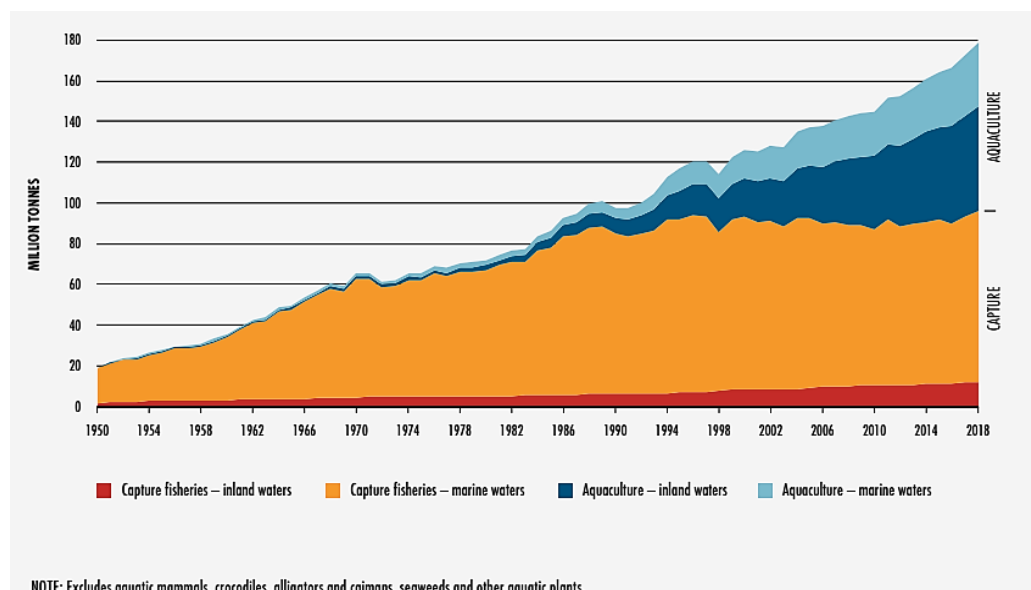


**Figure 1.1.** World fisheries and aquaculture production. Adapted from report (The state of world fisheries and aquaculture, (FAO, 2020))

To meet the demand, fish farming is required, and aquaculture operation is growing faster than other any other major food sector. The Food and

Agriculture Organization of the United Nations reported an average annual rate of 5.3 % between 2001 – 2018 (FAO, 2020). In the southeast Asian region, Malaysia is the seventh largest contributor to aquaculture production.

Malaysia is ranked fifth in term of total production of fishery and account for 6.9 % (SEAFDEC, 2018). Due to Malaysia long coastline of around 4780 km, the aquaculture industry is dominated by brackish aquaculture. In Malaysia freshwater aquaculture is predominant by pond culture (FAO, 2021). According to the department of fisheries (DOF) of Malaysia, the production of aquaculture is slightly reduced since 2010 to 2019 from 0.58 to 0.39 million tonne as shown in **Figure 1.2**, (DOF, 2020). The aquaculture industry contributes to about 12 % of the total GDP of Malaysia in 2020 (Department of Statistics Malaysia, 2020). Although aquaculture production is necessary to ensure world food security, it produces a large amount of wastewater that has repercussions on the environment.

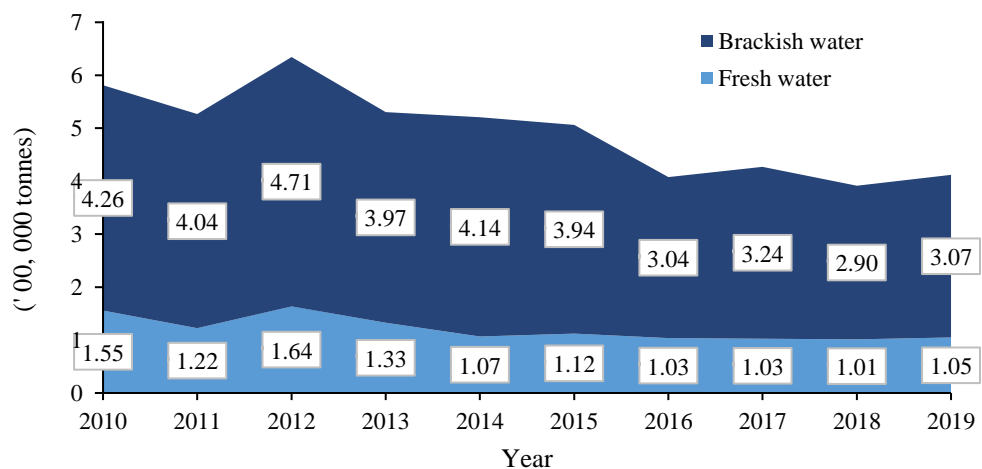


**Figure 1.2.** Aquaculture production in Malaysia (DOF, 2020)

## 1.2. Aquaculture wastewater

Aquaculture wastewater (AQW) consists mainly of suspended solids (SS), dissolved organic matter, and nutrients (i.e. nitrogen and phosphorus compounds) (Turcios and Papenbrock, 2014). The total solid in AQW is mainly composed of uneaten food and fish feces (Akinwole, Dauda and Ololade, 2016). Dissolved organic matter in AQW is the decomposition of uneaten feed or food metabolism in fish (Dauda *et al.*, 2019) and mainly contains nitrogen and phosphorus (Boyd and Massaut, 1999). Nitrogen and phosphorus retention varies in fish, with average nitrogen and phosphorus retained between 10 – 49 % and 17 – 40 %, respectively, from the utilized feed. Additionally, nitrogen (3.6 – 35 %) and phosphorus (15 – 70 %) in feces and excretory products (37 – 72 % nitrogen and 1 – 62 % phosphorus) are released (Dauda *et al.*, 2019). Phosphorus is excreted in the form of particulate matter (fecal) (Sugiura *et al.*, 1999). Although nitrogen is excreted in the form of ammonia (NH<sub>3</sub>) (Lazzari and Baldisserotto, 2008) and is typically suggested to be less than 1 ppm in the culture tank, as it is toxic to fish (Dauda *et al.*, 2019). Also, NH<sub>3</sub> occurs in AQW in unionized and ionized form (NH<sub>3</sub> and NH<sub>4</sub><sup>+</sup>) and the equilibrium ratio depends on the pH and water temperature (Ebeling and Timmons, 2012). Further, NH<sub>3</sub> is converted into nitrite (NO<sub>2</sub><sup>-</sup>) and nitrate (NO<sub>3</sub><sup>-</sup>) (Dauda, Akinwole and Olatinwo, 2014). High concentration of NO<sub>2</sub><sup>-</sup> significantly reduce the growth of fish (Romano and Zeng, 2013). Although NO<sub>3</sub><sup>-</sup> is the final product of NH<sub>3</sub> oxidation and is known to be non-toxic to fish species at low concentrations

(Dauda and Akinwale, 2015) and can accumulate to a level as high as 300 – 400 ppm over time (Dauda *et al.*, 2019).

Nitrogen and phosphorus are the main final product of the fish farming which make aquaculture high risk for environmental pollution (Lazzari and Baldisserotto, 2008) and further cause eutrophication (Dauda *et al.*, 2019). In addition to this, the effluent of fish farm is rich in nutrients (Ahmad *et al.*, 2022) and can be recovered (Zhou *et al.*, 2019; Beckinghausen, Odlare, *et al.*, 2020). Further, the circular economy of the AQW industry could be improve through recovery (Beckinghausen, Reynders, *et al.*, 2020). Therefore, there is need to treat the AQW wastewater before it is released into the environment. Moreover, ammonia is a form of nutrient, and it will be useful if it can be recovered.

### **1.3. Oil palm industry waste**

Malaysia is the world's second largest producer of palm oil and accounts for 28 % (19.92 million ton) of the world's production (FAO, 2018). The palm industry causes various type of wastes including empty fruit bunches (EFB), palm kernel shell (PKS), mesocarp fiber or oil palm fiber (OPF), and palm oil effluent (POME). The generation of solid biomass waste about 40,072.17 million tonnes per annum, while POME was produced at 136,328 million tonnes per year, been projected by 2030 (Jafri *et al.*, 2021). Among the waste, 15.73 million tons of OPF were produced annually (Wafti *et al.*, 2017). OPF were produced from different types of biomasses waste

such oil palm trunk, empty fruit bunches, and oil palm frond. The OPF contains cellulose (25.0 %), hemicellulose (25.7 %), lignin (25.5 %), and ash (5.8 %) on dry weight basis and having the heating value of 17.15 MJ/kg dry wt (Kaniapan *et al.*, 2021). Having the 2<sup>nd</sup> highest heating value of OPF compared to other biomass waste from the palm industry (Kaniapan *et al.*, 2021). At present 98.4± 1.0 % of OPF is used to produce electricity and steam for palm oil extraction, while the rest is sold on the market (Kong *et al.*, 2014).

The growth in the waste generation poses great challenges to the environmental sustainability in relation to waste management, and greenhouse gas emission from waste biomass. Reutilization of waste biomasses has gained many interests among the researchers. Biochar, value-added product, can be formed from OPF using slow pyrolysis. The biomass conversion to biochar results in the sequestration of around 50 % of the initial carbon compared to the less amount preserved after biological degradation (less than 10-20 % after 5-10 years) and burning (3 %) (Kong *et al.*, 2014).

The NH<sub>3</sub>-N occurs in wastewater in dissolved form and can be removed via coagulation and flocculation, biofloc technology, and adsorption process. In flocculation and coagulation process when the chemicals are added to the wastewater the NH<sub>3</sub> in the wastewater react with the chemical and removed (Rishel and Ebeling, 2006). However, in the biofloc technology, the microorganism decomposes the NH<sub>3</sub> into nitrogen and hydrogen (Fatimah *et al.*, 2019). In the adsorption process the NH<sub>3</sub>-N



molecules are interact with the adsorbent surface via surface functional groups, or ion exchange process or physically adsorbed in the pore of the adsorbent (El-sherbiny, El-chaghaby and El-Shafea, 2019).

#### **1.4. Problem statement**

The prime sources of  $\text{NH}_3\text{-N}$  in AQW are the excretion of fish, organic matter produced by the algae and decomposition of fecal. (Hargreaves and Tucker, 2004).  $\text{NH}_3\text{-N}$  is toxic to aquatic species and recommended to be less than 1 ppm in fish culture tank (Dauda *et al.*, 2019). Moreover, direct discharge of AQW to the river will pollute the water, affecting the growth of aquatic species in the receiving water bodies, as well as the loss of the nutrients. Therefore, it is necessary to treat the AQW to recover the nutrients prior to discharge.

Most of the latest studies in the literature, focuses on high initial concentrations of  $\text{NH}_3\text{-N}$  (>10ppm) and reported using synthetic wastewater. (Aghoghovwia, Hardie and Rozanov, 2020; Xu *et al.*, 2022). The synthetic wastewater did not represent the actual wastewater scenario as it contains other various pollutants which inhibit the performance of the adsorbent (Yao *et al.*, 2022). Low concentration of  $\text{NH}_3\text{-N}$  in AQW, further worsen the removal as low concentration shall have very little interaction between the adsorbent and the adsorbate molecule. Therefore, in this study, the recovery potential OPF biochar for low concentration condition of  $\text{NH}_3\text{-N}$  in actual AQW was investigated. Different preparation methods for biochar

production were evaluated to understand the removal mechanism of the NH<sub>3</sub>-N in lower concentration. Among the methods, partially oxidized biochar (with injection of air) shows the best performance.

Malaysia is one of the major producers of the palm oil and generates biomass wastes. The growth of palm industry waste poses a great challenge to the environment (Khatun *et al.*, 2017). Direct incineration of OPF is illegal in Malaysia (Kaniapan *et al.*, 2021), and because of the poor utilization and abundant availability of OPF in Malaysia, there is an urgent need for reutilization of this waste. Not only to be reutilized but also to enhance it to a value-added commercial product. Many has reported converting to biochar and AC for dyes, pesticides, heavy metals, and analyte (Marsin *et al.*, 2018). But very limited on nutrients removal especially NH<sub>3</sub>-N (Ricky *et al.*, 2016; Zahrim *et al.*, 2017; Ismail *et al.*, 2018; Nasir *et al.*, 2018). So far only four studies have been reported on OPF and cost analysis was not done. In this study, the cost of analysis on the pilot scale was calculated for commercialization of the product.

## 1.5. Objectives of the study

The aim of this study is to investigate the feasibility of oil palm fiber biochar to recover  $\text{NH}_3\text{-N}$  from AQW via adsorption. The objectives of this study are as follows:

- To optimize the preparation conditions of OPF biochar for low concentration  $\text{NH}_3\text{-N}$  adsorption.
- To optimize the adsorption parameters, and to evaluate the kinetics, mechanism, isotherms, and thermodynamics.
- To analyze the costing of OPF biochar production.

## 1.6. Novelty

Limited studies on carbon-based adsorbent have been found for the removal of low concentrations of  $\text{NH}_3\text{-N}$  from wastewater, especially AQW. Biochar and activated carbon produced from different raw materials have been tested for  $\text{NH}_3\text{-N}$  (<15 ppm). Limited studies have been done on concentration of less than 5 ppm (Sichula *et al.*, 2011; Zahrim *et al.*, 2017; Karia *et al.*, 2022). However, most studies have been done on synthetic wastewater (Hussain *et al.*, 2007; Shi, Wang and Zheng, 2013; Khalil, Sergeevich and Borisova, 2018). Three studies using different types of activated carbon, that is commercial activated carbon, chicken feather, and maize cob, were tested for the adsorption of  $\text{NH}_3\text{-N}$  from AQW by Karia *et al.*, (2021), Moon *et al.*, (2017), and Sichula *et al.*, (2011), respectively. The

performance of the adsorbents was poor and could only achieve less than 60% removal of  $\text{NH}_3\text{-N}$ . Moreover, the initial concentration of  $\text{NH}_3\text{-N}$  was reported to be higher than 15 ppm. In addition to this, the economic feasibility and the cost of the biochar production at a pilot plant scale was evaluated.

Thus, in this study, OPF biochar shall be prepared and tested for its recovery efficiency for low concentration  $\text{NH}_3\text{-N}$  in AQW. Also, to the best of our knowledge, studies have not been reported applying OPF biochar for low concentration recovery of  $\text{NH}_3\text{-N}$  from AQW.

### **1.7. Scope of study**

This research is narrow down to the scope low initial concentration of  $\text{NH}_3\text{-N}$  as reported highly to fish as well as other aquatic species. The bio-adsorbent raw material that was focusing on in this study was oil palm waste (OPF). The physical, chemical, and morphological structures of the OPF biochars were studied while their adsorption uptake adsorption efficiency/capacity were examined. The best-performing biochar for  $\text{NH}_3\text{-N}$  was further use for the effect of various operating parameters such as shaking speed, contact time, temperature, pH and dosage. The results were also compared with those of the biochars in the literature.

## **1.8. Organization of dissertation**

Chapter 1: Introduction start with overview of aquaculture production as well as the AQW including the presence of nutrients and pollutants has been discussed. The waste of the oil palm industry and its application in various fields are described. The toxicity of the  $\text{NH}_3\text{-N}$  on aquaculture species and the recovery with biochar has been outlined. The objective of palm waste is also mentioned, while the novelty and scope of the study explain how deeply the adsorption research and operating factors parameters will be studied in the work.

In Chapter 2: Literature review, the concentration of nutrients in the AQW has been reported with the addition of various treatment methods to remove pollutants and nutrients from the AQW. On other hand, a brief study on biochar, production method of biochar, pollutant removal by biochar, and adsorption mechanism has been discussed. Furthermore, a literature study on activated carbon and biochar prepared from OPF and its application is described for different pollutants and nutrients. Moreover, a detail study of the adsorption isotherms, kinetics, and thermodynamic is reviewed in the end of the chapter.

In Chapter 3: Methodology, besides laboratory testing and characterization studies, materials (chemicals and reagents,) and equipment used, are explained. Along with the production of biochar and activated

biochar, adsorption study and its parameters are discussed in detailed with collection of real AQW collection with its initial readings.

In Chapter 4: Results and discussion, all the collected results are shown in graphical and images form, in consecutive order from batch adsorption tests in preliminary screening stage, all characterizations, parameter evaluation, thermodynamics, adsorption isotherm, and kinetics. The analysis and discussion of the mechanism are carried out based on the experimental findings. Also, cost analysis of the biochar is also calculated using optimized OFP biochar preparation conditions from the lab to a pilot scale.

Lastly, in Chapter 5: Conclusion, the deductive reasoning is stated based on the results explained in Chapter 4. For future references and advancements in the research, recommendations are also made on the relevant areas of the research.

## CHAPTER 2

### LITERATURE REVIEW

#### 2.1. Characteristics of AQW

Based on the literature, the characteristics of the AQW are shown in **Table 2.1**. These pollutants and nutrients need to be removed from AQW before being discharge to the environment.  $\text{NH}_3\text{-N}$  is highly toxic and is recommended less than 1 ppm in the fish tank (Dauda *et al.*, 2019). Otherwise, it can decrease the growth and the immune response system (hemolymph THC) of fishes (Romano and Zeng, 2013).  $\text{NO}_2\text{-N}$  is the intermediate product of ammonia oxidation and generally recommended to be less than 0.5 ppm. However,  $\text{NO}_2\text{-N}$  is not stable and convert to  $\text{NO}_3\text{-N}$ . Further,  $\text{NO}_3\text{-N}$  is considered safe as it not harmful most of fish at concentration as high 200 ppm. Phosphorus causes eutrophication (Dauda *et al.*, 2019). A higher concentration of COD will cause less DO in the water. This may disturb live stability of the aquatic environment. TSS are considered extremely harmful since they can block fish gills and cause death, while TDS increase nitrogenous compound and stress cultured fish (Dauda *et al.*, 2019). Salts are using for reducing stress in fish, and lime is used for the treatment of ponds for acidity during the preparation of the pond (Dauda *et al.*, 2019). The pH range 6 – 9 is necessary for optimal growth, however, an acidic pH ~ 4 or less is lethal to fish (Ndubuisi *et al.*, 2015). In general high concentrations of the nutrients (phosphorus and nitrogen) can also cause

the eutrophication and promote the growth of floating macrophyte hence reduced the sunlight penetration disrupts the underwater photosynthesis of phytoplankton hence decreasing the DO in aquatic environment (Kurniawan *et al.*, 2021). So, it is required to treat the AQW and recover the valuable nutrients before it is being release to the receiving water bodies.



**Table 2.1.** Characteristics of AQW

Temp. (°C)	DO (ppm)	pH	TSS (ppm)	TDS (ppm)	NH <sub>3</sub> -N (ppm)	NO <sub>2</sub> -N (ppm)	NO <sub>3</sub> -N (ppm)	TN (ppm)	PO <sub>4</sub> <sup>3-</sup> -P (ppm)	BOD (ppm)	COD (ppm)	Cl <sup>-</sup> (g/l)	SO <sub>4</sub> <sup>2-</sup> (ppm)	CaCO <sub>3</sub> (ppm)	Ref.
-	1.9-16.8	6-9.3	0.7-3.3	-	0.0-7.7	0.0-1.4	0.2-16.8	0.6-14.0	0.0	-	-	-	-	-	Boyd <i>et al.</i> , 2000
-	6.2	7.7	-	-	0.8	0.2	19 ± 10	-	20 ± 12	5.3	-	5	85	-	Kioussis, Wheaton and Kofinas, 2000
27.4 ± 0.8	5.0 ± 0.9	7.3±0.1	-	-	0.5 ± 0.1	0.1 ± 0.1	7.2 ± 12.8	-	-	-	-	-	-	-	Dauda and Akinwole, 2014
27	4.9	7.2	1125	2275	3.0	0.3	5.0	-	-	-	-	-	-	-	Akinwole, Dauda and Ololade, 2016
-	-	7.8	-	-	0.3 ± 0.1	2.4 ± 0.7	51.8 ± 0.2	-	-	-	17 ± 3.4	-	-	-	Zou <i>et al.</i> , 2018
23.4 ± 2.6	7.2 ± 1.0	6.2 ± 0.6	-	-	0.6 ± 0.2	0.5 ± 0.1	26.6 ± 3.2	27.7 ± 2.3	-	-	-	-	-	-	Chunjie Li <i>et al.</i> , 2019
28	-	8.1	254 ± 29	-	1.6 ± 0.2	1.5 ± 0.0	35.8 ± 0.4	-	3.9 ± 0.1	-	-	-	-	148.9 ± 2.3	W. Liu <i>et al.</i> , 2019
-	-	7.5	-	-	≤ 0.1	0.3	152.8	-	16.1	-	38.4	147.3	420.6	-	Tejido-núñez <i>et al.</i> , 2019s

**Table 2.1.** Continued

Temp. (°C)	DO (ppm)	pH	TSS (ppm)	TDS (ppm)	NH <sub>3</sub> -N (ppm)	NO <sub>2</sub> -N (ppm)	NO <sub>3</sub> -N (ppm)	TN (ppm)	PO <sub>4</sub> <sup>3-</sup> -P (ppm)	BOD (ppm)	COD (ppm)	Cl <sup>-</sup> (g/l)	SO <sub>4</sub> <sup>2-</sup> (ppm)	CaCO <sub>3</sub> (ppm)	Ref.
30 ± 2	6.7 ± 0.7	7.8 ± 0.2	-	-	1.1 ± 0.3	0.3 ± 0.2	0.4 ± 1.0	-	-	-	-	-	-	-	John, Krishnapriya and Sankar, 2020
-	-	7.8 ± 0.0	83 ± 4	-	24.8 ± 1.4	<0.01	<0.3	-	0.7 ± 0.1	-	-	-	-	-	Ng and Chan, 2021
-	3.1	7.9	-	-	3.5	-	-	-	-	-	-	-	-	-	Karia <i>et al.</i> , 2022
-	-	7.2	-	-	0.0	0.0	21.82	-	0.7	-	-	-	-	-	Stamenković, Steinwall and Wulff, 2021
-	-	-	-	-	0.2 ± 0.0	0.1 ± 0.1	0.5 ± 0.4	-	0.2 ± 0.1	-	-	-	-	-	Iber and Kasan, 2021
-	-	7.5	492	-	50.1	-	-	-	2.8	-	139	-	-	-	Kurniawan <i>et al.</i> , 2022
33.4	2.1	8.9	-	734	1.3	0.8	-	-	0.1	2.2	1184	-	-	-	Saxena <i>et al.</i> , 2022s

## 2.2. Treatment technologies for AQW pollutants

**Figure 2.1** illustrates types of wastewater treatment processes used to improve the AQW, quality. Physical, chemical, and biological methods have been applied to aquaculture systems to reduce the concentration of nutrients and other pollutants in effluent before disposing to the environment.

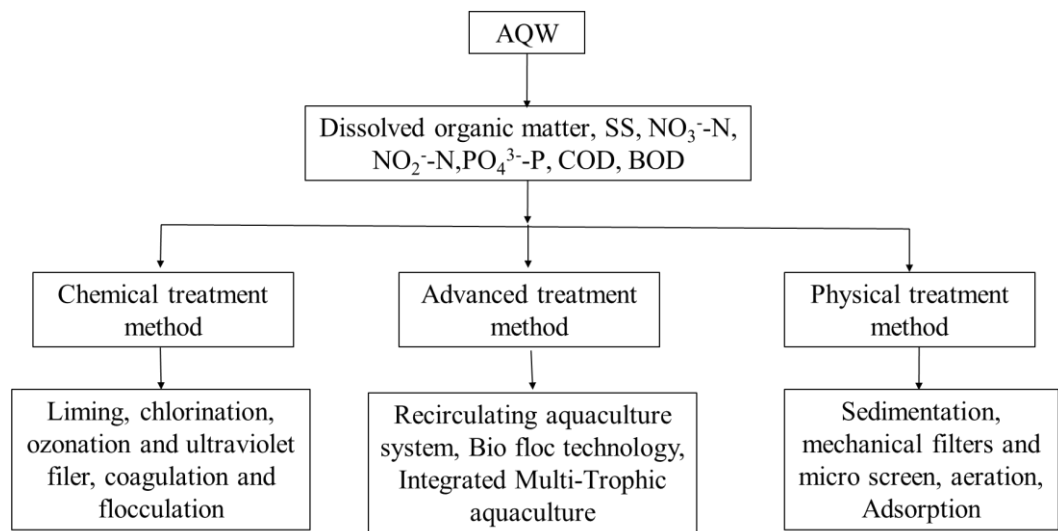


**Figure 2.1.** AQW treatment methods

In aquaculture systems, wastewater can be treated chemically by various methods. In liming, the pH of the water was increased by passing water from lime filter as a result reduced the soluble phosphorus and free CO<sub>2</sub>. Chlorination is a very common method used for disinfectant (Metcalf and Eddy, 2003; Crittenden, Trussell and Hand, 2012). It has been reported, that deactivation rate of bacteria increases from 0.19 to 0.3 s<sup>-1</sup> with the chlorine concentration from 2 to 4 ppm in AQW (Liltved and Landfald, 1995).

Ultraviolet or ozone treatment for AQW is a common method specifically used in recirculating aquaculture system (RAS) (Ling and Weimin, 2010). This method successfully eliminates parasites, pathogens, and bacteria, etc., that can harm fish (Davis, 2010). Ozonation is, very advantageous in the RAS, and it not only decreases the organic load but also sterilizes the system to make it more helpful for fish growth (Ling and Weimin, 2010). In the AQW system, ozone nearly decomposed all  $\text{NO}_2^-$ -N while reduced total ammonia (TAN) concentration to 0.1 ppm (Chen *et al.*, 2015). The combination of ultraviolet irradiation and ozonation (20 ppb) remove all bacteria as well as 66.67 – 83.33 % of  $\text{NO}_2^-$ -N and 37.5 – 47.5 % of TSS from AQW as shown in **Table 2.2** and **2.3** (Summerfelt *et al.*, 2009).

**Table 2.2.** Particles removal efficiency of various techniques for AQW treatment

Technique	Modification	Removal efficiency (%)	Particle size ( $\mu\text{m}$ )	Remarks	Ref.
Sedimentation (centrifugal separation)		$37.1 \pm 3.3$	-	Used as a primary settler nutrient recovery	Davidson and Summerfelt, 2005
	Swirl separator	60–63 (feed waste), 59–71 (fecal solid)	-	-	Lee, 2015
		46	-	-	Lee, 2014
		> 90	> 250	-	Pfeiffer, Osborn and Davis, 2008
	Radial separator	$77.9 \pm 1.6$	-	-	Davidson & Summerfelt, 2005
Filtration	Fluidized sand filtration	> 65	23 – 55	Final filtration component in RAS	Pfeiffer, Osborn and Davis, 2008
	Micro-screen drum filter	~ 50 (filter aperture size 100 $\mu\text{m}$ ) 100 (filter aperture size 18 $\mu\text{m}$ )	-	-	Dolan, Murphy and Hehir, 2013
	Drum screen filter	$34.22 \pm 8.85$ (Powder feed), $52.41 \pm 16.77$ (Pellet feed)	-	-	Ali, 2013
	Inclined belt filter + coagulant / flocculent	95	-	-	Ebeling, Welsh and Rishel, 2006
	Granular filter	100 40 - 50	> 50 < 10	- -	Malone and Beecher, 2000

**Table 2.2.** Continued

<b>Technique</b>	<b>Modification</b>	<b>Removal efficiency (%)</b>	<b>Particle size (µm)</b>	<b>Remarks</b>	<b>Ref.</b>
Filtration	Polystyrene floating filter or sand medium filter	60	-	-	Steicke, Jegatheesan and Zeng, 2007
RAS wastewater management	-	85 – 98	-	-	Martins <i>et al.</i> , 2010
Ozonation	Ozonation + UV irradiation	37.5 – 47.5	-	-	Summerfelt <i>et al.</i> , 2009
Coagulation and flocculation	Addition of chemicals	99	-	Polymer	Ebeling, Rishel and Sibrell, 2005
		99	-	Alum + polymer	Rishel and Ebeling, 2006
		95.1	-	FeCl + polymer	Sharrer, Rishel and Summerfelt, 2009
		> 90	-	FeCl <sub>3</sub> , PAS	Zhang <i>et al.</i> , 2014

**Table 2.3.** Nutrient recovery from AQW using different treatment methods

Method	Process	Removal efficiency (%)						System	Ref.
		NO <sub>2</sub> <sup>-</sup> -N	NO <sub>3</sub> <sup>-</sup> -N	NH <sub>3</sub>	TN	PO <sub>4</sub> <sup>3-</sup>	TP		
	-	-	-	-	-	-	65 – 96	-	Martins et al., 2010
RAS and wastewater management	Denitrification	-	49 – 71	-	-	-	-	Woodchip bioreactor	Lepine et al., 2018
	Denitrification	78.3	-	-	-	93.5	-	Suspended growth bioreactors	Liu et al., 2019
Ozonation	Injection of ozone	55.5	-	-	-	-	-	Ozone + TiO <sub>2</sub> /Al <sub>2</sub> O <sub>3</sub> membrane	Chen et al., 2015
		66.7– 83.3	-	-	-	-	-	Ozonation + UV irradiation	Summerfelt et al., 2009
Coagulation and flocculation	Generally, used addition of chemicals	-	-	-	-	92 – 95	-	Optimum polymer doses	Rishel and Sibrell, 2005
		50	68	64	-	92 – 99	-	Alum + polymer	Rishel and Ebeling, 2006
		-	-	99.1	-	99.1	-	Chitosan	Chung, Li and Chen, 2005

**Table 1.3.** Continued

Method	Process	Removal efficiency (%)								System	Ref.
		NO <sub>2</sub> <sup>-</sup> -N	NO <sub>3</sub> <sup>-</sup> -N	NH <sub>3</sub>	Dissolved Nitrogen	Sedimentary Nitrogen	TN	PO <sub>4</sub> <sup>3-</sup>	TP		
IMTA	Different tropic species are grown together	-	-	-	-	-	49.4	-	99	Tetraselmis suecica	Michels et al., 2014
		99.3	45.5	-	-	-	-	-	47	FeCl + Polymer	Sharrer, Rishel and Summerfelt, 2009
BFT	Using carbon as a source for microorganism growth	-	-	-	-	-	-	-	> 80	FeCl <sub>3</sub> , PAS	Zhang et al., 2014
		-	-	-	36.4	89.8	-	-	-	Biofloc + continuous aeration	Liu <i>et al.</i> , 2019
		-	-	-	-	-	92.2	-	-	Biofloc + denitrification + LED light	Changwei Li <i>et al.</i> , 2019
		-	-	52.3	-	-	-	-	-	Biofloc + quorum sensing	Fatimah et al., 2019



In coagulation and flocculation, chemicals are added to wastewater to increase particle size and convert the dissolved or colloidal substance into insoluble SS (Metcalf and Eddy, 2003; Stechemesser and Dobiás, 2005). Generally, aluminum and iron-based coagulants such as aluminum sulfate, aluminum chloride, ferric sulfate, ferrous sulfate, etc. are used. Other chemicals like hydrated lime and magnesium carbonate also used as a coagulant (Bratby, 2006). Various coagulants and flocculants have been studied for the removal of TSS and nutrients from AQW. According to the literature, the removal efficiency of TSS and  $\text{PO}_4^{3-}$  is greater than 90 %, however,  $\text{NO}_2^-$ -N (50 – 99.3 %),  $\text{NO}_3^-$ -N (45.5 – 68 %),  $\text{NH}_3$  (64 – 99.1 %), and total phosphorus (TP, 47 – > 80 %), as shown in **Table 2.2** and **Table 2.3**. Moreover BOD, and COD were reduced to 97.3 % and 96.4 %, respectively (Rishel and Ebeling, 2006).

In RAS, nutrients are controlled by using a biological method and the treated water is recycled. Due to recycling, the RAS process has advantages including, little water usage, a lower environmental impact because of nutrient recovery (Martins *et al.*, 2010) and having improved hygienic conditions (Summerfelt *et al.*, 2009; Tal *et al.*, 2009). The nitrification process has been reported to convert  $\text{NH}_3$  (toxic) to  $\text{NO}_3^-$  (less toxic) in RAS (Crab, Avnimelech and Defoirdt, 2007; Dauda, Akinwole and Olatinwo, 2014). Recently, different biofilters are used in the nitrification process for AQW (Martins *et al.*, 2010). Such as, emerge fixed-film filters and submerged fixed-film filters (Malone and Pfeiffer, 2006; Dauda, Akinwole and Olatinwo, 2014). Organic matter and SS removal efficiencies were found

to be 85 – 98 % while for phosphorus removal efficiency was 65 – 96 % in RAS (Martins *et al.*, 2010). Research on the nitrification and denitrification process shows a different tendency for the removal of nutrients. The NH<sub>3</sub> removal rate in the denitrification tank (using pumice stone) with the addition of methanol is, 116.9 g-N/m<sup>3</sup> packing volume per day, which is higher than the nitrification process (Pungrasmi *et al.* 2016). Also, the efficiency removal of NO<sub>3</sub><sup>-</sup>-N for denitrifying wood bioreactor (Lepine *et al.*, 2018) is lower than suspended growth bioreactors (SGBRs) shown in **Table 2.3** however, SGBRs also removes 93.48 % of PO<sub>4</sub><sup>3-</sup> (W. Liu *et al.*, 2019).

For sustainable aquaculture, biofloc technology (BFT) is now receiving more attention in the fish culture system (Bossier and Ekasari, 2017; Dauda *et al.*, 2018). In BFT, water is treated inside the pond and no need for extra equipment as compared to RAS in which the treatment is performed outside of the culture (Vinatea *et al.*, 2018). In this method, carbon is used as a source material for bacteria growth to convert NH<sub>3</sub> into nitrogen gas (Ekasari, Crab and Verstraete, 2010; Luo *et al.*, 2014; Dauda and Akinwole, 2015; Sgnaulin *et al.*, 2018). It was found that at in the C/N ratio of 15, the concentration of NH<sub>3</sub>-N and NO<sub>3</sub><sup>-</sup>-N were < 1 ppm while the NO<sub>2</sub><sup>-</sup>-N was less than 50 ppm (Dauda *et al.*, 2018). Also, similar results were observed by Sgnaulin *et al.*, (2018) for NO<sub>2</sub><sup>-</sup> (0.1 ppm), total NH<sub>3</sub> (0.96 ppm) and NO<sub>3</sub><sup>-</sup> (0.9 ppm). Formation of biofloc with addition of continuous aeration has lower removal of dissolved nitrogen compounds (Liu *et al.*, 2019) compared to combine BFT with denitrification and blue LED light (Changwei Li *et al.*, 2019) and addition of the quorum sensing signal (C6-

HSL) (Fatimah *et al.*, 2019) as shown in **Table 2.3**. However, research is needed to improve the oxidation or removal efficiency of  $\text{NH}_3$  and  $\text{NO}_2^-$  in the biofloc system because small bioflocs are less efficient for  $\text{NH}_3$  and  $\text{NO}_2^-$  oxidation (Souza *et al.*, 2019). Besides, RAS and BFT, integrated multi-trophic aquaculture (IMTA) also one of the advanced methods for fish farming.

Various trophic species are grown together in IMTA (Martan, 2008), and waste of one species is used as a feed for others by providing collective interaction between the species (Chopin *et al.*, 2001; Troell *et al.*, 2003; Neori *et al.*, 2004; Turcios and Papenbrock, 2014; Buck *et al.*, 2018). Michels *et al.*, (2014) found that *tetraselmis suecica* significantly convert the nitrogen and phosphorus into algal biomass as a primary nutrient for fish. Similar outcomes were found by Abreu *et al.*, (2011) using *G. Vermiculophylla* as shown in **Table 2.3**. On the contrary, seabream and grey mullet reduced total sludge by 85 % and nitrogen in sludge by 98 % (Shpigel *et al.*, 2016) as well as tilapia, shrimp, and *Sarcocornia ambigua* reduced the total sludge production by 48.57 % and have no effect on the recovery of nitrogen and phosphorus (Poli *et al.*, 2019) when these species were grown together. Also, sea urchin and cucumber consumed 3.8 – 16.3 % and 11.7 – 45.9 % of fish waste respectively, when injected to the culture as a feed (Israel, Lupatsch and Angel, 2019).

Various physical methods have been also adopted for the treatment AQW. These methods were originally developed for conventional

wastewater treatment plants. In AQW, visible and large particles were separated mechanically by various inexpensive methods alike sedimentation, physical straining, and sand filtration, etc. The smaller particles were removed using coagulation and flocculation, flotation, and membrane filtration (Lekang, 2007).

For AQW with a low overflow rate of 1 m/h, 85 – 90 % of the solid is generally removed by sedimentation (Cripps and Bergheim, 2000). Recently, many modifications have been adopted in the sedimentation for AQW in order to achieve higher efficiency, as shown in **Table 2.2**. The swirl and radial separator remove  $37.1 \pm 3.3$  % and  $77.9 \pm 1.6$  % solid particles from AQW respectively (Davidson and Summerfelt, 2005). However, greater than 90 % of the suspended particle larger than 250  $\mu\text{m}$  was removed through swirl separator in a recirculating aquaculture system (RAS) (Pfeiffer, Osborn and Davis, 2008). In addition to this, hydrocyclones remove solid particles based on centrifugal force inside the free vertex flow of wastewater and were used by Lee, (2014, 2015) for AQW. However, study shows that raw fish sludge (not suitable) has significantly lower plant biomass (82.6 % less) compared to commercial fertilizer and anaerobic digested sludge (Yogev *et al.*, 2020). Besides sedimentation, filtration has been used for AQW.

For larger particles ( $> 15$  mm) bar filter racks are employed and specially designed screens are used for smaller particles ( $< 6$   $\mu\text{m}$ ) (Lekang, 2007). Some studies reported that the sand filter removes more than 65 % of

the SS particle (23 – 55  $\mu\text{m}$ ) when used as a final filtration component in RAS (Pfeiffer, Osborn and Davis, 2008). Higher removal efficiency was observed for larger particles (Malone and Beecher, 2000; Ali, 2013) and smaller aperture size of filter media (Dolan, Murphy and Hehir, 2013) as shown in **Table 2.2**. Furthermore, an inclined belt filter with the addition of alum ( $\text{Al}_2(\text{SO}_4)_3 \cdot 18\text{H}_2\text{O}$ ) and polymer (Hychem, CE 1950) removed 95% SS and 80 %  $\text{PO}_4^{3-}$ . The  $\text{PO}_4^{3-}$  was recovered by chemical reaction with alum and polymer (Ebeling, Welsh and Rishel, 2006).

Aeration is used to remove dissolved gases by providing oxygen to the wastewater pond through water surface or using mechanical equipment at the bottom of the pond. A sufficient amount of oxygen is also necessary for aquatic life and to prohibit the natural aging of pond soil (Rogers, 1989). During aeration, the  $\text{CO}_2$  degassing occurs while meeting the oxygen deficiency in the pond system and increasing the production of fish (Brune *et al.*, 2003). Further, with continuous aeration and organic carbon, heterotrophic bacteria decrease dissolve nitrogen from 22 – 14 % and sedimentary nitrogen from 49 – 5 % and are converted to bacterial biomass (Liu *et al.*, 2019).

Many techniques and methods have been highlighted, however the usage of this very much dependent to the types of fish cultured system (Turcios and Papenbrock, 2014). Also, there is need to investigate the pros and cons of the methods and techniques suggested.

### **2.3. Advantages and disadvantages of current treatment methods**

Various methods have been used for AQW treatment as discussed in the above section. Each method has their own pros and cons. Sedimentation can be used as secondary treatment for thickness of the sludge however it's difficult to recover the nutrient as a primary treatment because of low concentration (Cripps and Bergheim, 2000). Aeration and liming is used for DO and pH of the pond water, respectively, hence improved the pond productivity (Rogers, 1989; Wurts and Masser, 2013). Chlorination generally oxidized the organic compound and kills the microorganism, but higher than 0.05 ppm in water makes it lethal to fish (Wedemeyer, 1996; Stickney, 2000). The advantages and disadvantages of AQW treatment method are shown briefly in the **Table 2.4**.

Furthermore, the conventional technique is not sufficient to reduce phosphorus, nitrogen, and toxic heavy metals etc. There is no advanced technology available for the treatment of wastewater to treat most of the pollutant in a single step. Various factor can be take into account for the selection of particular treatment i.e. required level of clean up, waste type and concentration, effluent heterogeneity, as well as economic factors (Rajasulochana and Preethy, 2016). The recovery of nutrients from wastewater is difficult to remove using primary and secondary treatment. However, adsorption is one of the methods used in the final treatment for the organic and inorganic pollutants removal even at low concentrations of adsorbate molecule.

**Table 2.4.** Advantage and disadvantages AQW treatment methods

Method	Description	Advantage	Drawbacks	Ref.
Sedimentation	Particle settled due to gravity and effect on retention time in settling tank	Used for secondary thickness of sludge in aquaculture system	Cannot be used as primary nutrient recovery due to low concentration of the nutrient	Cripps and Bergheim, 2000
Mechanical filters and micro screen	-	Inexpensive and simple	Require very low velocity	Lekang, 2007
Aeration and circulation	Addition and redistribution of oxygen	Improve pond water and soil quality Uniform DO and temperature Higher quality product	-	Rogers, 1989
Adsorption	Using solid material as adsorbent	Cost effective, simple design, excellent approach for removal of pollutants	Required regeneration of adsorbent	Sukmana <i>et al.</i> , 2021
Liming	Addition of lime	Increasing pH and hardness Increasing pond production	-	Wurts and Masser, 2013
Chlorination	Using chlorine compound as disinfectant	Oxidized organic compound	Dichlorination should be done	Stickney, 2000
		-	> 0.05 ppm dosage is lethal for fish	Wedemeyer, 1996
BFT	Using carbon for the growth of bacteria	Productivity improvement, less environmental impact, Almost no need for water exchange	-	Bossier and Ekasari, 2017
		-	Constant accumulation of suspended solid	Ekasari, Crab and Verstraete, 2010; Luo <i>et al.</i> , 2014; Sgnaulin <i>et al.</i> , 2018s

Adsorption has advantage because of simple design and involved low investment (initial cost and required land) compared to other methods (Rashed, 2013; Crini and Lichtfouse, 2019; Sukmana et al., 2021)

#### **2.4. Nitrogen compound removal or recovery from AQW by adsorption**

In adsorption process, the liquid or gas molecules accumulates on the surface of solid and is classified into physical and chemical adsorption, based on the type of attraction between the solute and adsorbent. Physical adsorption is a reversible process and caused by Van der Waals force between the adsorbate molecule and adsorbent however, chemisorption is irreversible and occur between solute and solid surface (adsorbent) through of chemical reaction (Lehr and Keeley, 2005; Ahmad *et al.*, 2019). Various sorbents and adsorption mechanisms (pore diffusion, electrostatic attraction, hydrogen bonding, ion exchange, memory effect, ion complexation, and chemical reaction) had reported to remove nitrogen compounds from wastewater (Dai *et al.*, 2020).

Several types of sorbents including zeolite-based, gastropod shells, carbon-based, clay-based, and biopolymer-based, etc. had been reported for the removal of nitrogen compounds from AQW and the adsorption capacity/efficiencies of numerous adsorbents have been summarized in **Table 2.5** for better clarity. However, a brief review has been done here based on adsorbents type.



**Table 2.5.** Adsorption capacity / efficiency of adsorbents for AQW nitrogen compound removal

Adsorbents	Adsorption capacity / efficiency					Operational parameters	Model	Study	Ref.
	NH <sub>4</sub> <sup>+</sup>	NH <sub>3</sub>	NH <sub>3</sub> -N	NO <sub>3</sub> <sup>-</sup>	NO <sub>2</sub> <sup>-</sup>				
<b>Zeolite-based adsorbents</b>									
Zeolite 13X	8.6 mg/g	-	-	-	-	25 °C, 0.67 hr	Langmuir	Batch	Zheng <i>et al.</i> , 2008
NCLP	7.3 mg/g	-	-	-	-	25 °C, 20 g/L, 48 hr	Langmuir	Batch	Yin <i>et al.</i> , 2018
Commercial zeolite 13X	17.6 mg/g	-	-	-	-	2 hr, 100 g/L	Freundlich	Batch	Ahmadiannamini <i>et al.</i> , 2017
Z3	15.2 mg/g	-	-	-	-	0.5 g/L, 48 hr	Langmuir	Batch	Bernal and Lopez-Real, 1993
Z2	-	14.2 mg/g	-	-	-		Langmuir	Batch	
CCZBs	-	-	0.18 mg/g	-	-	25 °C, 9.2 hr	Langmuir	Batch	Tian <i>et al.</i> , 2016
Commercial zeolite	18.5 %	-	-	58.3 %	12.1 %	10 g/L, RT, overnight	-	Batch	El-sherbiny, El-chaghaby and El-Shafea, 2019
Natural zeolite	32 %	-	-	-	-	18 °C, 10 g/L, 3.75 hr	-	Batch	Şahin <i>et al.</i> , 2018)
Zeolite + bentonite	38 %	-	-	-	-		-	Batch	
Natural zeolite	-	-	76.6 %	-	-	26.5 °C, 5 week, 5 ×10 <sup>-9</sup> g/L	-	Fish rearing tank	Aly <i>et al.</i> , 2017
Mordenite sample 1&2	8.7 mg/g	-	-	-	-	22 – 26 °C, 24 hr, 0.05 g/L	Langmuir	Batch	Zhou and Boyd, 2014
<b>Gastropod shell-based adsorbent</b>									
Calcined gastropod shell (CGS)	-	-	-	9.8 mg/g		2 g/L, 6 hr	Pseudo 2 <sup>nd</sup> order	Batch	Saliu <i>et al.</i> , 2019s

**Table 2.5.** Continued

Adsorbents	Adsorption capacity / efficiency					Operational parameters	Model	Study	Ref.
	NH <sub>4</sub> <sup>+</sup>	NH <sub>3</sub>	NH <sub>3</sub> -N	NO <sub>3</sub> <sup>-</sup>	NO <sub>2</sub> <sup>-</sup>				
<b>Carbon-based adsorbents</b>									
Activated carbon	-	65.3 %	-	-	-	22 °C, 0.33 g/L, 9 hr	-	Fish rearing tank	Sichula <i>et al.</i> , 2011
Pyrolyzed chicken feathers fiber (PCFF)	-	-	39.13 %	-	-	11.7 g/L, RT, 1.25 hr	Langmuir	Batch	Moon <i>et al.</i> , 2017
Biochar (RSII)	4.5 mg/g	-	-	-	-	45 °C, 1.5 hr	Freundlich	Batch	Khalil, Sergeevich and Borisova, 2018
Activated carbon filter	17.8 %	-	-	89.3 %	89.6 %	23.2 °C, 0.9-1.8 hr	-	Continuous	Jegatheesan <i>et al.</i> , 2007
98% DD chitosan	-	89 %	-	-	-	0.02 g/L, 25 °C, 0.5 hr	-	Batch	Chung, 2006
Chitosan foam 0.10 % (m/v)	-	32.8 %	-	-	57.2 %	25 °C, 25 hr	-	Batch	Zadinelo <i>et al.</i> , 2018
Chitosan (Q2)	-	94.3 %	-	-	-	25 °C, 3 hr	-	-	Bernardi <i>et al.</i> , 2018
<b>Clay-based adsorbents</b>									
Bentonite hydrochar composite	23.7 mg/g	-	-	-	-	1- 10 g/L, 30 °C, 6 hr	Langmuir	Batch	Ismadji <i>et al.</i> , 2016
Bentonite Clay 1	~ 100 %	-	-	-	-	-	-	Continuous	
Bentonite Clay 1	0.5 mg/g	-	-	-	-	18 °C, 10 g/L, 3.75 hr	-	Batch	Şahin <i>et al.</i> , 2018
Bentonite Clay 1	97.8 %	-	-	-	-	20 ppm, 75 g/L, 27 °C, 3 hr	-	Batch	Zadinelo <i>et al.</i> , 2015

**Table 2.5.** Continued

Adsorbents	Adsorption capacity / efficiency					Operational parameters	Model	Study	Ref.
	NH <sub>4</sub> <sup>+</sup>	NH <sub>3</sub>	NH <sub>3</sub> -N	NO <sub>3</sub> <sup>-</sup>	NO <sub>2</sub> <sup>-</sup>				
<b>Other adsorbents</b>									
PAA.HCl hydrogel	-	-	-	> 53 %	> 85 %	0.1 g/L, 3 hr	-	Batch	Kioussis, Wheaton and Kofinas, 2000
Aged refuse	1.4 mg/g	-	-	-	-	20 g/L, 0.67 hr, 250 rpm and at ambient temperature	Freundlich	Batch	Anijiofor <i>et al.</i> , 2018
Fe <sub>3</sub> O <sub>4</sub> @CNT	-	-	-	55 %	-	-	-	Batch	Nezhadheydari <i>et al.</i> , 2019
Desulfurization slag (DS)	0.1 mg/g / 45.1 %	-	-	-	-	30 ppm, 40 g/L, 2 hr, and 30 °C	Pseudo 2 <sup>nd</sup> order	Batch	Yang <i>et al.</i> , 2017

Few studies have been found in the literature that worked on the recovery of the nutrient from the spent sorbent. The  $\text{NH}_4^+$  was recovered from the spent zeolite (clinoptilolite) by injection of NaOH to the continuous column process following the stripping and scrubber in the regeneration process and convert to  $(\text{NH}_4)_2\text{SO}_4$  as a final product (Lubensky and Ellersdorfer, 2021). Similar method has been used for the recovery of  $\text{NH}_4^+$  by injection of NaCl/NaOH to the zeolite (clinoptilolite) bed for the regeneration. The material balanced showed that with addition of the air stripping at total of 1267 mg of  $\text{NH}_4^+$  is recovered in the solution (Ellersdorfer, 2018). Also, 95 % of  $\text{NH}_3$  is recovered from the spent zeolite during the regeneration (NaCl/NaOH) subsequently air stripping and scrubber process (Deng, Elbeshbishy and Lee, 2016). Addition of the regeneration process could increase the cost of the process however, it would be economical feasible to direct used the spent sorbent as a nutrient-rich zeolite fertilizer (Wu and Vaneeckhaute, 2022).

## **2.5. Biochar**

According to the International Biochar Initiative (IBI), biochar is standardized “as a solid material obtained from the thermochemical conversion of biomass in a limited oxygen environment”. The biochar and charcoal preparation method (pyrolysis) is the same as both are obtained from carbonaceous raw materials (Aller, 2016). The main characteristics that distinguish the two materials, however, are their starting materials and their final application. Biochar is applied as a soil amelioration or an adsorbent

(having high porosity, nutrient content) whereas charcoal is used for heat generation. It has been reported the biochar term is not applied for the charred materials, which are obtained from coal and petroleum etc. (non-renewable source). Also, having the sorption properties, biochar can be used for the purification of gases and wastewater. Research has been conducted on the biochar which shows the immobilization of heavy metals, sulfamethoxazole, antibiotics etc from the pharmaceutical residue and industrial wastewater (Saletnik *et al.*, 2019). Furthermore, having large application in agronomic sector, and environmental management, the biochar market is increasing faster, with a global market price of \$80–13,480/oven-dried metric tonne. Additionally, the biochar market is expected to reach up to \$3.14 billion by 2025, with an annual growing rate of 13.1 % (Rashidi and Yusup, 2020).

### **2.5.1. Preparation of biochar**

Currently, various methods are used to produce biochar. However, depending on the feedstock and the required characteristics of the biochar for its application, the selection of pretreatment methods is very limited. According to the definition, biochar is normally prepared by heating the biomass at high temperatures in the absence or limited supply of oxygen (Kambo and Dutta, 2015). The various physical and chemical characteristics of biochar is based on technology used, such as pyrolysis, hydrothermal carbonization, and torrefaction.

Pyrolysis is the thermochemical decomposition of biomass in an inert atmosphere at high temperature (300 – 650 °C). The main product of pyrolysis is carbon rich solid material (biochar), volatile matters (condense to liquid as a bio-oil), and the remaining is “non condensable” gases, such as CH<sub>4</sub>, CO<sub>2</sub>, CO, and H<sub>2</sub>. Pyrolysis can be further divide in fast, and slow pyrolysis depends on the heating rate, and reaction time (Mohan, Pittman and Steele, 2006).

Slow pyrolysis is generally used for the production of biochar as it gives high yield of solid (25 – 30 %) than other pyrolysis process (Brownsort, 2009). In this process, the biomass is heated to a temperature range of 300 – 650 °C using long residence time (few minutes to several hours), and a low heating rates (10 – 30 °C/min) (Onay and Kockar, 2003). The slow heating rate and low operating temperatures favor high solid product yield (Kambo and Dutta, 2015).

Fast pyrolysis yield more bio-oil than other products such as gases and solid because the bio-oil could be directly used as source of energy for many processes (Czernik and Bridgwater, 2004). In fast pyrolysis the biomass is rapidly heated with the heating rates (> 120 °C/min), short residence times (< 2 sec), and at temperature range of 500 – 1000 °C. High amount of bio-oil (75 %) is obtain in fast pyrolysis process while small quantity of biochar (12 %) and non-condensable (13%) gases is produced. The produce bio-oil during fast pyrolysis t could be use a source of energy (Shakoor *et al.*, 2020).

Carbonization is a thermochemical process that convert biomass into charcoal. The carbonization process occurs when the biomass or carbonaceous material is slowly heated to temperature  $> 300$  °C in the presence of limited oxygen and to obtain maximum fixed carbon. During carbonization  $300 - 400$  °C, the cellulose and hemicellulose completely decompose and produce richer fixed carbon biochar. If heating continues over  $400$  °C, a high rich carbon material (charcoal) is achieved (Amer and Elwardany, 2020).

Hydrothermal carbonization (HTC), also called wet torrefaction, in which the organic feedstock is converted into a carbon rich solid product via thermochemical process. During HTC, the biomass is heated in a confined system under pressure ( $2 - 6$  MPa) for 5 to 240 minutes while being immersed in water at a temperature between  $180$  and  $260$  °C. (Mumme *et al.*, 2011). Typically, there is no control over the reaction pressure throughout the process in which the water saturation vapor pressure is corresponding to the reaction temperature (autogenic process). Liquid (bio-oil mixed with water), hydrochar, and small fraction of gases (mainly  $\text{CO}_2$ ) are the main products of HTC process. Hydrochar is the desired product in the HTC process, having the mass yield of around  $40 - 70$  % (Yan *et al.*, 2010). After hydrochar preparation before being used as adsorbent or fuel, it must go through a number of processes such as mechanical dewatering, filtering, and drying (Kambo and Dutta, 2015).

Torrefaction is a thermochemical process in which the sample is heated to temperature range of 200 – 300 °C in the absence of oxygen with a residence time of 30 min to several of hours (Kambo and Dutta, 2015). During this process, the slowly decomposition of biomass or waste material releases CO<sub>2</sub>, H<sub>2</sub>O and increases the carbon content in the material which possesses high energy density, hydrophobic behavior, homogenous, etc. and has high quality (equal to coal). The quality of rich carbon material depends on the torrefaction temperature and holding time because the depolymerization of biomass occurred in this process. The torrefaction process has been reported to increase the carbon content to 92.6 % of the *Leucaena leucocephala* woody biomass, suitable for the combustion. Biochar prepared from coffee residue through torrefaction exhibits a higher calorific value (31.12 MJ/Kg) and energy yield (48.08 %) (Jeyasubramanian *et al.*, 2021).

### **2.5.2 Nutrients removal/recovery by biochar**

Biochar has been used to remove various pollutants from wastewater, such as organic pollutants, heavy metals, nitrogen and phosphorus, etc. (Deng, Zhang and Wang, 2017) which cause harm to the environment. Deng, Zhang and Wang, (2017), reported that biochar has been employed for the removal of different types of pollutants in wastewater and the percentage of biochar usage for the adsorption of nutrients *i.e.* nitrogen and phosphorus is about 13 % from other studies such as organic matter, heavy metals, etc. (Deng, Zhang and Wang, 2017).



**Table 2.6** summarizes studies reported in the literature on biochar adsorption nutrients. Some wastewaters such as livestock contains abundant of nutrients, especially nitrogen and phosphorus.

**Table 2.6.** Nutrient removal by biochar from wastewater

Type of nutrients	Raw material	Pyrolysis temperature (°C)	Pyrolysis time (hr)	Adsorption temperature (°C)	Adsorption capacity/ efficiency	Model fitted	Ref.
<b>NH<sub>4</sub><sup>+</sup></b>	Bamboo waste	400	1	RT	3.9 mg/g	Redlich-Peterson / Elovich	Chen <i>et al.</i> , 2017
	Sugarcane harvest residue	550	1	22.5	22 mg/g	Langmuir / PSO	Li <i>et al.</i> , 2017
	Pine sawdust	550	2	RT	3.4 mg/g	Redlich-Peterson / PSO	Yang <i>et al.</i> , 2018
	Pine sawdust	300	-	20	5.38 mg/g	PSO	
	Fruit pericarp	300	4	25	4.1 mg/g	Langmuir / PSO	Xue <i>et al.</i> , 2019
	Rice straw	600	4	-	0.4 mg/g	-	Meng <i>et al.</i> , 2019
	Rice straw	600	0.17	25	1.4 mg/g	PSO	Song <i>et al.</i> , 2019
	Wood chips	700	-	-	6.7 mg/g	Langmuir	Hailegnaw <i>et al.</i> , 2019
	Rice straw	300	0.33	25	7.5 mg/g	PSO	Gong <i>et al.</i> , 2019
	Pineapple peel	300	2	-	4.4 mg/g	Langmuir / PSO	Hu <i>et al.</i> , 2020

**Table 2.6.** Continued

Types of nutrients	Raw material	Pyrolysis temperature (°C)	Pyrolysis time (hr)	Adsorption temperature (°C)	Adsorption capacity/ efficiency	Model fitted	Ref.
NH <sup>4+</sup>	Grape skin	-	-	RT	38 %	Freundlich	Aghoghovwia, Hardie and Rozanov, 2020
	Coffee husk	350	1	RT	1.6 mg/g	Langmuir / PFO	Vu and Do, 2021
	Peanut shell	500	2	30	3.8 mg/g	Langmuir / PSO	An <i>et al.</i> , 2021
	Wood chips	700	-	RT	0.96 mg/g	Langmuir	Begum <i>et al.</i> , 2021
	Corn straw	500	2	RT	4.4 mg/g	Langmuir / PSO	Li <i>et al.</i> , 2021
	Rice husk	550	3	28	0.1 mg/g	Freundlich	Thao <i>et al.</i> , 2021
	Pineapple peel	400	4	-	13.4 mg/g	Dubinin-Radushkevich	Otieno <i>et al.</i> , 2021
	Rice straw	550	-	25	24.3 mg/g	Langmuir	Lv <i>et al.</i> , 2021
	Sorghum straw	300	0.5	25	3.5 mg/g	Langmuir / PSO	Xu <i>et al.</i> , 2022

**Table 2.6.** Continued

<b>Types of nutrients</b>	<b>Raw material</b>	<b>Pyrolysis temperature (°C)</b>	<b>Pyrolysis time (hr)</b>	<b>Adsorption temperature (°C)</b>	<b>Adsorption capacity/ efficiency</b>	<b>Model fitted</b>	<b>Ref.</b>
<b>NO<sub>3</sub><sup>-</sup></b>	Soybean straw	500	2	25	42 mg/g	PSO	Yin, Wang and Zhao, 2018
	Corn cob	600	2	30	3.3 mg/g	Langmuir / PSO	Zhao <i>et al.</i> , 2018
	Bamboo wastes	460	2	25	~5 mg/g	Langmuir	Viglašová <i>et al.</i> , 2018
	Rice straw	300	0.33	25	~10.7 mg/g	PSO	Gong <i>et al.</i> , 2019
	Rice straw	600	4	10	0.80 mg/g	-	Meng <i>et al.</i> , 2019
	Wood chips	700	-	-	11.3 mg/g	Langmuir	Hailegnaw <i>et al.</i> , 2019
	Rice straw	300	2	30	< 0 mg/g	-	Zhou <i>et al.</i> , 2019
	Wood biochar	900 - 1000	-	23	0.3 mg/g	-	Rahman, Nachabe and Ergas, 2020
	Rubber tyre	-	-	RT	87 %	-	Aghoghovwia, Hardie and
	Grape skin	-	-	RT	85.6 %	-	Rozanov, 2020

**Table 2.6.** Continued

Types of nutrients	Raw material	Pyrolysis temperature (°C)	Pyrolysis time (hr)	Adsorption temperature (°C)	Adsorption capacity/ efficiency	Model fitted	Ref.
NO <sub>3</sub> <sup>-</sup>	Pinewood wastes	600	2	22	4.2 mg/g	Langmuir / PFO	Vijayaraghavan and Balasubramanian, 2021
	Rice straw	550	-	25	2.3 mg/g	Langmuir	Lv <i>et al.</i> , 2021
	Rice husk	550	3	28	0.13 mg/g	Freundlich	Thao <i>et al.</i> , 2021
PO <sub>4</sub> <sup>3-</sup>	Wood	600	10	25	7.67 mg/g	Langmuir / PSO	Kizito <i>et al.</i> , 2017
	Soybean stover	700	3	40	~ 65 mg/g	Freundlich / Elovich	Karunanithi <i>et al.</i> , 2017
	Raw sludge	650	0.5	25	92.86 %	Langmuir	Xu, Zhang and Deng, 2018
	Soybean straw	500	2	25	77 mg/g	PFO	Yin, Wang and Zhao, 2018
	Crawfish waste	800	2	25	70.9 mg/g	Langmuir / PSO	Park <i>et al.</i> , 2018
	Sesame straw	700	2	25	34.17 mg/g	Freundlich / PSO	Yin <i>et al.</i> , 2018
	Wood waste	600	-	25	116.4 mg/g	Redlich-Peterson / PSO	Xu <i>et al.</i> , 2018

**Table 2.6.** Continued

Types of nutrients	Raw material	Pyrolysis temperature (°C)	Pyrolysis time (hr)	Adsorption temperature (°C)	Adsorption capacity/ efficiency	Model fitted	Ref.
<b>PO<sub>4</sub><sup>3-</sup></b>	Sewage sludge	600	3	RT	49.95 mg/g	Langmuir / PSO	Yin, Liu and Ren, 2019
	Broussonetia papyrifera leaves	500	2	25	~7.5 mg/g	Freundlich / PSO	Qiu <i>et al.</i> , 2019
	Egg shell and rice straw (1:1)	800	2	25	~225 mg/g	Langmuir / PSO	Liu, Shen and Qi, 2019
	Hickory wood chips	600	1	25	8.34 mg/g	Langmuir / PSO	Zheng <i>et al.</i> , 2019
	Pinewood wastes	600	2	22	18.4 mg/g	Langmuir /PFO	Vijayaraghavan and Balasubramanian, 2021

Using biochar as adsorbent is not only reducing the eutrophication but can be also recycled for the enhancing the soil fertility, and nutrient resources. A maximum adsorption capacity (9.67 mg/g) for  $\text{NH}_3\text{-N}$  was observed onto biochar when corn cob was pyrolyzed at 600 °C for 2 hr (Deng, Zhang and Wang, 2017). Also, biochar prepared from cow dung represent a remarkable adsorption capacity (25.84 mg/g at 25 °C) of  $\text{NH}_3\text{-N}$  (Deng, Zhang and Wang, 2017). Modification of corn cob biochar with calcium and magnesium significantly improved the adsorption capacity of  $\text{PO}_4^{3-}$  and a highest adsorption capacity of 319.63 mg/g was achieved (Fang *et al.*, 2015). The result indicating that increasing the anion exchange capacity of biochar by using of calcium and magnesium improve its phosphate adsorption efficiency. Also, two studies have been found in which the ammonia spent biochar was used for the growth of ryegrass (Taghizadeh-Toosi *et al.*, 2012) and water spinach (Shang *et al.*, 2018). From the discussion above, it can be concluded that biochar can be used to adsorb the nitrogen and phosphorus from wastewater and can be further applied as a fertilizer if the biochar is made from green material.

Biochar prepared from various feedstocks using different conditions such as gas flow, heating rate, temperature, heating rate, and time etc. shows various characteristics. it has been reported that using rice husk and empty fruit bunch biochar has different CEC, surface area, and pore volume using same preparation condition (Yavari *et al.*, 2017). In addition to this, biochar from peanut shell, wheat straw, and corn straw have different functional groups, pH, surface area, and electrical conductivity (Gai *et al.*, 2014).

Biochar made from different feedstocks and various conditions involve in various adsorption mechanisms for inorganic and organic pollutants, including physical and chemical interaction such as Vander Waals forces, surface complexation, ion exchange, electrostatic interaction, and pore filling (Barquilha and Braga, 2021). Van der Waals forces occurs when the molecules aligned having opposite charge (Roy, Kar and Das, 2015). Electrostatic interactions occur between the surface of biochar and ionizable species and strongly influenced by pH of the solution (Li *et al.*, 2019). Surface complexation is another adsorption mechanism in which the ionic species forms complexes on the surface of biochar. A complex is formed when a central atoms are surrounded by ligands (Barquilha and Braga, 2021). In ion exchange process, the biochar could be impregnated with the ions such as  $K^+$ ,  $Na^+$ ,  $Mg^{2+}$ , and  $Ca^{2+}$  and further exchanged for the target atom or molecule in the adsorption process. During ion exchange process, the solid phase must be insoluble in the medium (Barquilha and Braga, 2021). Pore-filling is a physical adsorption method and occurs in adsorbent materials, such as activated carbon and biochar, due to high surface area and large volumes of micro and mesopore (Barquilha and Braga, 2021).

## **2.6. OPF biochar**

**Table 2.7** shows the adsorption efficiency/capacity of biochar and activated carbon for various pollutants from wastewater. Few studies have been found on the removal of nutrients.



**Table 2.7.** OPF based adsorbent for removal of different pollutants from wastewater

Pollutants	Preparation conditions	Operation parameters	Adsorption Capacity/ efficiency	Model fitted	Ref.
Pb <sup>2+</sup>	Powder oil palm empty fruit bunces	10 g/L, 2 hr, RT	94.3 %	PSO	Daneshfozoun, Abdullah and Abdullah, 2016
	Fine sized of oil palm EFB fiber + Fe <sub>2</sub> O <sub>3</sub> solution, sonicated for 5 min followed by shaking for 10	10 g/L, 25 °C, 2.5 hr	48.7 mg/g	-	Daneshfozoun, Abdullah and Abdullah, 2017
	EFB fiber + 10mM NaOH for 12 hr at RT, washed with DI water, dried (60 °C, 48 hr)	14 g/L, 2 hr	0.19 – 0.6 mg/g	-	Ricky <i>et al.</i> , 2016
NH <sub>3</sub> -N	EFB fiber + 10mM NaOH for 12 hr at RT	15.7 g/L, 0.67 hr, 27 °C	0.53 – 10.89 mg/g	-	Zahrim <i>et al.</i> , 2017
	Pyrolysis (450 °C, 2 hr) Activation (600 – 900 °C, 0.25 – 4 hr)	6.67 g/L, 2 hr	16 – 32 %	-	Ismail <i>et al.</i> , 2018
	0.6 M citric acid + EFB, dried at 50 °C for 24 hr followed by raising temperature to 120 °C for 90 min, washed, dried (50 °C, 24 hr)	35 g/L, 2 hr	79.5 %	Langmuir	Nasir <i>et al.</i> , 2018
Methylene blue	Carbonization (450 °C, 15 °C/min, 0.5 hr), Activation (Biochar + 1 M HNO <sub>3</sub> , 132 °C, 1 hr, 35 psi)	2 g/L, 30 °C, 24 HR	62.52 mg/g	Langmuir / PSO	Ibrahim <i>et al.</i> , 2021

The best removal efficiency of 79.5 % was observed using citric acid activated EFB (Nasir *et al.*, 2018). Also, the NaOH modified EFB represents 0.83 mg/g and 10.89 mg/g of NH<sub>3</sub>-N at a concentrations of 50 and 4000 ppm, respectively (Zahrim *et al.*, 2017). Moreover, one study has done adsorption isotherm study on NH<sub>3</sub>-N removal using modified citric acid EFB and its follow Langmuir model which mean the adsorption is monolayer but have not conducted the kinetics or thermodynamic to understand the adsorption mechanism (Nasir *et al.*, 2018). Also, biochar or activated carbon from OPF has not been investigated for the adsorption mechanism of NH<sub>3</sub>-N removal using OPF based biochar. In addition to this, OPF biochar is also used for other pollutant such as heavy metals and dye (Marsin *et al.*, 2018). In case of Pb<sup>2+</sup> the powder EFB follows pseudo- second order (PSO) model shows chemisorption (Daneshfozoun, Abdullah and Abdullah, 2016). However, methylene blue adsorption onto activated biochar exhibit monolayer chemisorption (Ibrahim *et al.*, 2021).

## **2.7. Cost analysis of biochar**

The production cost of biochar is a significant factor in its application and marketing. In cases where biochar is the prime product, the cost must cover operating expenses such as the costs of feedstock, transport, labor, maintenance, production, distribution, and others to ensure the long-term business feasibility. The price of biochar varies depending on the product sites countries. The price arranges from \$0.09/kg in the Philippines to as high as \$8.85/kg in the UK (Ahmed *et al.*, 2016). The cost of biochar production

appears to be lower than that of synthetic fertilizer. According to the World Bank (April 2022) the price of phosphorus fertilizers is as high as 954 US \$/ton and nitrogen fertilizers (Urea) 925 US \$/ton (Marciniczyk, Ok and Oleszczuk, 2022). By applying a high biochar rate, ranging from 2.5 – 20 ton/ha, significant changes in crop productivity are achieved (Joseph *et al.*, 2013). Nutrient enriched biochar can decrease this dosage level and providing the fertilization for long time hence reducing agricultural cost (Marciniczyk, Ok and Oleszczuk, 2022). The high wastewater production has not only adverse effect on environment, although requires large financial outlays (Jones *et al.*, 2021). Moreover, in Europe the average price for biowaste landfilling is 30 €/ton (Marciniczyk, Ok and Oleszczuk, 2022). Biochar-based fertilizer could be a profitable sector if wastes has been used for biochar preparation, waste heat is used for pyrolysis process, nutrient rich obtained biochar is further targeted for fertilization (Stávková and Maroušek, 2021).

## CHAPTER 3

### RESEARCH METHODOLOGY

#### 3.1. Introduction

This chapter consist of the research methodology adopted for this research work. The research work was divided into three phases. The first phase is to produce biochar and further activate the biochar via activating agents. In the second phase, the process parameter study has been evaluated using OPF biochar. In third phase, the adsorption isotherms, kinetics, and thermodynamic study was investigated for adsorption mechanism as well as cost analysis of the biochar. At each stage, the adsorption efficiency/capacity was evaluated. The schematic flow chart of the whole research is presented in **Figure 3.1**.

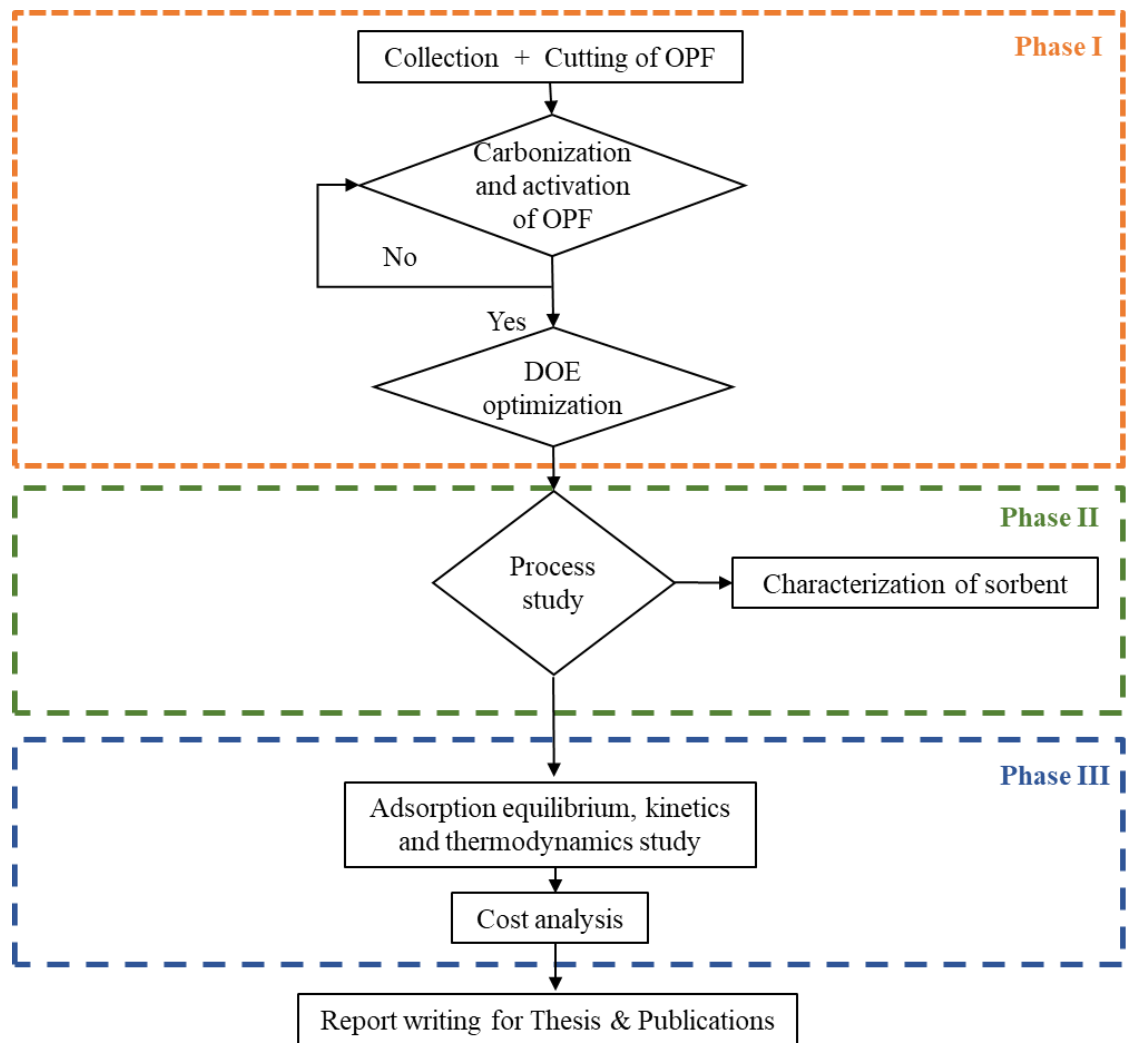


**Figure 3.1.** Schematic flow chart of the research study

### 3.2. Materials

The materials and chemicals used in this study are listed in **Table 3.1**.

**Table 3.1.** List of materials and chemicals

<b>Materials</b>	<b>Manufacturer/supplier</b>	<b>Purity (%)</b>
Oil palm fiber	Tian Siang Oil Mill (Air kuning) Sdn. Bhd	-
Ammonium sulfate ((NH <sub>4</sub> ) <sub>2</sub> SO <sub>4</sub> )	Merck Chemicals Germany	≥ 99
65 % HNO <sub>3</sub>	R&M chemical Malaysia	65
37 % HCl	R&M chemical Malaysia	37
85 % H <sub>3</sub> PO <sub>4</sub>	R&M chemical Malaysia	85
98 % H <sub>2</sub> SO <sub>4</sub>	R&M chemical Malaysia	98
Glacial CH <sub>3</sub> COOH	R&M chemical Malaysia	99.8
30 % H <sub>2</sub> O <sub>2</sub>	R&M chemical Malaysia	30
Silver nitrate (AgNO <sub>3</sub> )	GENE chemicals	99
Barium acetate	SYNERLAB	99
Sodium hydroxide (NaOH)	R&M chemical Malaysia	99
Sodium chloride (NaCl)	R&M chemical Malaysia	99
Test 'N Tube™ Vials, 0.4 – 50.0 ppm NH <sub>3</sub> -N (HR)	Hach company USA	-
Nitrogen gas	Linde Malaysia Sdn. Bhd.	99
Compressed air	Linde Malaysia Sdn. Bhd.	99

### 3.3. Apparatus

The equipment's use in this study is listed in **Table 3.2**.

**Table 3.2.** List of apparatus

<b>Apparatus</b>	<b>Purpose</b>	<b>Model</b>	<b>Manufacturer/Supplier &amp; Country</b>
Grinder	Biochar grinding	ZM 200	Retsch /Germany
Sieve analysis	Sieving as per the required particle size	-	Fisher Scientific (M) Sdn. Bhd/USA
Oven	Drying	UF110	Memmert/Germany
pH meter	Checking the pH of solution	HQ30d	Hach USA
Vis-spectrophotometer	NH <sub>3</sub> -N measurement	DR3900	Hach USA
BET surface area	To measure the surface area of the sorbet	Autosorb 1	Quantachrome instruments ASIC/USA
FESEM and EDX	Image analysis and elemental content	JSM-6701F	JEOL /Japan
ATR-IR	To identify the functional group	Perkin Elmer spectrum 2	Perkin Elmer/USA
Heating mental	Activation of biochar	MS ES302	Lab Medical Science Sdn.Bhd/UK
Thermo gravimetric analyzer	Proximate analysis of biochar	TGA/DSC 3 <sup>+</sup>	Mettler Toledo/USA
Orbital shaker	For shaking of the solution	KS 4000 i	IKA

### 3.4. Preparation of OPF

The raw OPF was provided by Tian Siang Oil Mill (Air Kuning) Sdn. Bhd. Located in Kampar, Perak, Malaysia. Raw OPF was collected from the bedding processing mill within the palm oil factory, which was pre-cleaned

and polished. The collected OPF were then cut into small pieces in a range of 1 – 2 cm and stored in the plastic bag at room temperature prior to use. The raw and cut OPF is shown in **Figure 3.2**.

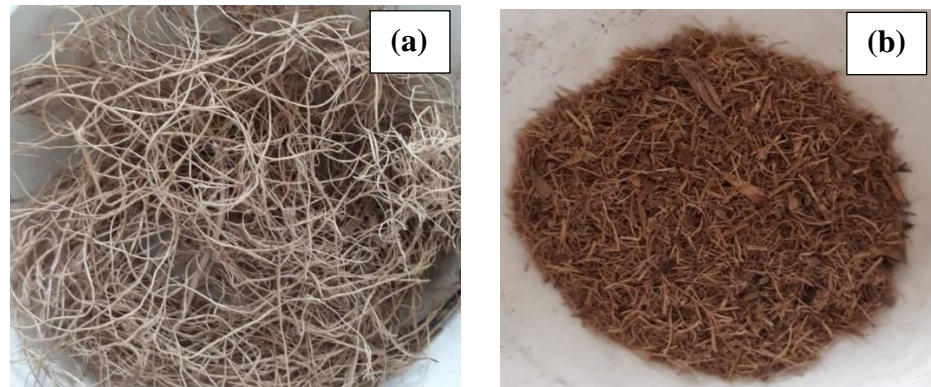


**Figure 3.2** Raw (a) and Cut (b) OPF

#### **3.4.1. Preliminary preparation of biochar with and without Air**

10 g of OPF was put into the vertical fixed bed carbonization unit and carbonized at different temperature (200 °C – 500 °C) keeping holding time (1 hr), and heating rate (15 °C/min) constant. For the samples prepared without air, nitrogen gas (N<sub>2</sub>) was flowed at a rate of 300 ml/min. For the sample prepared with air, 100 ml/min of air was flown into the carbonization unit. The injection of air was strictly controlled through mass flow controller to avoid combustion. A preliminary study was conducted on using different air flow before choosing the actual range for DOE. In preliminary study it was found that the flow more than 150 ml/min will be an oversupply of oxygen and the biochar tend to form ash. Also, at higher temperature more



than 400 °C can burn the biochar and convert to ashes. Further, the air was injected to partially oxidize the biochar and improve the surface functional group. After the carbonization process, the biochar samples were cooled in N<sub>2</sub> and air environment, respectively. The conditions were based on the adsorption efficiency of NH<sub>3</sub>-N by increasing the carbonization temperature the adsorption efficiency decreases by Gai *et al.* (2014). After, cooling, the biochar samples were crushed and sieved to a particle size of less than 250 µm. The prepared samples were thoroughly washed with distilled water until the filtrate was clear for removing the contaminants and till neutral pH because the biochar surface contains some organic compounds which can readily leached into the water. These organic compounds condensed on the surface of biochar during cooling process. The biochar samples were then oven dried at 105 °C for 2 to 4 hr until no changes in weight were observed and sealed in a container and stored in a desiccator for further use.

### **3.4.2. Preliminary preparation of activated biochar**

The best biochar prepared from Section 3.4.1 were further activated via chemical and physical activation. This is to test whether this could further improve the adsorption efficiency/capacity of the adsorbent. 5 g of the OPF biochar added to a 1M solution (100 ml) of HNO<sub>3</sub>, HCl, H<sub>3</sub>PO<sub>4</sub>, H<sub>2</sub>SO<sub>4</sub>, CH<sub>3</sub>COOH or H<sub>2</sub>O<sub>2</sub> and heated to 100 °C for 2 hr with a continuous stirring of 200 rpm (Shim, Park and Ryu, 2001; Tan *et al.*, 2014; Kim *et al.*, 2020; Niyousha *et al.*, 2020). The modified biochar samples are labeled BC-HNO<sub>3</sub>, BC-HCl, BC-H<sub>3</sub>PO<sub>4</sub>, BC-H<sub>2</sub>SO<sub>4</sub>, BC-CH<sub>3</sub>COOH, and BC-H<sub>2</sub>O<sub>2</sub>. For

physical activation, CO<sub>2</sub> activation was tested. The OPF biochar is activated at various holding time (0.5 – 2 hr) keeping activation temperature (300 °C) and CO<sub>2</sub> injection (300 ml/min) constant (Iberahim *et al.*, 2022). After, activation the activated samples were cooled down in the presence of N<sub>2</sub>. After cooling, samples were prepared as described in Section 3.4.1 prior to usage.

### 3.4.3. Optimization via DOE

Design Expert 13.0 software was used to optimize the preparation OPF biochar. The experimental design suggested by the software is given in **Table 3.3**.

In optimization study, a standard response surface methodology (RSM) design has been applied using central composite design (CCD). CCD is a suitable statistical approach for sequential testing that can readily fit the quadratic surface. The RSM technique not only determines the best optimum conditions for the minimum number of experimental tests but also gives the information to estimate results in order to design a process. RSM is a systematic and efficient procedure for studying interaction effect of various parameters (Iberahim *et al.*, 2019). On the other hand, the factorial design gives many experimental runs with a modest number of parameters. For examples for 3 factors, the RSM design calculate 10 experimental runs while factorial design gives 27 runs.

The adsorption efficiency for NH<sub>3</sub>-N in the current study was chosen as a response. Variance analysis (ANOVA) was applied using the statistical model. Only significant coded term was obtained for NH<sub>3</sub>-N in the final empirical model. The model significance can be calculated by probability value (p-value) and Fisher variance ratio (F-value), which quantifies how effectively the model explain the variance in the data around its mean value. Larger the F-value is, the more significant that term is, while for the p-value, the term is only significant if the value is less than 0.05 and not significant if its value exceeds 0.1. (Iberahim *et al.*, 2022).

Based on preliminary study, the carbonization parameters were varied as factors and adsorption capacity/efficiency as the response. **Table 3.3.** shows the details. Upon input to the software the software generated a series of runs as per **Table 3.4.** The alpha value was 0.5.  $t$  was fixed as 0.5 to obtain the inscribe designed as the limits are specified.

**Table 3.3.** Input parameter range for DOE design

Temperature (°C)	200 – 400
Holding time (min)	30 – 270
Air injection (ml/min)	50 – 250

**Table 3.4.** Design of experiments

<b>Run</b>	<b>Temperature (°C)</b>	<b>Holding time (min)</b>	<b>Air flowrate (ml/min)</b>
1	200	30	50
2	400	30	50
3	200	270	50
4	400	270	50
5	200	30	250
6	400	30	250
7	200	270	250
8	400	270	250
9	250	150	150
10	350	150	150
11	300	90	150
12	300	210	150
13	300	150	100
14	300	150	200
15	300	150	150
16	300	150	150
17	300	150	150
18	300	150	150
19	300	150	150
20	300	150	150

### **3.5. Synthetic NH<sub>3</sub>-N solution preparation**

The synthetic wastewater for NH<sub>3</sub>-N was prepared based on the measured averaged value of NH<sub>3</sub>-N from two actual aquaculture farm wastewater (Air Kuning) Kampar (4°13'25.3"N, 101°09'02.4"E), and Kampar (4°18'58.2"N, 101°05'27.8"E), Perak. Between the two farms the one having the higher concentration of NH<sub>3</sub>-N was chosen. The initial concentration of 10 ppm NH<sub>3</sub>-N was prepared by dissolving 0.0472 g the ammonium sulfate ((NH<sub>4</sub>)<sub>2</sub>SO<sub>4</sub>) in 1L of distilled water.

### 3.6. Collection and characterization of actual AQW

For collection of AQW sample, a commercial hyphen fishpond in Air Kunning, Kampar ( $4^{\circ}13'25.3''\text{N}$ ,  $101^{\circ}09'02.4''\text{E}$ ), Perak, Malaysia was chosen in this study. Also, the concentration of the pond changes and it mostly depends on the weather (rainy or dry season). In rainy season the concentration reduces. The pond produced approximately 16.67 metric tonnes of wastewater and the discharge after 3-4 months of harvesting into the river. Currently, there is no treatment for the wastewater in the fish farm and directly discharge to the river. Three different samples from the same pond were taken at various locations as shown in the **Figure 3.2** and combined as a mixed sample. **Table 3.5** shows the parameters measured and its methods.



**Figure 3.3.** Sampling of AQW from fishpond

**Table 3.5.** AQW parameters and its measurement methods

<b>Parameters</b>	<b>Measurement methods</b>
<b>pH</b>	Multimeter (HQd30, Hach)
<b>Salinity</b>	Multimeter (HQd30, Hach)
<b>DO</b>	Multimeter (HQd30, Hach)
<b>NH<sub>3</sub>-N</b>	Salicylate Method (Test 'N Tube™ Vials, 0.4 – 50.0 ppm NH <sub>3</sub> -N (HR), Hach method 10031)
<b>PO<sub>4</sub><sup>3-</sup>-P</b>	Ascorbic acid method (TNT plus 845, Hach method 10209/10210)
<b>Total phosphorus (TP)</b>	Ascorbic acid method (TNT plus 845, Hach method 10209/10210)
<b>NO<sub>3</sub><sup>-</sup>-N</b>	Cadmium reduction method (Reagent powder pillows, NitraVer ®5)
<b>NO<sub>2</sub>-N</b>	Ferrous sulfate (reagent powder pillows, NitriVer®2)
<b>COD</b>	Digestion method (COD HR vial 20 – 1500 ppm)
<b>Turbidity</b>	Turbidity meter (HI 98703, Hanna instrument USA)

### 3.7. NH<sub>3</sub>-N adsorption

For both synthetic and actual AQW, the concentration of NH<sub>3</sub>-N was determined by Salicylate Method using a vis spectrometer. The adsorption efficiency/capacity of NH<sub>3</sub>-N was measured by following equations:

$$\text{Adsorption efficiency (\%)} = \frac{C_i - C_f}{C_i} \times 100 \quad (3.1)$$

$$\text{Adsorption capacity (mg/g)} = \frac{C_i - C_f}{W} \times V \quad (3.2)$$

Where  $C_i$  and  $C_f$  is the initial and final concentrations (ppm) of the solution respectively.  $V$  is the volume of the solution in liters (L), and  $W$  is the mass (g) of adsorbent used.

For the preliminary adsorption study, 200 ml of  $10.0 \pm 1$  ppm of synthetic  $\text{NH}_3\text{-N}$  was tested using 1.0 g of biochar. The solution was shaken at 150 rpm, for 90 min at RT. For actual AQW, 200 ml of the wastewater was used for each run in the process parameter study. All the experimental work was repeated twice for accuracy and an averaged data was reported.

### **3.7.1. Process study**

The identified optimized adsorbent was further used for adsorption process study of actual AQW. This was carried out by changing, one parameter at a time, while holding the others fixed. The following are the evaluated parameters: temperature ( $25\text{ }^\circ\text{C} - 40\text{ }^\circ\text{C}$ ), contact time (15 – 240 min), shaking speed (50 rpm – 250 rpm), pH (3 – 11), and dosage (0.5 – 4 g) using 200 ml of actual AQW.

### 3.7.2. Adsorption kinetics, isotherms, and thermodynamics study

The measurement of adsorption isotherm was done by using different dosage of the OPF biochar. The results were fitted to Freundlich and Langmuir isotherms models. The Freundlich and Langmuir isotherms assume heterogeneous adsorptive energies on the adsorbent surface and homogeneous monolayer surface sorption, respectively (Goh *et al.*, 2019). Equation 3.3 and 3.4 are Langmuir, while equation 3.5 and 3.6 are Freundlich, which are non-Linear and Linear isotherm models, respectively (Tran *et al.*, 2017).

$$q_e = \frac{Q_{max}^0 K_L C_e}{1 + K_L C_e} \quad (3.3)$$

$$\frac{1}{q_e} = \left( \frac{1}{Q_{max}^0 K_L} \right) \frac{1}{C_e} + \frac{1}{Q_{max}^0} \quad (3.4)$$

$$q_e = K_F C_e^n \quad (3.5)$$

$$\log q_e = n \log C_e + \log K_F \quad (3.6)$$

Where  $q_e$  (mg/g) is the amount uptake at equilibrium,  $C_e$  (ppm) is the equilibrium concentration of the adsorbate,  $Q_{max}^0$  (mg/g) is the maximum saturated monolayer adsorption capacity of an adsorbent, and  $K_L$  (L/mg) is the constant related to the affinity between the adsorbent and adsorbate,  $K_F$  is the Freundlich constant, and  $n$  (dimensionless) is the Freundlich intensity



parameter and shows the magnitude of the adsorption driving force or surface heterogeneity. If  $n = 0$  the process is irreversible, Linear if  $n = 1$ , unfavorable if  $n > 1$ , favorable if  $n < 1$ . An intercept of  $1/Q_{\max}^0$  and a straight line with a slope of  $(1/Q_{\max}^0 K_L)$  is obtained when  $1/q_e$  is plotted against  $1/C_e$ . Hall separation factor was used for the adsorption favorability, where  $R_L$  is dimensionless, favorable if  $0 < R_L < 1$ , If  $R_L = 0$  the process is irreversible, Linear if  $R_L = 1$  and unfavorable if  $R_L > 1$  (Hall *et al.*, 1966).

The kinetic models of pseudo first order (PFO) and pseudo second order (PSO) were used for the analysis of adsorption kinetics. The experimental findings, from various contact times, were applied to the models. The following equations represent the non-Linear and Linear PFO model, respectively, (Tran *et al.*, 2017).

$$q_t = q_e(1 - e^{-k_1 t}) \quad (3.7)$$

$$\ln(q_e - q_t) = -k_1 t + \ln(q_e) \quad (3.8)$$

Where  $k_1$  is the rate constant (1/min), and  $q_t$  and  $q_e$  of the amount of adsorbate uptake at per mass of adsorbent at time  $t$  and at equilibrium of PFO equation. The PSO kinetic model is significantly influenced by the amount of adsorbate on the adsorbent surface and the equilibrium amount adsorbed. The rate is proportional to the number of the active sites on the adsorbent

surface. The following equation represent the non-Linear and Linear model of PSO (Tran *et al.*, 2017).

$$q_t = \frac{q_e^2 k_2 t}{1 + k_2 q_e t} \quad (3.9)$$

$$\frac{t}{q_t} = \left(\frac{1}{q_e}\right)t + \frac{1}{k_2 q_e^2} \quad (3.10)$$

Where  $k_2$  is the PSO adsorption rate constant (g/mg min).

The linearized intra-particle diffusion model is stated as (Weber and Morris, 1963):

$$q_t = k_p \sqrt{t} + C \quad (3.11)$$

Where  $k_p$  ( $\text{mg/g} \times \text{min}^{1/2}$ ) is the rate constant and  $C$  ( $\text{mg/g}$ ) is the constant related to boundary layer thickness, a higher value of  $C$  is related to a higher value in the limiting boundary layer. However, from the intra-particle diffusion model, the initial adsorption behavior ( $R_i$ ) was measured. If  $R_i = 1$  shows no initial adsorption behavior, weakly initial adsorption behavior if  $1 > R_i > 0.9$ , intermediately initial adsorption when  $0.9 > R_i > 0.5$ , the value of  $R_i$  at  $0.5 > R_i > 0.1$  shows strong initial adsorption, if  $R < 0.1$  shows approaching completely initial adsorption (Wu, Tseng and Juang, 2009).

For the investigation of thermodynamics parameters, at various temperatures (25 °C – 40 °C) the OPF biochar was shaken while holding the other process condition fixed. The Gibbs free energy was calculated from the following equation (Tran *et al.*, 2017).

$$\Delta G^\circ = -RT \ln K_C \quad (3.12)$$

The relationship between the  $\Delta G^\circ$ ,  $\Delta H^\circ$ , and  $\Delta S^\circ$  is describe as follow:

$$\Delta G^\circ = \Delta H^\circ - T\Delta S^\circ \quad (3.13)$$

$$\ln K_C = -\frac{\Delta H^\circ}{R} \times \frac{1}{T} + \frac{\Delta S^\circ}{R} \quad (3.14)$$

Where  $\Delta G^\circ$  is the standard free energy change for ion exchange (J/mol), T is the absolute temperature (K), and R is the universal gas constant (8.314 J/mol K),  $K_C$  is the equilibrium constant, and must be dimensionless (Zhou, 2017),  $\Delta H^\circ$  represents the enthalpy, while  $\Delta S^\circ$  indicates the entropy (J/mol K). From the Linear plot of  $\ln K_C$  and  $1/T$ , the slope and intercept were used for measuring the value of  $\Delta H^\circ$ , and  $\Delta S^\circ$ .

### 3.8. Characterization

Different adsorbent samples having the lowest and the highest adsorption were characterized via various techniques to justify the results.

These methods include Attenuated Total Reflectance (ATR), Field Emission Scanning Electron Microscope (FESEM), Energy Dispersion X-ray (EDX), Brunauer-Emmett-Teller (BET), Cation Exchange Capacity (CEC), Point Zero Charge (pHzc), Zeta potential, and Thermogravimetric analysis (TGA). Brief description of each technique is given below.

### **3.8.1. Attenuated Total Reflectance (ATR-FTIR)**

ATR is popular sampling technique for Fourier transform infrared (FTIR) spectroscopy. ATR-FTIR easily and quickly examines a wide range of sample types such as, solids, semisolids, powders, liquids, and pastes. The ATR-FTIR is used to investigate the information about functional groups of the samples. This method of spectroscopy is mostly used to produce qualitative analysis of a sample, and from the peaks, we can determine the functional groups of the material. ATR-FTIR machine measures the infrared frequencies in a very short period. In this study, the ATR-IR was conducted on the machine Perkin Elmer ATR-IR spectrum 2. The crystal of the ATR-FTIR was cleaned and the sample was placed directly on the plate in order to cover the crystal. The arm is then lock to the position over the crystal and turned clockwise until the metal tip is close to the plate. Click on the scan, for acquiring the preview of spectrum and pressure gauge. To obtain a uniform disc of the sample, handle is continuously twisted until the force gauge reads between 60 – 80. Click on the scan to get the final spectrum and then further analyzed the spectrum.

### **3.8.2. Field Emission Electron Microscopy (FESEM)**

To investigate the surface morphology of the adsorbent samples, FESEM was performed using the machine model JEOL JSM-6701F. A small quantity of the sample was pasted onto the sample plates and then coated with the beam very finer layer of gold metal for 60 seconds to avoid charging during the electron emissions. The sample was placed in high vacuum environment to develop a good quality of image scanning. The images of the FESEM image of the adsorbents were observed at different magnification such as 350X, 500X, 1000X, and 2000X.

### **3.8.3. Energy Dispersion X-ray (EDX)**

The EDX detector installed with the FESEM apparatus determines the presence of elements on the surface of the material. The sample preparation is similar to that of the FESEM, and the examination can be performed on the FESEM machine.

### **3.8.4. Brunauer-Emmett-Teller (BET)**

The pore properties of the adsorbent, such as specific surface area, pore volume, and pore size distribution were determine using by Quantachrome Instruments ASIC by nitrogen adsorption-desorption isotherms. Before the BET analysis the samples were degassed first at 110 °C for 5 hr on the sample of 0.5 g inside the analysis tube, to remove the

unwanted pre-adsorbed matter on the sample surface. After the degassing process, the sample was put in liquid nitrogen at 77 K. The software that was attached to the analyzer automatically collected the data for the nitrogen adsorption and desorption process. Further, the BET equation was used to determine the specific surface area from the adsorption isotherm.

### 3.8.5. Cation Exchange Capacity (CEC)

To determine the cation exchange capacity (CEC) of the samples, a similar protocol from AOAC method 973.09 was used (Rippy and Nelson, 2007; Huff and Lee, 2016). Briefly, 0.5 g of the samples were taken and was placed in 100 ml of conical flask with the addition of 50 ml of 0.5M HCl. The samples were shaken for 2 hr at 120 rpm. The mixture was filtered and rinsed through Whatman cellulose filter paper with a 100 ml portion of New Human Up 900 deionized water until no sign of precipitation was observed by adding few drops of dilute (0.028M) AgNO<sub>3</sub>. The washed samples with the filter paper were added to 50 mL of with 0.5M Ba(OAc)<sub>2</sub> solution. After then, the samples were shaken for another 2 hr, filtered, and washed New Human Up 900 deionized water. The sample residue was thrown away and the filtrate were titrated with 0.025 M NaOH solution until the pink color appeared as phenolphthalein is used an indicator. Each test was repeated twice. The CEC was measured using the following equation:

$$\frac{\text{cmol}}{\text{Kg biochar}} = \frac{\text{ml} \times \text{molarity of NaOH} \times 100}{\text{gram sample}} \quad (3.15)$$

### **3.8.6. Point Zero charge (PHzc) and Zeta Potential**

The pH drift technique was used for the determination of the point zero charge ( $pH_{PZC}$ ) of the biochar samples. 0.1M NaCl solution (50 ml) was added to a 100 ml conical flask. The solution initial pH ( $pH_i$ ) was adjusted between 3 and 11 by addition of 0.1M HCl or NaOH. After fixing the pH, 0.2 g of biochar was put into the flask and shaken it at room temperature for 24 hr. The solution was filtered after 24 hr using Whatman filter paper, and the final pH ( $pH_f$ ) of the filtrate was determined using pH meter (PHC201, Hach). The difference between the initial and final pH values ( $\Delta pH = pH_i - pH_f$ ) were plotted against  $pH_i$ . The pH at which the  $\Delta pH = 0$  is a pH value at the point of zero charge (Hafshejani *et al.*, 2016). The zeta potential was measured using Litesizer™ 500, (Anton Paar, Austria) using the same pH range.

### **3.8.7. Thermogravimetric analysis (TGA)**

Proximate analysis of the adsorbent samples was determined using TGA analyzer (Mettler Toledo, USA). The adsorbent sample was kept in the presence of nitrogen and the temperature was increased at a rate of 20 °C/min to 110 °C and kept constant at 110 °C for 6 min to measure the water content in the sample. Then the temperature was raised to 900 °C at a heating rate of 20 °C/min and kept constant for 10 min at 900 °C to calculate the volatile matter content of the sample. At 900 °C air was injected for 25 min to

determine the fixed carbon content of the sample (Min, Ahmad and Lee, 2017).

### **3.8.8. Ultimate analysis**

The ultimate analysis of the adsorbent was performed using an elemental CHN analyzer (LECO CHN628S, USA). This examination determined the percentage of carbon, nitrogen, and hydrogen in the adsorbent. The technique used in the ultimate analysis to determine the composition of combustion element is pyrolyzed a sample of 100 mg at 950 °C with excess oxygen in a helium atmosphere. The test is referred to ASTM D5291 standard, and this is one of the best quantitative measurements of elemental composition.

### **3.9. Cost analysis**

Economic analysis of the biochar is necessary to evaluate the cost benefit of the current research project. The cost calculation was done based on the production of 1000 kg biochar/day, 320 days/year of production, two men per shift (3 shifts) for 24 hr/day at RM 18/hr. The respective power of the machines was converted into kilowatt-hour (kWh) unit, as given in **Equation 3.16**, and electricity prices are taken form Tenaga National, Malaysia for commercial consumers which is 0.38/kWh (Tenaga, 2022).



$$\begin{aligned} \text{Cost per kg} &= \text{time (hr)} \times \text{electricity consumption of device (kW)} \\ &\times \text{electricity cost per kWh} \end{aligned} \quad (3.16)$$

The total fixed capital investment was calculated by the summation of the total equipment cost and the total capital cost. The annual operating cost and capital cost, shown in **Table 3.6**, are based on the percentage given by Peters and Timmerhaus, (1991).

**Table 3.6.** Estimated cost measurement method for pilot plant based on the percentage in Peters and Timmerhaus, (1991).

<b>Services</b>	<b>Cost measurement</b>
Equipment installation	25 % of purchased equipment
Instrumentation	6 % of purchased equipment
Piping and material transport	80 % of purchased equipment
Electrical installation	10 % of purchased equipment
Building	12 % of fixed capital investment
Yard improvement	10 % of purchased equipment
Service facility	30 % of purchased equipment
Land	8 % of purchased equipment
Engineering and supervision	30 % of purchased equipment
Construction expenses	1.5 % of fixed capital investment
Contractor fee	1.5 % of fixed capital investment
Contingency	5 % of purchased equipment
Maintenance labor	15 % of operating labor
Supervision	15 % of operating labor
Fringe and benefits	16 % of operating labor
Maintenance supplies	2 % of purchased equipment
Operating supplies	15 % of Maintenance supplies
General and administrative	2 % of operating labor
Property insurance and tax	20 % fixed capital investment
Depreciation	3 % of building + 10 % purchased equipment

The annual production and cost of biochar was calculated from equation 3.17 and 3.18 respectively.

$$Annual\ production = \frac{biochar\ (kg)}{day} \times \frac{320\ days}{year} \quad (3.17)$$

$$Cost \left( \frac{\text{per}}{\text{kg}} \right) = \frac{\text{Total operating cost (RM)}}{\text{Total annual biochar production (kg)}} \quad (3.18)$$

Malaysia produces large quantity of OPF as a waste from palm industry, so the raw material was provided free of cost. The pilot scale plant for biochar was designed based on laboratory work. First the OPF was received from the palm oil company and stored for further used. In laboratory scale, the OPF was cut into smaller particle so in the pilot plant a shredder is needed covert the OPF to smaller size. Further, in our work the vertical carbonization unit has been used for the conversion of OPF into biochar however for bigger scale a horizontal rotary kiln is necessary for biochar production. The constant rotation of the rotary kiln will provide a constant homogenize heat to all the OPF particles. In laboratory scale the biochar cool down easily while having large amount of biochar in pilot scale a rotary cooler is essential for the cooling process as the process is continuous. After cooling process, the biochar is directly stored and then packages. All the prices of the equipment's were taken from the Alibaba online website (Alibaba, 2022).

## CHAPTER 4

### RESULTS AND DISCUSSION

#### 4.1. Preliminary carbonization

Biochar was prepared by injecting of two different types of gases *i.e.* N<sub>2</sub> and air. Various temperatures have been evaluated keeping the holding time constant and testing the removal capacity and efficiency of NH<sub>3</sub>-N removal. After the carbonization process, the optimized OPF biochar was physically and chemically activated and further tested for NH<sub>3</sub>-N adsorption.

##### 4.1.1. N<sub>2</sub> and air carbonization of OPF

In N<sub>2</sub> and air injection, the prepared biochar was tested for the removal of NH<sub>3</sub>-N as given in **Figure 4.1**. At a holding time of 1 hr, and 300 ml/min injection of N<sub>2</sub>, when the pyrolysis temperature was increased from 200 °C to 350 °C the adsorption efficiency increased from 4.4 % to 48.4 %. The adsorption efficiency decreases further increase in temperature and reach to 5.3 % at 500 °C. However, in the case of air injection, the highest adsorption efficiency of 65.8 % was noticed at 300 °C. Further increase in carbonization temperature decreases the performance. The higher adsorption efficiency in injection of air is expected due to the addition of oxygen functional groups. The best performance was noticed at 300 °C, 1 hr, 100 ml

air/min. The decrease in the adsorption efficiency at high pyrolysis temperature is caused by the loss of oxygen functional groups (Gai *et al.*, 2014). Because at higher pyrolysis temperature, the loss of volatile matter diminishes the oxygen functional groups which decrease the negative surface charge on the carbon surface and hence decrease the NH<sub>3</sub>-N removal. Next, activation was tried to further improve the performance of the adsorption.

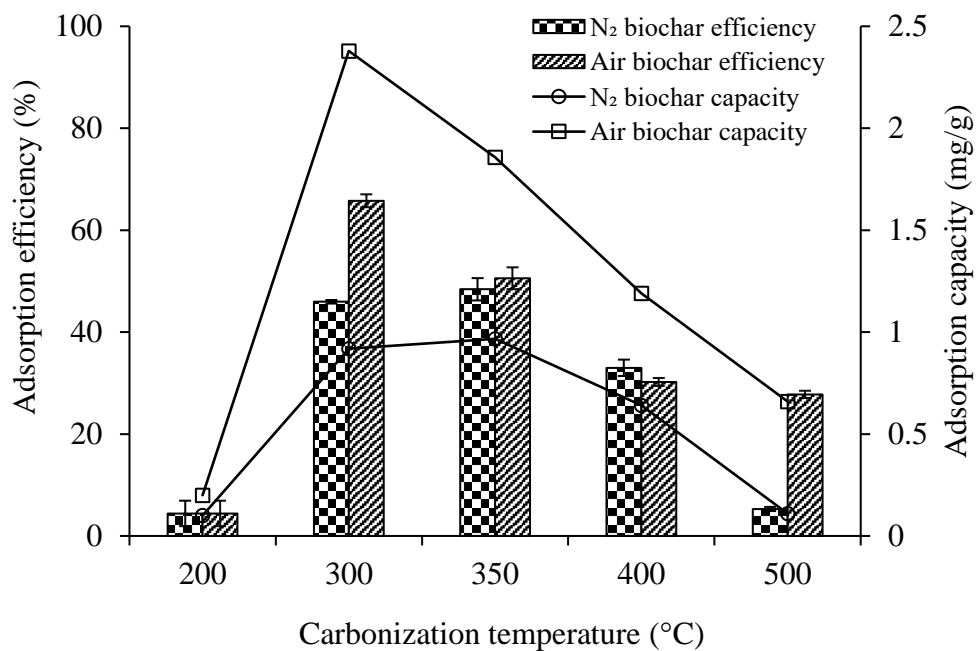


**Figure 4.1:** Adsorption efficiency/capacity of NH<sub>3</sub>-N (10 ppm) onto carbonized biochar

#### 4.1.2. Activation of carbonized OPF

The biochar prepared at 300 °C, 1 hr, 100 ml air/min from the above section was further physically activated with the injection of CO<sub>2</sub> (300 ml/min) at 300 °C at different activation times. This method is chosen for

physical activation because CO<sub>2</sub> activation could improve the BET surface area and porosity of the sorbents (Iberahim *et al.*, 2022). The adsorption efficiency/capacity of NH<sub>3</sub>-N onto activated carbon is shown in **Figure 4.2**.

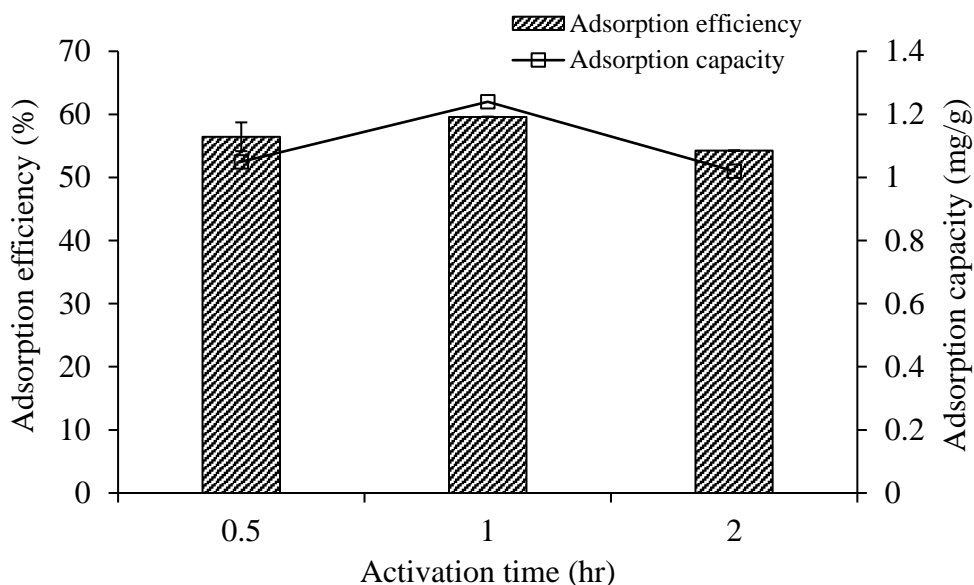


**Figure 4.2:** Adsorption efficiency/capacity of NH<sub>3</sub>-N (10 ppm) onto CO<sub>2</sub> activated biochar

The adsorption efficiency of activated biochar decreases from 59.6 % to 54.3 % when the activation time was increase from 0.5 hr to 2 hr. The physical activation process did not improve the adsorption efficiency of air carbonized biochar. Because during physical activation, the injection of CO<sub>2</sub> burn off the biochar sample at higher holding time which decreases the oxygen functional groups and hence reduced the adsorption efficiency. Also, in our study it has been found that oxygen functional groups play an important role in NH<sub>3</sub>-N adsorption. Next, the best biochar prepared at 300 °C, 1 hr, 100 ml air/min was activated using chemical activation with various types of oxidation agents. The performance of chemically activated biochar and its adsorption efficiency/capacity are given in **Figure 4.3**. In the oxidized

samples, only BC-HNO<sub>3</sub> represents the highest adsorption efficiency of 41 % but still lower compared to biochar (65.8 %). The remaining modified sample exhibits leaching. Form these results, it can be concluded that in this study the adsorption efficiency of the NH<sub>3</sub>-N did not improve even by applying various oxidizing agents.

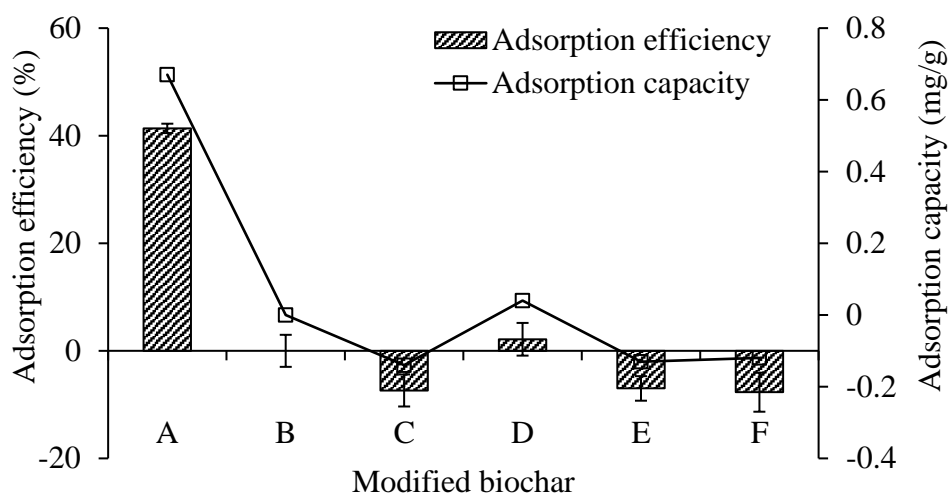


**Figure 4.3:** NH<sub>3</sub>-N (10 ppm) adsorption efficiency/capacity onto modified biochar. (A = BC-HNO<sub>3</sub>, B = BC-CH<sub>3</sub>COOH, C = BC-HCl, D = BC-H<sub>2</sub>O<sub>2</sub>, E = BC-H<sub>2</sub>SO<sub>4</sub>, F = BC-H<sub>3</sub>PO<sub>4</sub>)

Activation temperature (50, 80, 100, and 150 °C) effect was also evaluated to confirm that chemical activation did not improve the adsorption properties of the biochar prepared by keeping HNO<sub>3</sub> concentration (1M) and activation time 2 hr constant. **Figure 4.4** represents the adsorption efficiency/capacity of NH<sub>3</sub>-N onto activated biochar. HNO<sub>3</sub> activation reduced the adsorption efficiency of NH<sub>3</sub>-N. Also, at activation temperature 50 °C, the biochar shows leaching however at 80 °C and 100 °C the biochar

shows positive results of 24 % and 41 % removal efficiency of NH<sub>3</sub>-N respectively. Overall, the efficiency has not shown any increment.

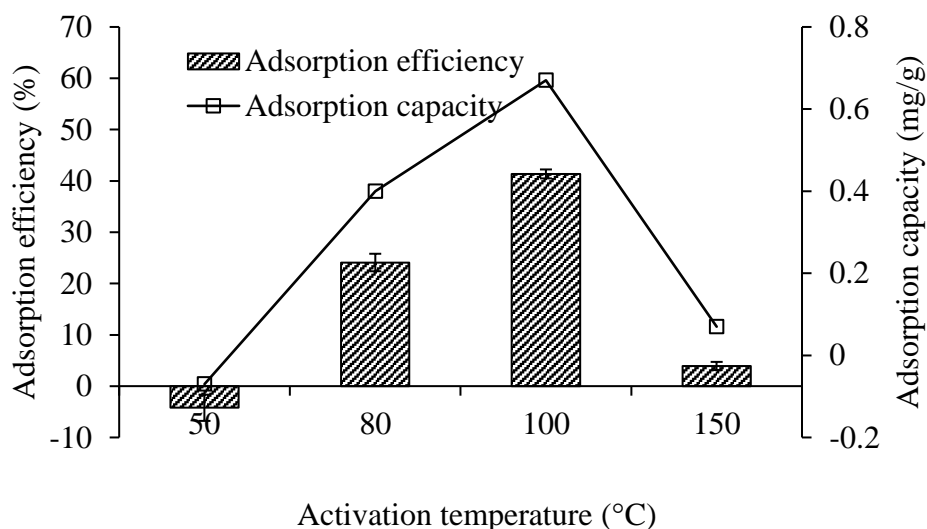


**Figure 4.4:** NH<sub>3</sub>-N (10 ppm) adsorption efficiency/capacity on HNO<sub>3</sub> activated biochar at different temperature

In addition to this, the effect of HNO<sub>3</sub> concentration was evaluated on the activation of biochar (300 °C, 1 hr, 100 ml air/min) keeping temperature (100 °C), and time (2 hr) constant. As the molarity of HNO<sub>3</sub> is increased from 0.1 to 1 M, the adsorption capacity of activated biochar increases from 7 % to 41 % as given in **Figure 4.5**. Further increase in HNO<sub>3</sub> concentration *i.e.* 2 M dissolved the biochar in the solution. Thus, only up to 1M can be tested. Although HNO<sub>3</sub> is a very high oxidizing agent, it did not enhance the adsorption efficiency of NH<sub>3</sub>-N as the final pH of the



solution (after adsorption test) was acidic (around 4) which cause the competitive adsorption between  $\text{NH}_4^+$  and  $\text{H}^+$ .

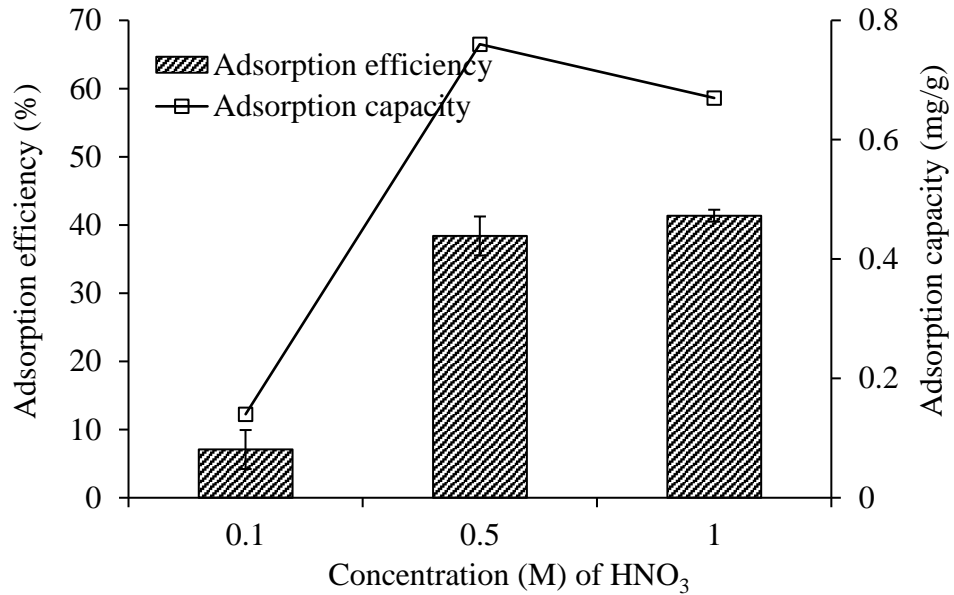


**Figure 4.5:**  $\text{NH}_3\text{-N}$  (10 ppm) removal efficiency/capacity onto  $\text{HNO}_3$  modified biochar at different molarity

Based on the preliminary results presented above, it can be concluded that the performance of carbonized OPF biochar did not improve with any type of activation for the removal of  $\text{NH}_3\text{-N}$ . It is expected that during chemical activation the value-added metals such as Mg, K, and Ca have been completely removed from the sorbent. Same goes to other metals such as Cu and Zn as shown in **Table 4.1**. Value-added metal could help in adsorption of  $\text{NH}_3\text{-N}$  via the ion exchange process (Yu *et al.*, 2016). In addition to this, the functional groups of the activated biochar did not improve using chemical activation, as shown in **Figure 4.6**. Moreover, adsorbent treated with acid washing reduces the common and useful active surface functional groups such as C=O, C=C, and -OH (Gai *et al.*, 2014). Nonetheless, the functional

group (C=O) drastically enhanced in BC-HNO<sub>3</sub>, which is responsible for NH<sub>3</sub>-N adsorption (Ibrahim *et al.*, 2021). However, the biochar produce in the presence of air which contains limited oxygen. The oxygen enriched the oxygen functional groups such as carboxyl and carbonyl which play a key role in the adsorption of NH<sub>3</sub>-N.

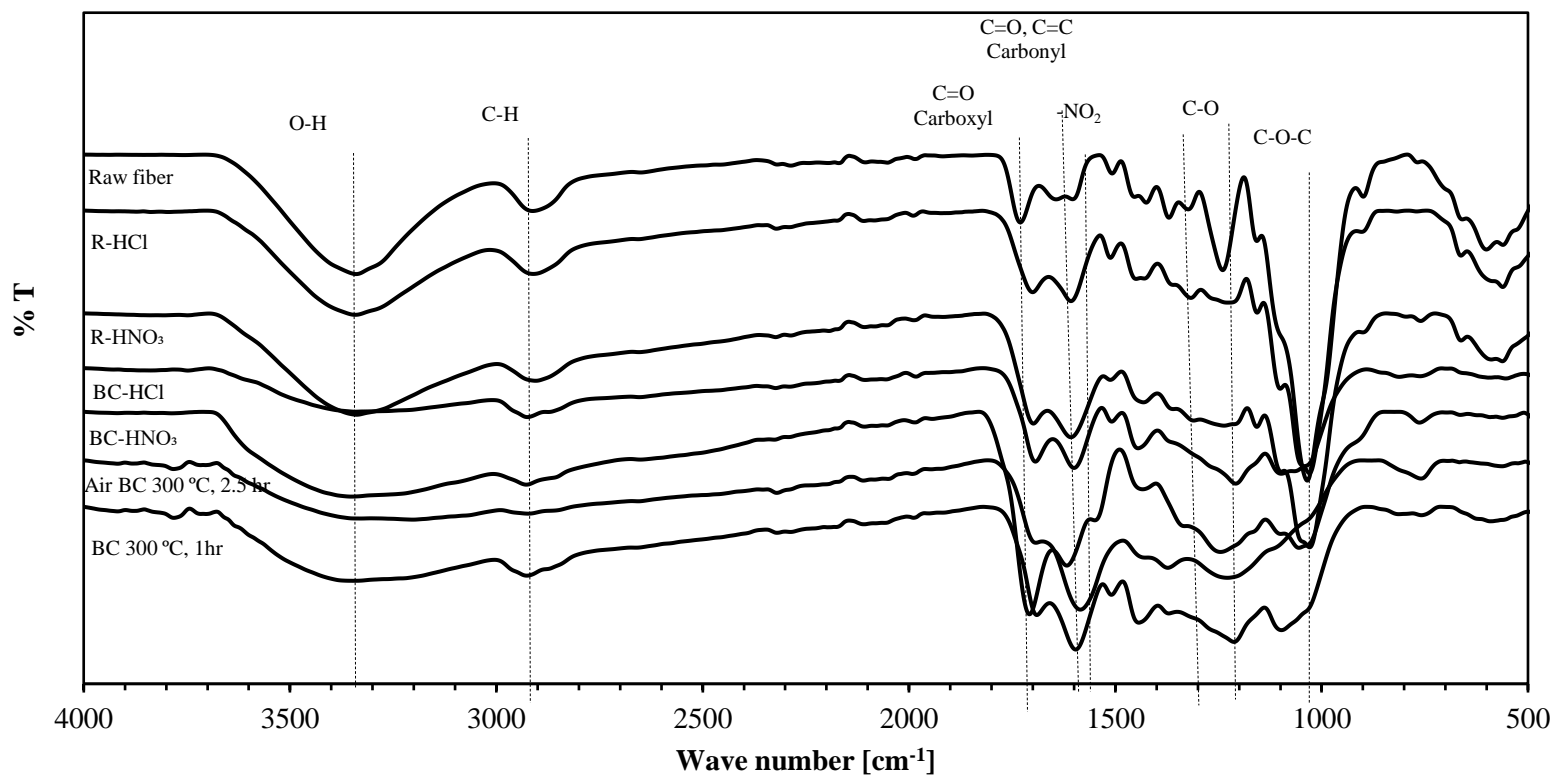


**Figure 4.6:** ATR-IR results of adsorbent samples

**Table 4.1:** EDX elemental analysis of the adsorbent samples

<b>Elements</b>	<b>OPF biochar</b>	<b>BC-HNO<sub>3</sub> (% weight)</b>	<b>BC-HCl (% weight)</b>
C	75.30	73.25	76.56
O	23.57	26.19	22.88
Mg	0.04	-	-
Al	0.05	0.04	0.03
K	0.24	-	-
Ca	0.06	-	-
Cu	0.51	0.25	0.25
Zn	0.36	0.18	0.20
Si	0.05	0.09	0.07

In this study we did not impregnate the adsorbent with metals, to reduce the cost of making the biochar and not to contaminate the biochar with metals as the spent biochar is expected to be used as soil conditioner or fertilizer in future. Thus, the next step in this research study is to optimize air injection procedure to produce OPF biochar via DOE software (version 13.0).

#### **4.2. Design of experiments for OPF biochar**

Response surface methodology (RSM) based on central composite design (CCD) has been applied in DOE software (version 13.0) for optimization. RSM is used for developing, improving, and optimization of the process using a combination of mathematical and statistical methods. It explains the effect of variables, alone or in combination, on the process. In

addition to this, a standard RSM design using CCD developed a set of consecutive experiments for various independent variables. During analysis, this experimental methodology develops an empirical model (quadratic model) which described the corresponding quantity of the process (Amiri, Shahhosseini and Ghaemi, 2017). However, to develop the 2<sup>nd</sup> order quadratic model, three level factorial design is needed. The factorial design gives more experiments compared to CCD. Therefore, CCD could be used for the optimization of suitable parameters with the minimal number of experiments and for the analysis of the interaction between parameters (Iberahim *et al.*, 2019).

#### **4.2.1. The design**

The preparation of air injection biochar was optimized using Design Expert® software 13.0. Three variables were chosen: air injection (50 – 250 ml/min), holding time (0.5 – 4.5 hr) and pyrolysis temperature (200 – 400 °C). The alpha value was fixed as 0.5. The adsorption efficiency was taken as the response. **Table 4.2** summarizes the experimental design. The design has 20 set of experiments, in which 6 were repeated to confirm the error.

**Table 4.2:** Design of experiments generated from Design-Expert® software

Run	$x_1$ : carbonization temperature (°C)	$x_2$ : holding time (min)	$x_3$ : air injection (ml/min)	$y_1$ : NH <sub>3</sub> -N adsorption efficiency (%)
1	300	150	150	62.5
2	200	30	250	4.69
3	300	150	150	59.24
4	300	150	150	60.33
5	300	150	100	71.56
6	300	150	150	67.39
7	300	150	200	59.6
8	400	270	250	5.56
9	400	270	50	26.77
10	200	270	50	4.55
11	300	150	150	65.76
12	250	150	150	52.6
13	400	30	50	40.4
14	300	90	150	58.15
15	400	30	250	29.82
16	200	30	50	4.69
17	300	210	150	63.64
18	350	150	150	51.63
19	200	270	250	5.21
20	300	150	150	64.67

The results were configured in accordance with the empirical model developed by applying a polynomial equation (second-degree) (Iberahim *et al.*, 2019) as shown in Eq.4.1.

$$y = b_0 + \sum_{i=1}^n b_i x_i + \sum_{i=1}^n b_{ii} x_{ii}^2 + \sum_{i=1}^{n-1} \sum_{j=i+1}^n b_{jj} x_i x_j \quad (4.1)$$

Where y is the predicted response,  $b_0$  is the constant coefficient,  $b_i$  is the linear coefficient,  $b_{ij}$  is the interaction coefficient,  $b_{ii}$  is the quadratic

coefficient, and  $x_i$  to  $x_j$  are the coded values of the variables. The total number of experiments calculated was 20 (calculated from  $= 2^3 + 2k + 6$  where  $k$  is the number of factors).

The results indicates that the adsorption efficiency at carbonization temperature at 300° C is higher compared to 200 °C and 400 °C. Further, increasing the holding time (up to 150 min) increases the adsorption efficiency of NH<sub>3</sub>-N and further decreases. At higher injection rate of air, the biochar burns and have low effects on the removal of NH<sub>3</sub>-N. The highest adsorption efficiency of 71.6 % was achieved for NH<sub>3</sub>-N. After adsorption tests, a regression analysis was performed using a statistical correlation. Analysis of Variance (ANOVA) was used for the determination of significant parameters in the experiments. By relating the response with a significant parameter, the relationship between experimental and predicted results are correlated by ANOVA. The values of F and p indicate the significance of the coefficient. The model becomes significant if the p-value is less than 0.05, and insignificant if it increase 0.1 (Iberahim *et al.*, 2019).

#### **4.2.2. ANOVA analysis**

For the preliminary testing to optimize the best OPF biochar, the adsorption parameters were fixed. The response for the study was the adsorption efficiency of NH<sub>3</sub>-N. **Table 4.3** contains the variance analysis (ANOVA) results. Based on the results, the quadratic model was developed for the response was termed as “significant”. Only taking the significant

terms, the final empirical model in coded factors is stated as an equation (4.2).

**NH<sub>3</sub>N model:**

$$y_1 = +63.40 + 9.76x_1 - 4.09x_2 - 4.37x_3 - 4.78x_1x_2 - 4.06x_1x_3 - 48.14x_1^2 \quad (4.2)$$

In the above equation (4.2),  $x_1$ ,  $x_2$ , and  $x_3$  are used for the input variables of carbonization temperature, holding time, and air injection flow rate, respectively. The term with a positive and negative sign represents its synergistic and antagonistic effect respectively. The probability value (p-value) and Fisher's variance ratio (F-value) has been used for the significance of the derive model. These values indicate how effectively the model explains data variance around its mean value. The terms are "significant" if the F-value is larger, and p-value is <0.05. The model for the response is statistically significant as mentioned in **Table 4.3**. The variable  $x_1$  (carbonization temperature) was the most significant variable compared to others. Moreover, the validity of the empirical model can be verified by the coefficient of determination ( $R^2$  value), adequate precision, coefficient of variation (C.V.%), and standard deviation. The coefficient of determination ( $R^2$ ) of NH<sub>3</sub>-N is 0.9800. This indicates that about 98 % of the regression model is attributed to the studied experimental variables.



**Table 4.3:** ANOVA results for response surface quadratic model for NH<sub>3</sub>-N

	Sum of Squares	df	Mean Square	F-value	p-value
Model	11884.85	6	1980.81	106.10	< 0.0001
$x_1$	809.01	1	809.01	43.33	< 0.0001
$x_2$	142.19	1	142.19	7.62	0.0162
$x_3$	162.02	1	162.02	8.68	0.0114
$x_1x_2$	183.07	1	183.07	9.81	0.0080
$x_1x_3$	131.63	1	131.63	7.05	0.0198
$x_1^2$	10456.93	1	10456.93	560.09	< 0.0001
Residual	242.71	13	18.67		
Lack of Fit	192.11	8	24.01	2.37	0.1781
Pure Error	50.60	5	10.12		
R <sup>2</sup>	0.9800				
Adeq. precision	23.89				
Std. dev	4.32				
Mean	42.94				
C.V.%	10.06				

The model will give a more accurate predicted value that will be closer to the actual if the R<sup>2</sup> value is closer to 1.0 (unity). **Table 4.3** shows that the R<sup>2</sup> value for NH<sub>3</sub>-N is very high, indicating that the experimental and predicted results are very close to each other. The model could be applied to navigate the design space, as the adequate precision ratio is more than 4 (Iberahim *et al.*, 2019). **Figure 4.7** represent the predicted versus actual results for NH<sub>3</sub>-N adsorption. The findings shows that the model agreed well for the NH<sub>3</sub>-N adsorption efficiency as the predicted results are close to the actual values.

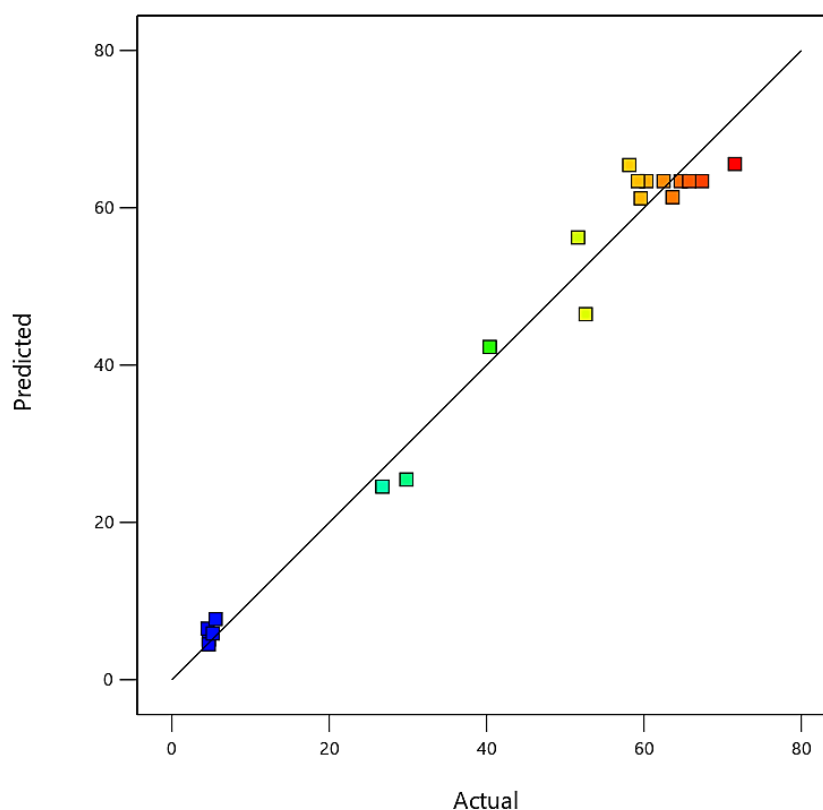


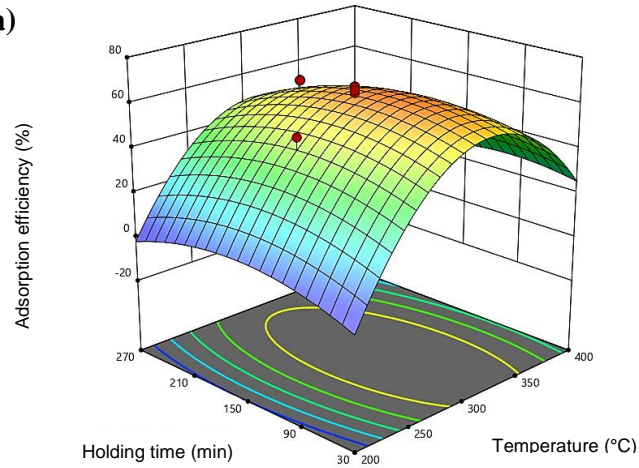
**Figure 4.7:** Predicted versus actual adsorption efficiency of NH<sub>3</sub>-N

#### 4.2.3. Effect of variables on NH<sub>3</sub>-N adsorption

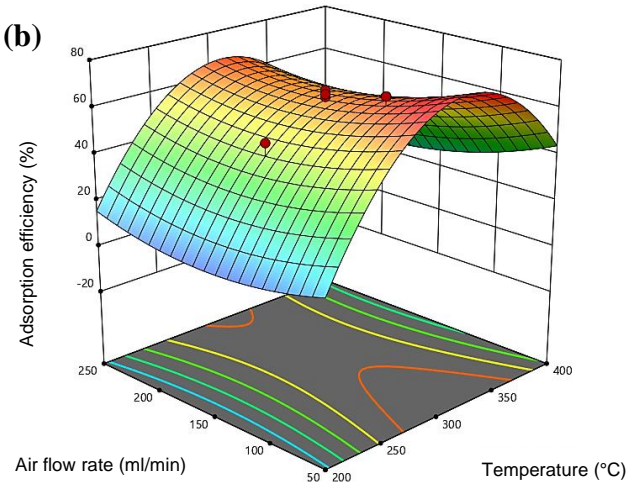
**Figure 4.8** shows the 3-D response surface graph for the input variables of NH<sub>3</sub>-N adsorption. It was noticed when the pyrolysis temperature increases to 300 °C the adsorption efficiency of NH<sub>3</sub>-N increases while decreases at higher temperature such as 350 and 400 °C. The decrease in the efficiency is occur because at higher temperature the biochar loses the oxygen functional group. It has been reported that oxygen functional group has positive correlation with the adsorption of NH<sub>3</sub>-N (Wang *et al.*, 2015). Also, it was found that at 300 °C the holding time of 2.5

hr was the best for the adsorption of  $\text{NH}_3\text{-N}$  and adsorption decreases with increasing the holding time.

(a)



(b)



(c)

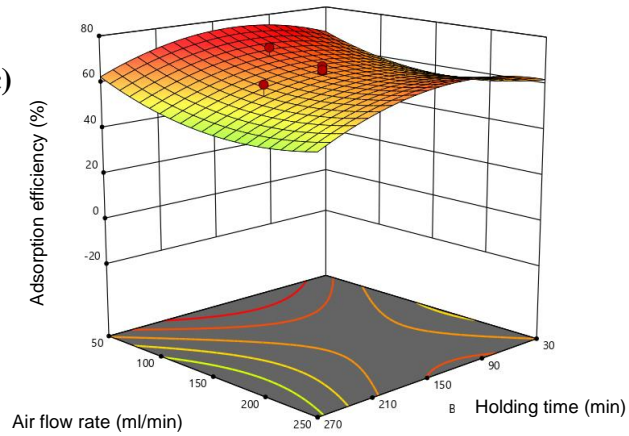


**Figure 4.8:** Response surface plot of (a) pyrolysis temperature versus holding time (b) pyrolysis temperature versus air flow rate, and (c) holding time versus air flow rate for  $\text{NH}_3\text{-N}$  adsorption

Increasing the holding time may cause an increase in quantity of volatile compound resulting in the decrease of negative surface charge at same carbonization temperature (Shaaban *et al.*, 2014). Increasing the air injection flow rate to 100 ml/min increases the adsorption efficiency of the NH<sub>3</sub>-N while decreases at higher injection flow rate at carbonization temperature 300 °C. Increasing the air injection more than 100 ml/min causes increased burn off of the OPF biochar and increased the ash content. Similar result has been found by (Xiao *et al.*, 2018) when increasing the holding time at the same carbonization temperature or keeping holding time constant and increase the temperature. Additionally, the injection flow rate shows the least effect on the adsorption of NH<sub>3</sub>-N. It was also noticed during experimental work that higher holding time and injection of air flow rate burn the biochar sample and convert it into ash. The highest adsorption efficiency and capacity of 71.6 % and 1.6 mg/g for NH<sub>3</sub>-N was observed respectively, at 300 °C, 2.5 hr, and 100 ml air/min and selected as OPF biochar for further studies.

#### **4.2.4. Validation of the model and optimization**

Using the software-developed model, the parameters were optimized to achieve the highest NH<sub>3</sub>-N adsorption efficiency. The solutions were automated by RSM according to set criteria. RSM recommended several solutions. Three (3) best solutions were chosen with the desirability close to unity as shown in **Table 4.4**.

**Table 4.4:** Model Validation of the predicted and experimental results

Temperature (°C)	Holding time (min)	Air flow rate (ml/min)	Desirability	Removal efficiency (%)		Error
				Predicted	Actual	
327.1	171.1	98.8	1	66.5	66.7	0.1
338.4	169.4	70.3	1	69.2	68.9	0.2
330.5	181.7	111.7	1	63.4	67.1	2.6

The biochar samples were prepared, and the experimental results were compared to the model predicted values as illustrated in **Table 4.4**. The actual experimental and predicted adsorption efficiency of  $\text{NH}_3\text{-N}$  were nearly the same, having less than 3 % error. Hence, the model was significant in predicting the removal efficiency of  $\text{NH}_3\text{-N}$ .

### 4.3. Effect of initial concentration of $\text{NH}_3\text{-N}$

The initial concentration of  $\text{NH}_3\text{-N}$  was investigated on the OPF biochar at a range of 5 – 20 ppm while the dosage (1 g), temperature (25 °C), and contact time (90 min), was kept constant. The removing efficiency of the  $\text{NH}_3\text{-N}$  decreases from 79.8 % to 61.5 % when the initial concentration of the solution was increased from 5 to 20 ppm as mentioned in **Figure 4.9**.

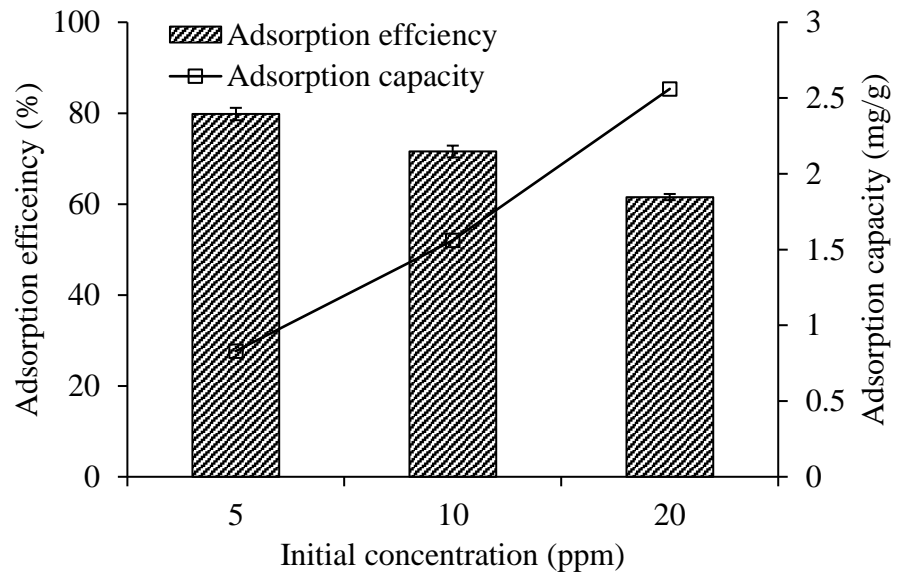


**Figure 4.9:** Effect of initial concentration of solution on adsorption efficiency of OPF biochar for  $\text{NH}_3\text{-N}$  recovery

At low concentration, the adsorption of  $\text{NH}_3\text{-N}$  occurs faster because of higher availability of the adsorbent site on the adsorbent surface and improve the adsorption efficiency. While at high concentration, the exterior surface of the adsorbent rapidly saturated by adsorbate molecules and hence, reduce the adsorption efficiency. Furthermore, due to the contact and collision between the adsorbent and adsorbate the adsorption capacity increases at higher initial concentration (Godini et al., 2017).

#### **4.4. Characterization of OPF biochar**

The characterization of the raw fiber, OPF biochar and spent OPF biochar discussed here. FESEM analysis was conducted to observe the morphologies of the raw fiber and the OPF biochar. **Figure 4.10** represents the raw fiber structure at different magnifications. The FESEM results show that the raw fiber structure is smooth, and non-porous structure. However, some pore can be seen in **Figure 4.10** it might be occur because of cutting the OPF as the pore looks open on both side and is difficult to contribute to the adsorption process.



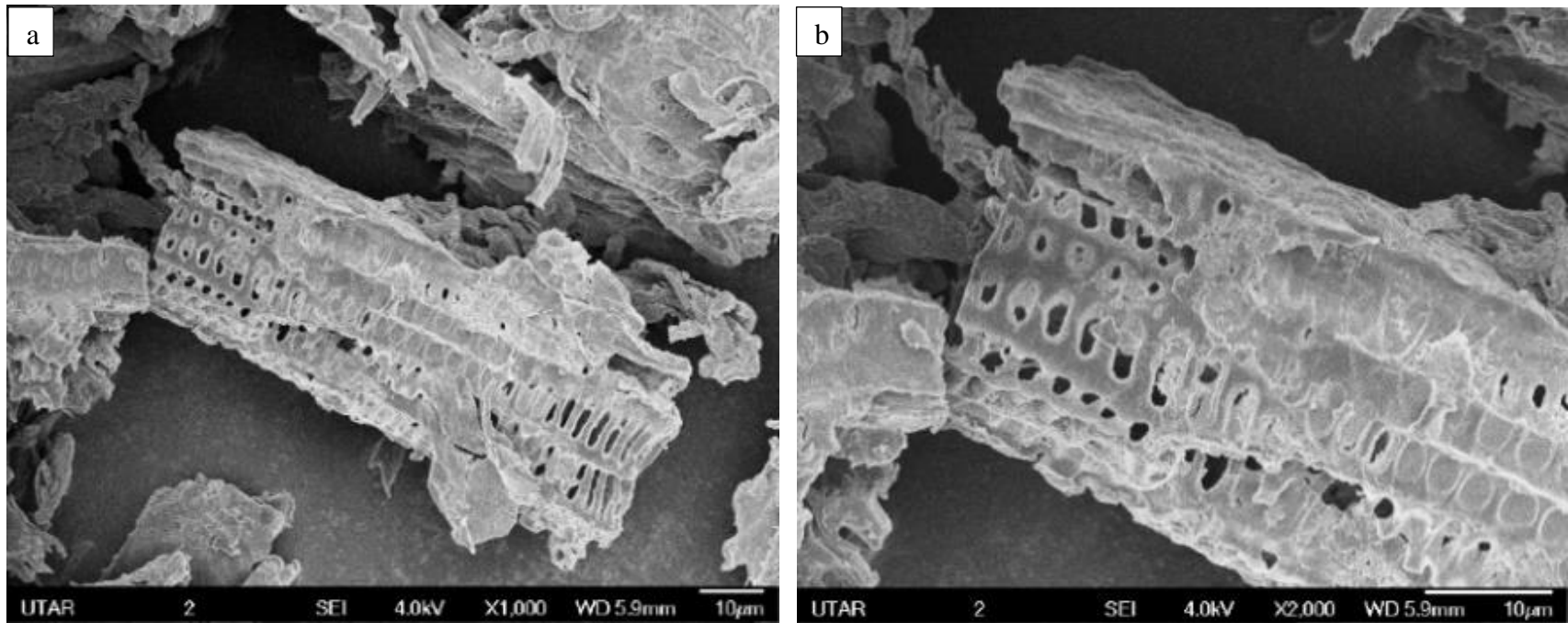


**Figure 4.10:** FESEM image of raw fiber at different magnification (a) 1000X, and (b) 2000X

The OPF biochar structure is well developed honeycomb like porous structure as given in **Figure 4.11**. The outer surface of the biochar is smooth and have no pore while the inner surface is porous and evenly distributed. The pores are formed as a result of the volatilization, destruction, and deformation of the lignocellulose structure of biomass when carbonized at high temperature. These pores structures are useful for liquid-solid adsorption and could enhance the recovery of adsorbate molecule (Shaaban *et al.*, 2014). The adsorbate molecule is expected to diffuse onto the adsorbent's upper surface, then into the pores, and finally attach (Min, Ahmad and Lee, 2017).

After adsorption of  $\text{NH}_3\text{-N}$ , the spent OPF biochar has a similar structure and no changes have been observed in the morphology, as shown in **Figure 4.12** compared to OPF biochar.

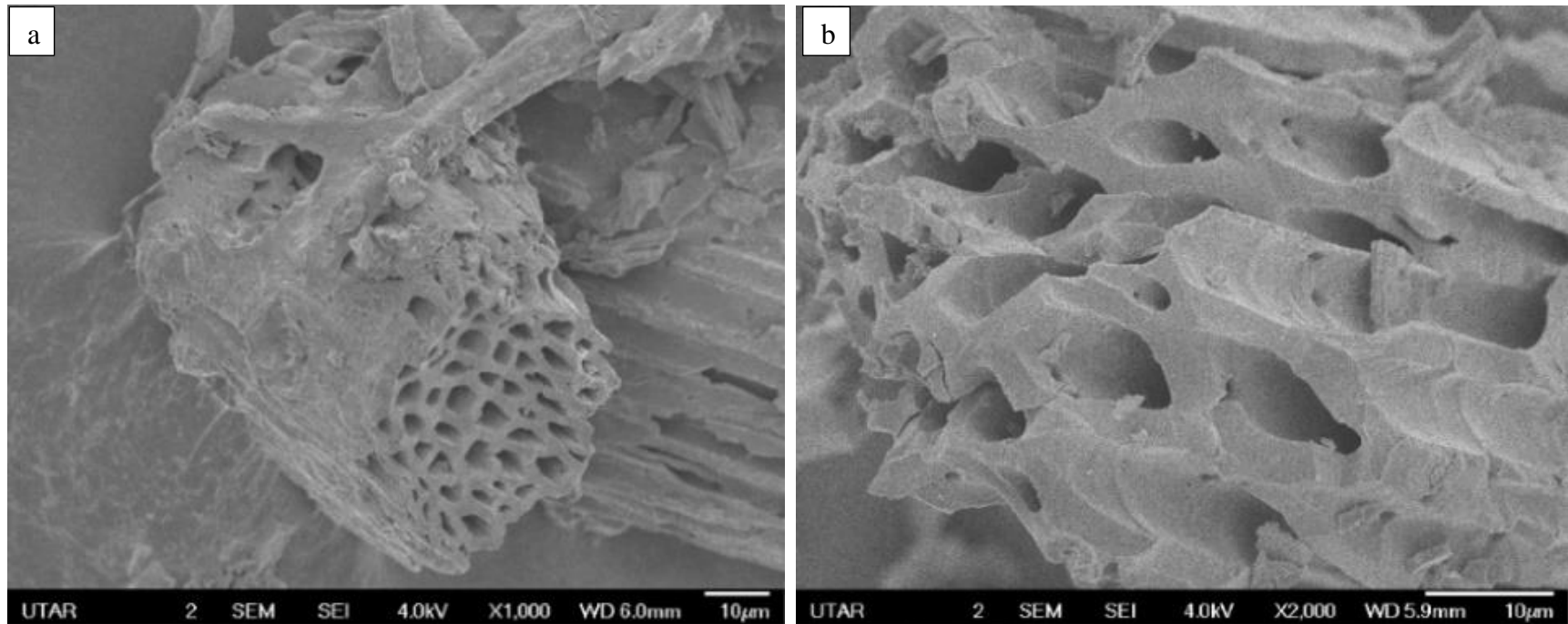


**Figure 4.11:** FESEM image of OPF biochar at different magnification

(a) 1000X, and (b) 2000X

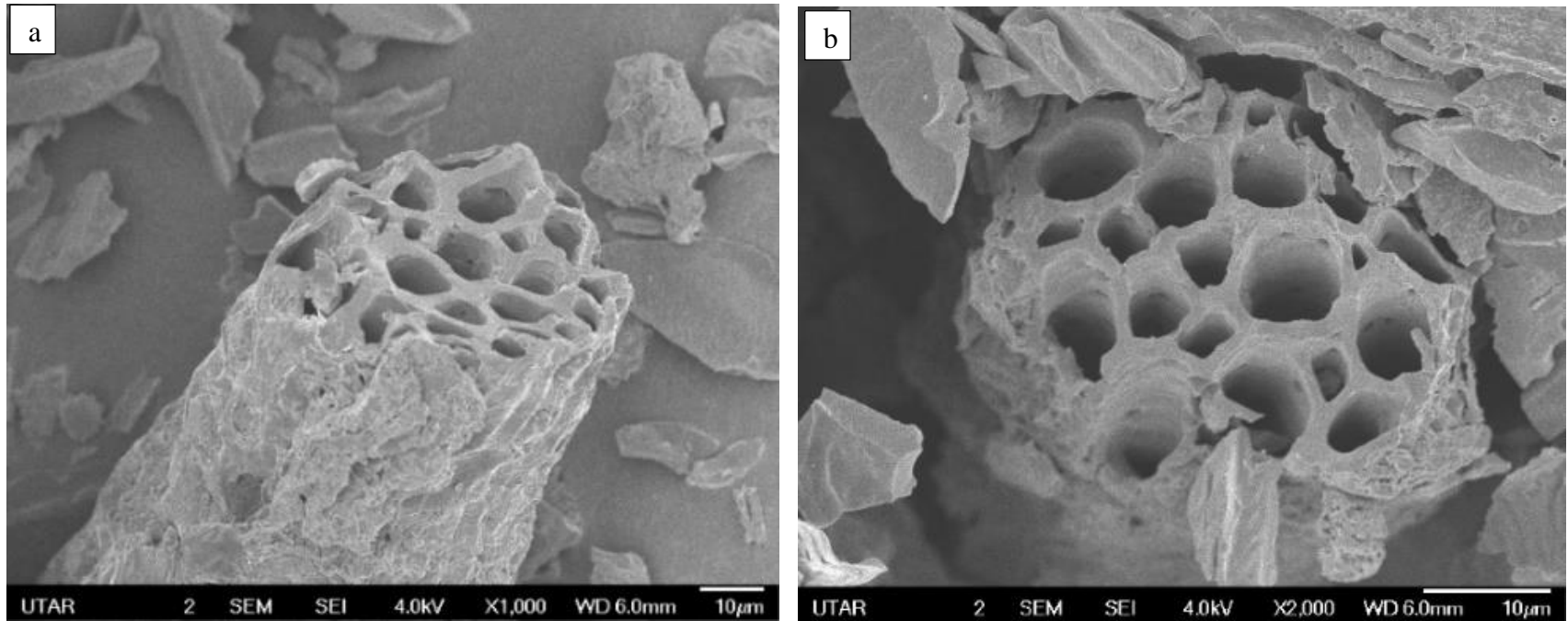


**Figure 4.12:** FESEM image of spent OPF biochar at different magnification (a) 1000X, and (b) 2000X

In addition to this, the proximate analysis in **Table 4.5** of the OPF biochar samples reveals that after the pyrolysis the percentage content of volatile matter decreases. During carbonization process the lignocellulosic compound destruction occur and vaporized from the material at higher temperature (Shaaban *et al.*, 2014). The decomposition of hemicellulose occurs in the temperature range of 224 – 333 °C while the cracking of cellulose happens at 327 – 370 °C. Unlike hemicellulose and cellulose, the degradation of lignin was observed in a wide range of temperature from 297 – 460 °C (Chen *et al.*, 2022). The fixed carbon content increases to 44.98 % because of the formation of more polyaromatic graphite like carbon structure in OPF biochar, and ash increases to 10.26 % as most of the volatile compounds are removed from the raw material. However, the moisture content is nearly similar in the sorbent samples. The ultimate analysis of the OPF biochar and spent OPF biochar, given in **Table 4.5**, represents that, the percentage weight of the elements such as carbon, hydrogen, and nitrogen are increased in the spent OPF biochar after treatment of AQW.

**Table 4.5:** Physical characteristics of raw fiber and OPF and spent

OPF biochar

Samples	Raw OPF	OPF biochar	Spent OPF biochar
BET Surface area (m <sup>2</sup> /g)	0.60	0.63	
Proximate analysis (% weight)			
Moisture content	4.0	6.0	
Volatile matter	76.2	47.8	
Fixed carbon	11.8	37.4	
Ash	8.0	8.9	
Ultimate analysis (% weight)			
C		61.5	63.1
H		3.9	4.2
N		1.4	2.3
EDX elemental (% weight)			
C	60.56	75.30	80.02
O	38.81	23.57	19.02
Mg	0.0	0.04	0.06
K	0.0	0.24	0.06
Ca	0.04	0.06	0.04
Al	0.03	0.05	0.05
Cu	0.30	0.51	0.45
Zn	0.19	0.36	0.28
Si	0.07	0.05	0.02

The increase in nitrogen and hydrogen is because of the adsorption of NH<sub>3</sub>-N. The carbon increase might be due to adsorption of some organic compound from the wastewater. The BET surface area of the OPF biochar sample did not improve as well, when the raw OPF is carbonized at 300 °C. this could be due to insufficient removal of volatile compound at lower temperature as noticed in the proximate analysis in **Table 4.5**. The OPF biochar still contains a high percent volatile matter. Similar result has been reported by others that biochar produced at lower temperature has a smaller

BET surface area compared to the ones prepared at high temperature (Shaaban *et al.*, 2014). When the volatile matter releases from the raw OPF the pores are formed during the formation of polyaromatic graphite like carbon structure polymerization structure which increase the BET surface area.

The SEM-EDX analysis is shown in **Table 4.5**. The results confirmed that after adsorption, the elemental composition of OPF biochar is significantly affected. The weight percent of some elements such as  $K^+$ ,  $Ca^{2+}$ ,  $Cu^{2+}$ , and Zn substantially reduces in spent OPF biochar after adsorption, demonstrating the  $NH_3$ -N recovery using ion exchange process. It has been reported that the positive ion on the surface of biochar can remove  $NH_4^+$  from the environment by ion exchange process (Dai *et al.*, 2020). Decreasing the metal content in the ash of biochar decrease the adsorption capacity of  $NH_4^+$ . When the pig manure biochar was treated with acid the value added metals such as  $K^+$ ,  $Ca^{2+}$  etc. were decreased in the pig manure biochar which causes a reduction in the adsorption capacity of  $NH_4^+$  from 13.66 mg/g to 4.72 mg/g (Yu *et al.*, 2016). However, the amount of carbon was increases because the OPF biochar was tested in real AQW and could adsorbed the organic carbon in wastewater treatment.

CEC is a crucial surface chemical characteristic that affects the adsorption of positively charged ions such as  $NH_4^+$  and reduces as the pyrolysis temperature increases (Gai *et al.*, 2014). OPF biochar produced at 300 °C has a higher CEC value than that of 400 °C as shown in **Figure 4.13**.

Lower CEC value at 400 °C is because of the loss of volatile matter with negative charge functional groups during the pyrolysis process (Mukherjee, Zimmerman and Harris, 2011; Rahman, Nachabe and Ergas, 2020).

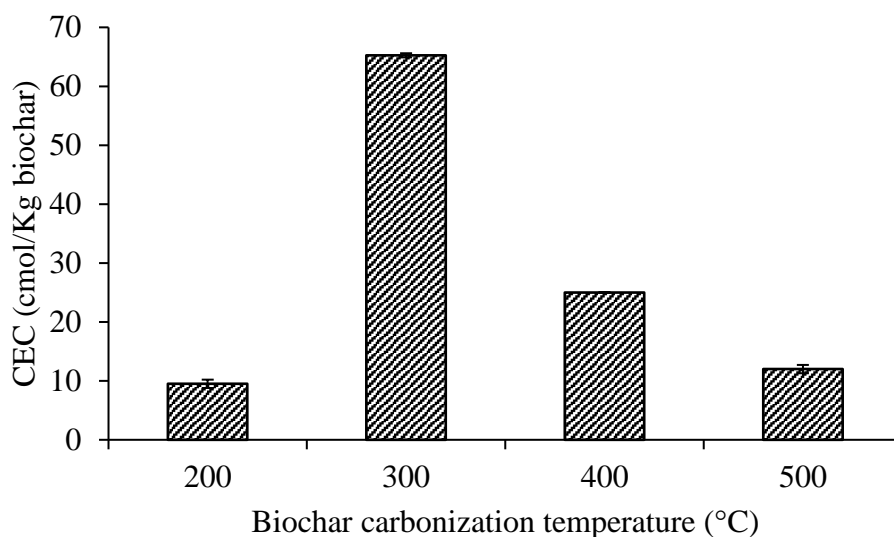


**Figure 4.13:** CEC of OPF biochar prepared at different carbonization temperature

Some researchers reported that negative charges on the carbonaceous material can be neutralized by positively charged ions such as  $\text{NH}_4^+$ ,  $\text{K}^+$ ,  $\text{Ca}^+$  etc. (Mukherjee, Zimmerman and Harris, 2011; Hale *et al.*, 2013).

In addition to this, the CEC of OPF biochar shows direct correlation to the recovery of  $\text{NH}_3\text{-N}$  adsorption as illustrate in **Figure 4.14**. The higher the CEC value of the adsorbent sample, the higher the adsorption efficiency of  $\text{NH}_3\text{-N}$ . The OPF biochar in **Figure 4.14** prepared at various conditions such as 200 °C, 0.5 hr ( $\square$ ), 300 °C, 1 hr ( $\times$ ), 300 °C, 2.5 hr ( $\Delta$ ), 400 °C, 0.5 hr ( $\circ$ ), 500 °C, 1 hr ( $\diamond$ ). Also, after the adsorption of  $\text{NH}_3\text{-N}$  the OPF biochar does not change the color and still brownish after the treatment.



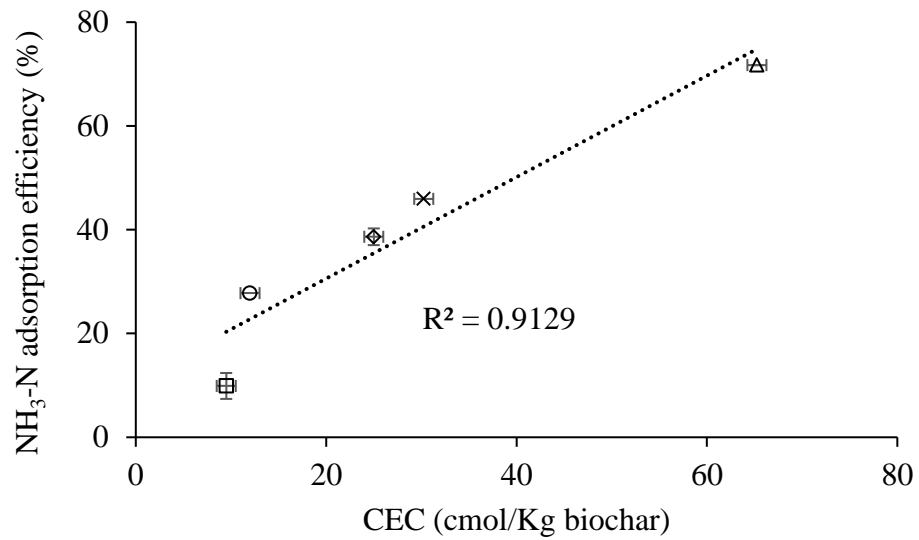


**Figure 4.14:** Effect of CEC of OPF biochar versus NH<sub>3</sub>-N adsorption efficiency

The ATR-IR results of the OPF biochar and spent OPF biochar is given in the **Figure 4.15**. The distinct peak at  $\sim 1600\text{ cm}^{-1}$  was corresponded to carbonyl C=O and aromatic C=C stretching vibration. The peak at  $\sim 1700\text{ cm}^{-1}$  reveals the carboxyl group C=O stretching. The peak at  $\sim 1246\text{ cm}^{-1}$  corresponds to aromatic alkoxy stretching, most probably from phenolic C-O bonds (Ibrahim *et al.*, 2021). The absorption band range from  $3000 - 3600\text{ cm}^{-1}$  corresponds to O-H. The smaller peak at  $2925\text{ cm}^{-1}$  represent C-H stretching. (Ahmad *et al.*, 2021). From the ATR-IR spectra, it is apparent that the intensity of C-O at  $\sim 1245$ , carbonyl at  $\sim 1600$  and carboxyl at  $\sim 1700$  peak increases and became more stable after NH<sub>3</sub>-N adsorption. It implies that during adsorption, those surface functional groups interact with NH<sub>3</sub>-N molecule. The increasing in the peaks demonstrating the formation of chemical bonds. It has also been reported that oxygen functional groups

adsorbed  $\text{NH}_4^+$  onto biochar via hydrogen bonding as well as electrostatic interaction (Cai *et al.*, 2016). The hydrogen bond or electrostatic force of attraction is formed between the positive charge  $\text{NH}_4^+$  molecule with the negative charge oxygen atom in the surface functional groups (C=O or C-O) of the biochar that cause the adsorption of  $\text{NH}_3\text{-N}$ .

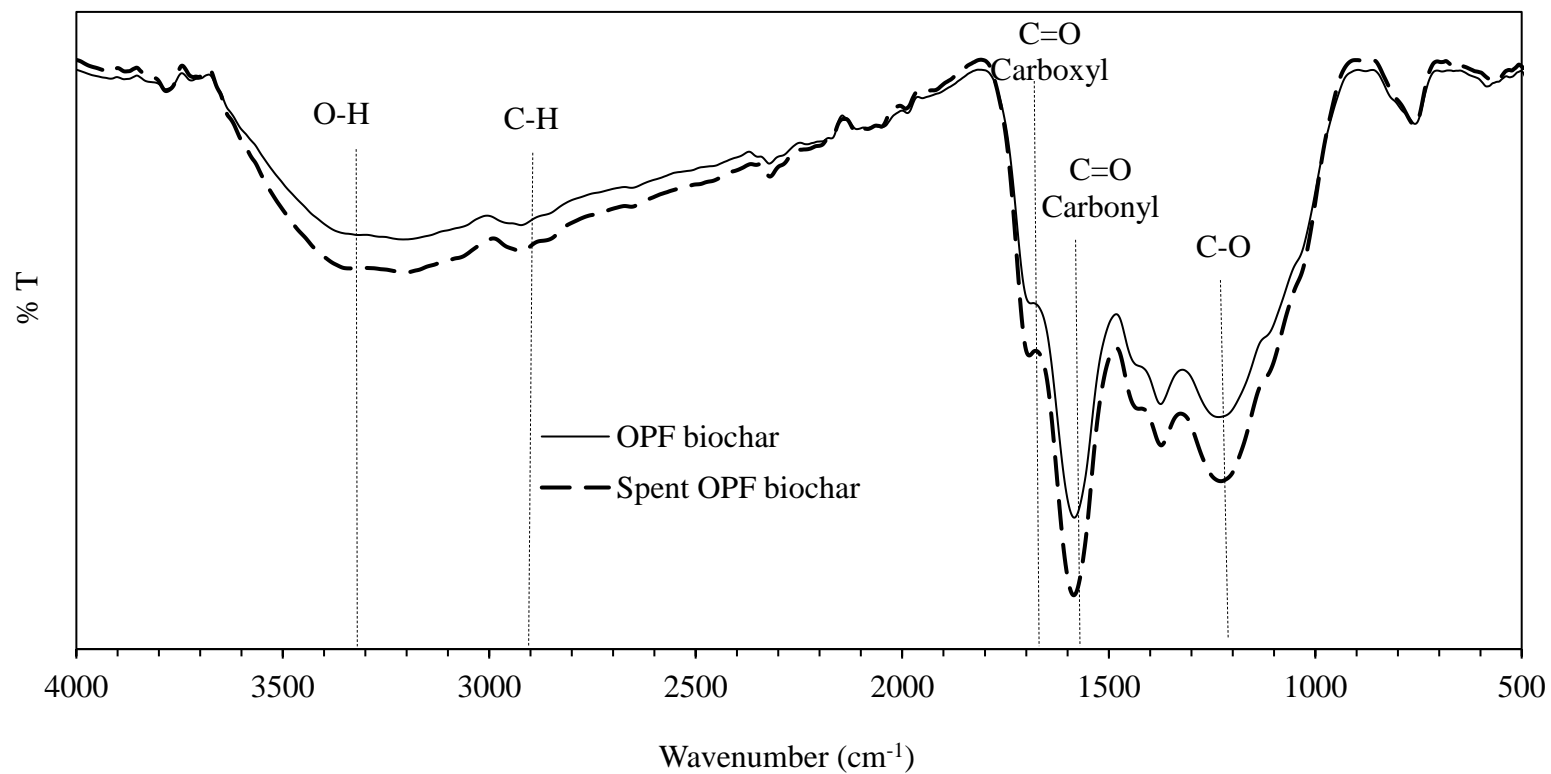


**Figure 4.15:** ATR-IR results of the OPF biochar at optimum adsorption condition (dosage (2 g), shaking speed (150 rpm), contact time (3 hr), pH (8.16), temperature (25 °C), and initial concentration of NH<sub>3</sub>-N (5.3 ppm))

Similar results have been observed for  $\text{NH}_4^+$  adsorption onto zeolite. After adsorption of the  $\text{NH}_4^+$ , the oxygen functional group increases and becomes more stable showing the formation of chemical bonds (Liu *et al.*, 2022). It can be concluded that oxygen functional groups take part in the recovery of  $\text{NH}_3\text{-N}$ .

Zeta potential analysis is performed for the predicting of the nutrients recovery (Yuan, Xu and Zhang, 2011). The pH at which the zeta potential becomes zero is the isoelectric point. As a function of pH, the pHzc and zeta potential values of the OPF biochar samples were determined and presented in **Figure 4.16**. The OPF biochar samples represent negative zeta potential. The negative charge on the OPF biochar decreases with the increase in the pyrolysis temperature. In the studied pH range, the zeta potential of the OPF biochar indicates that the surface of biochar is negatively charged, and the magnitude of the charge increases as pH increases. Similar results have been observed for the sorghum distiller grain biochar at acidic pH (3.0). The value of zeta potential was low at pH 3.0 (~ -5 mV) and became higher when the pH was increased to 10.0 (~ -48 mV). At pH 3.0 the adsorption capacity of  $\text{NH}_4^+$  was 3 mg/g and it increased to 12 mg/g when pH was increased to 9.0. This is because  $\text{NH}_4^+$  has positive charge and a higher negative value of the zeta potential facilitate adsorption through electrostatic attraction (Hsu *et al.*, 2019). A lower pH, the adsorption capacity of  $\text{NH}_4^+$  was low as well due to decrease in negative charges.

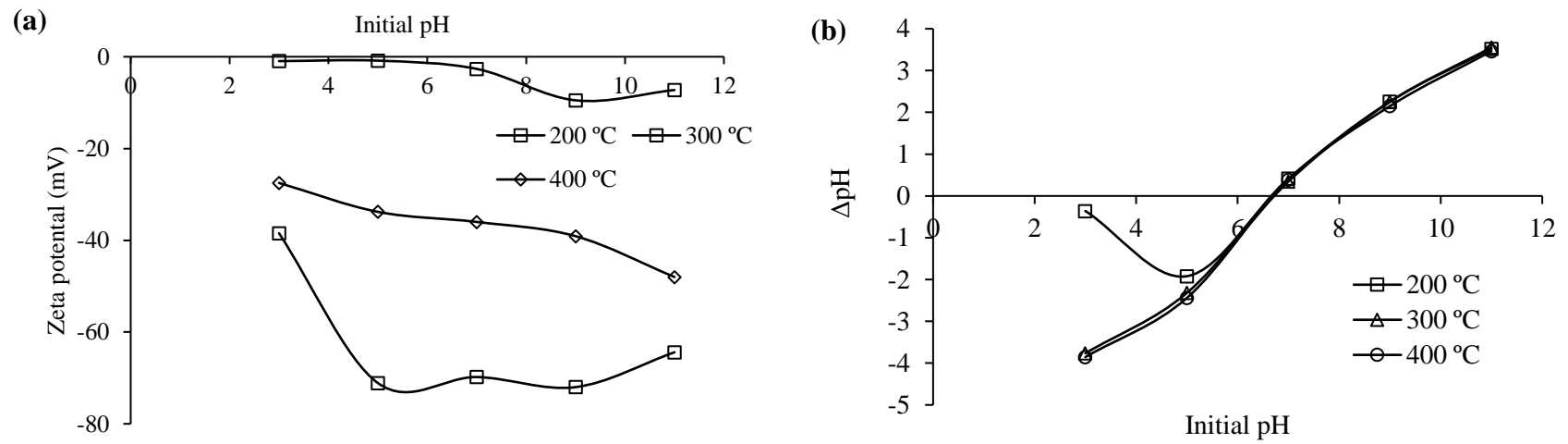


**Figure 4.16:** (a) Zeta potential and (b) pHzc of the OPF biochar samples

## **4.5. Adsorption process study on actual AQW**

The different process parameters have been evaluated for the optimization of NH<sub>3</sub>-N adsorption onto OPF biochar using actual AQW to reflect the actual adsorption scenario. Further, the process parameter data were used to find out the ruling adsorption mechanism of NH<sub>3</sub>-N onto OPF biochar using adsorption isotherms, and kinetics models.

### **4.5.1. Contact time**

The contact time effect on NH<sub>3</sub>-N removal was studied by changing the contact time from 15 to 240 min dosage (1 g), shaking speed (150 rpm), and temperature (25 °C) without any changes in pH. **Figure 4.17** shows that the adsorption efficiency of OPF biochar improved with increasing the contact time. At a contact time of 180 min, the highest adsorption of NH<sub>3</sub>-N of 61.54 % was observed. Further increase of time up to equilibrium (24 hr) shows very minimum increase only (63.5 %).

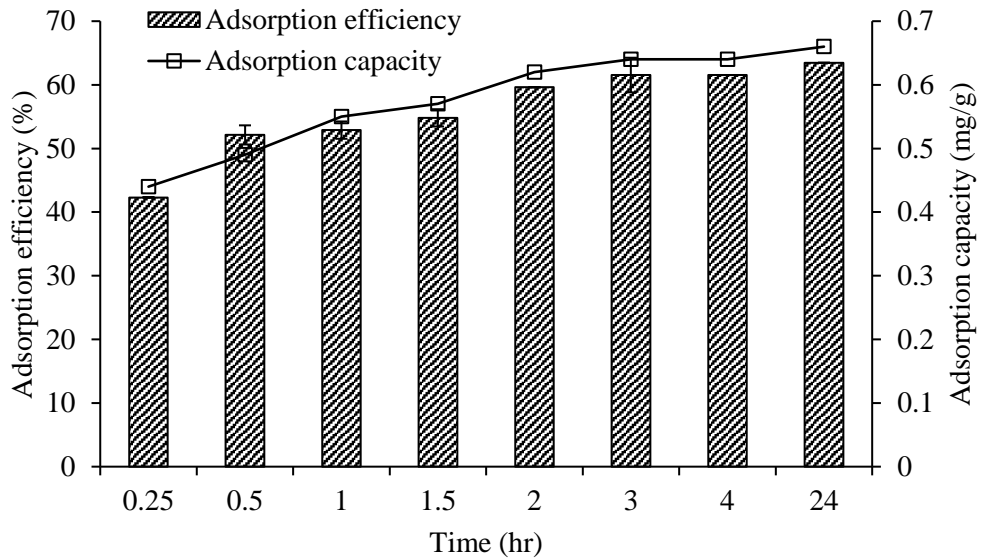


**Figure 4.17:** Effect of contact time of adsorption efficiency/capacity onto OPF biochar

Compared to the synthetic wastewater results shown in Section 4.3 (79.8 %), the  $\text{NH}_3\text{-N}$  removal efficiency was comparatively lower. The adsorption efficiency was lower in actual due to the presence of many other pollutants which hindered the adsorption of  $\text{NH}_3\text{-N}$ .

In the beginning of the adsorption process, the uptake was promoted by greater solute concentration gradient as well as a larger number of available adsorbent sites (Yang *et al.*, 2018). Furthermore, fast adsorption is also facilitated by the  $\text{NH}_4^+$  ion initial interaction with negatively charged surface anion groups including carboxylate ( $\text{COO}^-$ ) and hydroxyl ( $\text{OH}^-$ ). Following the first hour, the adsorption rate slow down, indicating the ionic equilibrium between the adsorbent and the aqueous solution (Kizito *et al.*, 2015). Similar findings were reported, whereby fast adsorption of  $\text{NH}_4^+$  occurred for 1 to 2 hours and it slowed and stabilized after 10 to 24 hours or

even after 4 hours due to the saturation and equilibrium of the adsorption sites (Gao *et al.*, 2015). The adsorption efficiency (61.5 %) was slightly greater than that of 120 min, hence the optimum contact time of 180 min was chosen for the next parameter.

#### 4.5.2. Effect of shaking

The impact of shaking speed was investigated by varying the orbital shaker's agitation speed from 50 to 250 rpm. While other operating parameters were remained unchanged. The removal efficiency of the  $\text{NH}_3\text{-N}$  versus shaking speed is illustrated in **Figure 4.18**. The uptake of  $\text{NH}_3\text{-N}$  increased initially when the speed was increased from 50 to 150 rpm, followed by a steady condition at 200 rpm. Increase in efficiency was occurred due to contact between the adsorbate and adsorbent, which promotes adsorbate diffusion toward the biochar surface indirectly.

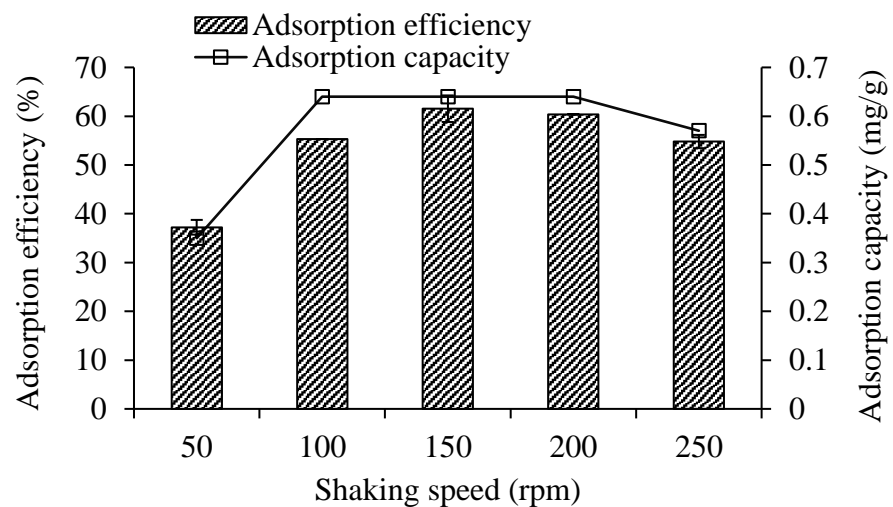


**Figure 4.18:** Effect of various shaking speed on the adsorption efficiency/capacity of  $\text{NH}_3\text{-N}$  onto OPF biochar



The increase of the adsorption efficiency with shaking speed is reported that the increase of turbulence and decrease of the thickness of the boundary layer, the rate diffusion surrounding sorbent from the bulk liquid to the liquid boundary layer surrounding sorbent enhances (Murithi, Onindo and Muthakia, 2012). It has been also suggested for good diffusion rate, increasing the shaking speed increases the external film mass transfer coefficient and hence enhanced the uptake (Murithi, Onindo and Muthakia, 2012). When the shaking speed exceeds 250 rpm, the removal efficiency reduces. The reduction in adsorption efficiency at 250 rpm is due to increase in kinetic energy of adsorbate and adsorbent which initiates collision between them. This enhances weakly bonded molecules of adsorbate detach from the adsorbent particles (Jamil *et al.*, 2014).

#### **4.5.3. Effect of OPF biochar dosage**

The impact of OPF biochar dosage on the effectiveness of NH<sub>3</sub>-N adsorption was studied in a range of 0.5 – 4 g by shaking speed (150 rpm), temperature (25 °C), contact time (180 min), and pH constant. The dose of OPF biochar influences the availability of adsorption sites. **Figure 4.19** shows that by increasing the biochar dose, the removal efficiency of NH<sub>3</sub>-N increased linearly.

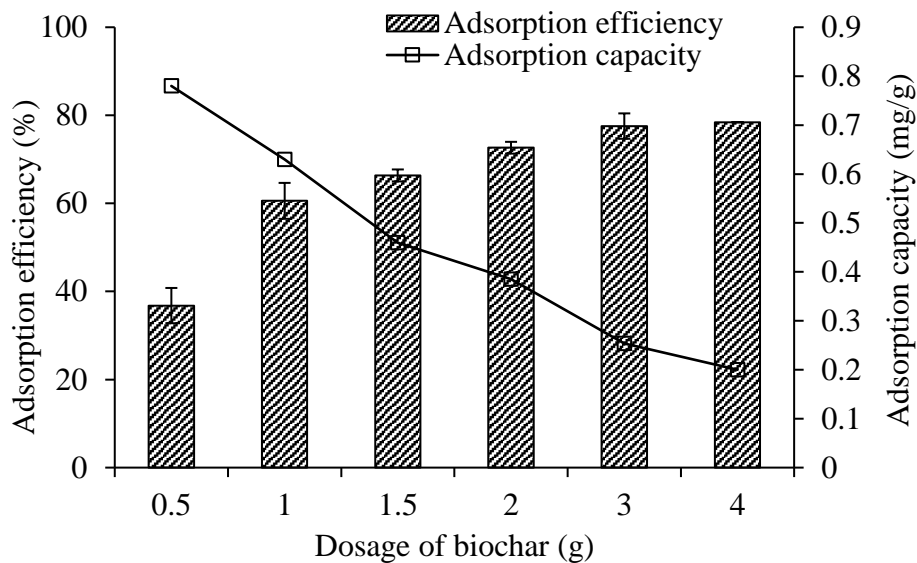


**Figure 4.19:** Effect of the OPF biochar dosage on the adsorption efficiency/capacity of  $\text{NH}_3\text{-N}$

More sorption sites are available with a higher dose, which helps  $\text{NH}_3\text{-N}$  to bind more onto the biochar surface. The removal efficiency does not improve much after 2 g of dose and did not achieve higher efficiency than 90 %. It is due to the overlapping of adsorbent layers phenomenon, the increase in adsorbent mass covers accessible active sites. Also, similar results for  $\text{NH}_4^+$  adsorption onto biochar has been observed (Kizito *et al.*, 2015). The decrease in adsorption capacity (mg/g) with increasing mass of the adsorbent is due to the split in concentration gradient between the solute concentration in the solution and the solute concentration on the surface of the adsorbent. At higher dosage the particle aggregation takes place, and as a result the capacity of  $\text{NH}_3\text{-N}$  decreases (Villabona-Ortíz, Figueroa-Lopez and Ortega-Toro, 2022). It has been reported that increasing the dosage of adsorbent led to the insufficiency of the adsorbate molecule in the solution with respect to the binding adsorbate molecule (Murithi, Onindo and

Muthakia, 2012). Thus, with an increase in the adsorbent amount, the amount of adsorbate molecule sorbed on the unit weight of the sorbent gets reduced, causing a decrease in adsorption capacity with increasing adsorbent dosage. Hence, 2 g was taken as the optimized dosage for the next parameter.

#### 4.5.4. Effect of pH

The influence of pH adjustment of the AQW was examined in the range of 3 – 11, keeping the dosage (2 g), temperature (25 °C), shaking speed (150 rpm), and contact time (180 min) constant. The pH was adjusted by adding 0.1M NaOH or HCl. The original pH of AQW was slightly alkaline (8.16). The removal efficiency and capacity without any pH adjustment were 72.6 %, and 0.4 mg/g respectively. When the pH of the solution was adjusted to an acidic pH (3.0), the removal efficiency of NH<sub>3</sub>-N immediately dropped to 58.5 %. However, when the pH adjusted to alkaline condition *i.e.*, 11 and increase in removal efficiency was noticed. Biochar represent high negative zeta potential at higher pH and facilitate the adsorption through electrostatic interaction (Hsu *et al.*, 2019), as mentioned in **Figure 4.20**. The findings for NH<sub>3</sub>-N at acidic pH were unfavorable because of protonation of the surface binding site of OPF biochar also the adsorbent contains extra positive charges from hydrogen ions, that might produce large repulsion (Kizito *et al.*, 2015). The OPF biochar performs best at alkaline and neutral pH values.

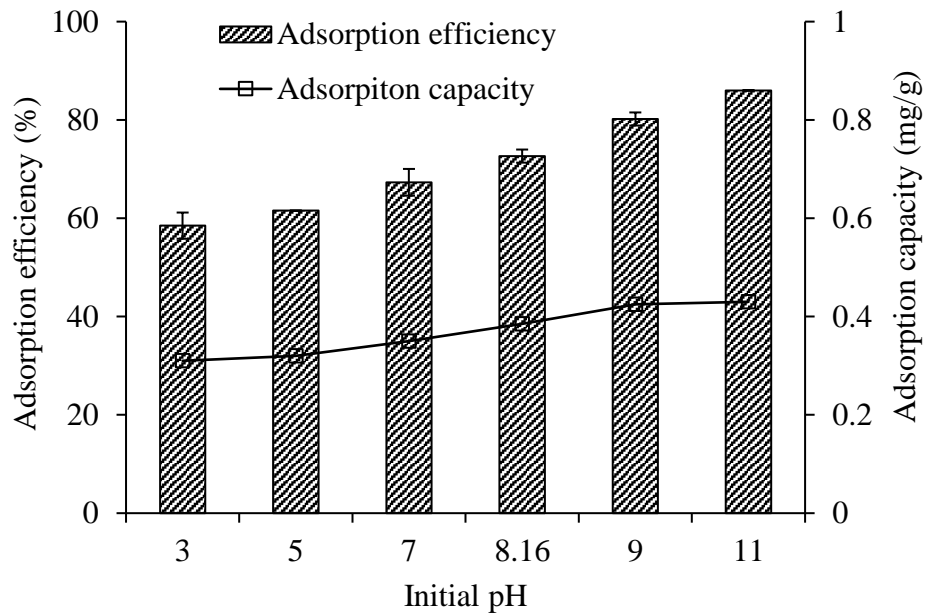


**Figure 4.20:** Effect of initial pH on the adsorption efficiency/capacity of  $\text{NH}_3\text{-N}$  onto OPF biochar

#### 4.5.5. Effect of temperature

The effect of temperature on  $\text{NH}_3\text{-N}$  was investigated from room temperature (25 °C) to 40 °C keeping dosage (2 g), shaking speed (150 rpm), and contact time (3 hr), constant. **Figure 4.21** shows that slightly increase in the adsorption efficiency of  $\text{NH}_3\text{-N}$  was occurred when temperature was increased from 25 to 40 °C. The increase in adsorption efficiency expresses that the adsorption onto OPF biochar was endothermic. For achieving the maximum adsorption, temperature higher than ambient temperature will be needed. This type of trend has been described that the diffusivity of the adsorbate from the external laminar layer in the micropore of biochar increases at higher temperature because of higher reaction rate between the surface functional groups of biochar and  $\text{NH}_4^+$  (Long *et al.*, 2008). Also, the

adsorption tests higher than 40 °C were not conducted because of the equipment limitation as well as economic reason as the change in the adsorption efficiency was not very high. Moreover, it is not feasible to change the temperature of the AQW in real application. Similar results has been reported that increasing the temperature enhanced the adsorption of  $\text{NH}_4^+$  (Kizito *et al.*, 2015).

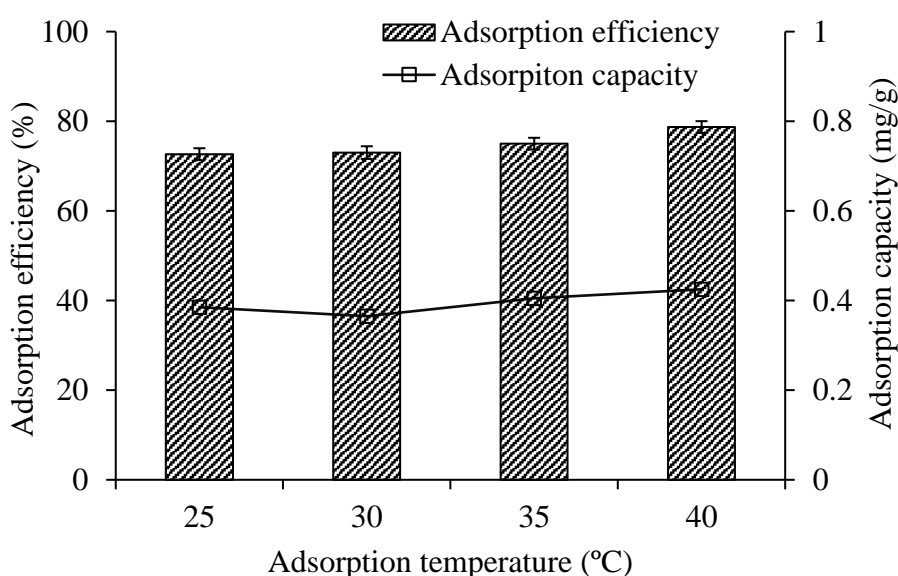


**Figure 4.21:** Effect of temperature on the adsorption efficiency/capacity of  $\text{NH}_3\text{-N}$  onto OPF biochar

#### 4.6. Thermodynamics analysis

The value of  $\Delta H^\circ$ , and  $\Delta S^\circ$  was calculated using the slope and intercept from the Linear plot of  $\ln K_C$  and  $1/T$  as shown in **Figure 4.22**. **Table 4.6** contains the measured value of  $\Delta H^\circ$ ,  $\Delta S^\circ$ , and  $\Delta G^\circ$ . The degree of entropy between the atom is represent by  $\Delta S^\circ$ .

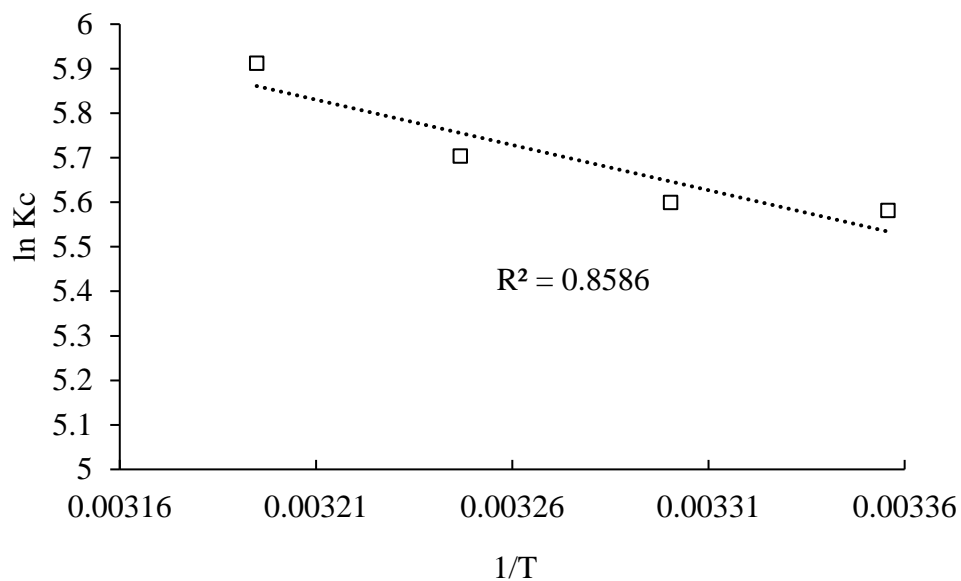


**Figure 4.22.** Linear plot of  $\ln K_c$  vs  $1/T$

**Table 4.6.** Thermodynamic parameters for adsorption of  $\text{NH}_3\text{-N}$  onto OPF biochar

Temperature (K)	$\Delta G^\circ$ (kJ/mol)	$\Delta H^\circ$ (kJ/mol)	$\Delta S^\circ$ (kJ/mol.K)	Ea (kJ/mol)
298	-13.83			
303	-14.11			
308	-14.61	16.90	102.72	35.12
313	-15.39			

The positive  $\Delta S^\circ$  of  $\text{NH}_3\text{-N}$  indicated an increase in randomness at OPF biochar interface during the adsorption process (Pholosi, Naidoo and Ofomaja, 2020).  $\Delta G^\circ$  is used to determine the spontaneous and nonspontaneous adsorption. The adsorption of  $\text{NH}_3\text{-N}$  onto OPF biochar is spontaneous as  $\Delta G^\circ$  value is negative which shows the process is thermodynamically favorable. The value of  $\Delta H^\circ$  was noticed in the range of

-20 to 40 kJ/mol for physical adsorption (Raghav and Kumar, 2018). In the present work, that adsorption type is physisorption and endothermic in nature because the value of  $\Delta H^\circ$  is positive. It is important to note that both PFO and PSO both showed good correlation and near to 1 so, the adsorption mechanism may be both physical and chemical adsorption as the thermodynamic parameters calculation also proven the occurrence of the physical adsorption. It has also reported that increasing the temperature, the value of the intercept, indicating the boundary diffusion, in the intraparticle diffusion increases, resulting in enhanced the surface adsorption (Pholosi, Naidoo and Ofomaja, 2020). Based on these results, the conclusion can be made that both physisorption and chemisorption. Similar findings are reported for the adsorption of  $\text{NH}_4^+$  onto biochar (Kizito *et al.*, 2015).

An Arrhenius plot of  $\ln K$  vs  $1/T$ , with slope equal to  $-(E_a/R)$  gives the activation energy ( $E_a$ ). The activation energy calculated for  $\text{NH}_3\text{-N}$  is presented in **Table 4.6**. The minimum energy required for starting a chemical reaction is called the activation energy. The positive value of  $E_a$  in the adsorption process implies that the process is endothermic (Ebelegi, Ayawei and Wankasi, 2020).

#### **4.7. Adsorption equilibrium and kinetics**

To further analyze the ruling factor for the adsorption capacity of the OPF biochar, the experimental data obtained from **Figure 4.19** were fitted

with Linear and non-Linear Langmuir and Freundlich models. The isotherm plots are illustrated in **Figure 4.23** and the results are presented in **Table 4.7**.



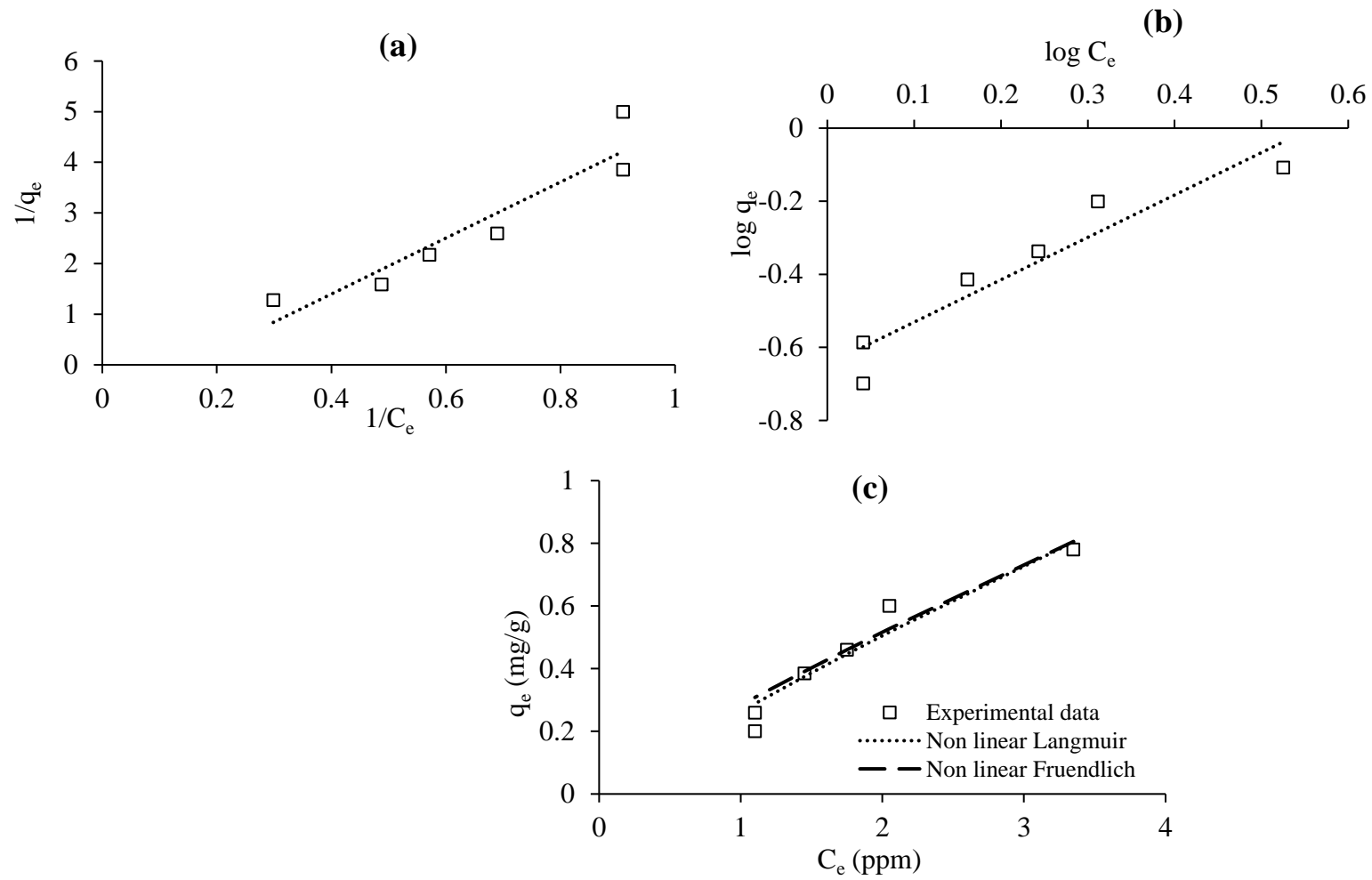


**Figure 4.23:** Adsorption isotherm (a) Linear Langmuir (b) Linear Freundlich (c) Linear and non-Linear

**Table 4.7.** Isotherm parameters for NH<sub>3</sub>-N adsorption onto OPF biochar

<b>Isotherms</b>	<b>Parameters</b>	<b>Linear model</b>	<b>Non-Linear model</b>
Freundlich	K <sub>F</sub> (mg/g)/(ppm) <sup>n</sup>	0.22	0.28
	n	1.16	0.86
	R <sup>2</sup>	0.9009	0.9518
	χ <sup>2</sup>	0.05	0.05
Langmuir	Q <sub>max</sub> (mg/g)	1.22	6.42
	K <sub>L</sub> (L/mg)	0.15	0.04
	R <sub>L</sub>	0.57	0.82
	R <sup>2</sup>	0.8794	0.9303
	χ <sup>2</sup>	1.07	0.04

According to **Table 4.7**, NH<sub>3</sub>-N adsorption by OPF biochar was heterogeneous because the correlation factor ( $R^2 = 0.9009$ ) of NH<sub>3</sub>-N of the Freundlich models agreed well compared to Langmuir models. The heterogeneous characteristics of biochar surface is strongly associated to the adsorption of NH<sub>3</sub>-N (Kizito *et al.*, 2015). Moreover, higher coefficient of determination ( $R^2 = 0.9518$ ) was observed in the case of non-Linear Freundlich model, when applied to experimental data and shows better fit compared to Linear model.

On the basis of  $R^2$  and  $\chi^2$  values, the comparison effectiveness of the non-Linear and Linear isotherm models can be evaluated. The error analysis of the non-Linear and Linear models in the form of isotherm models is shown in **Table 4.7**. A smaller value of  $\chi^2$  indicates a higher fit to the model. The non-Linear and Linear Freundlich models have the same error function value

of  $\chi^2$  implies that both models agreed well with the experimental findings. However, comparing the  $R^2$  values, the non-Linear Freundlich model agreed the most to experimental data.

The influence of contact time was used to measure the adsorption kinetics. The PFO and PSO non-Linear and Linear models were evaluated. The details are given in **Table 4.8**. **Figure 4.24** illustrates the model plots. The correlation coefficient ( $R^2$ ) value for the adsorption of  $\text{NH}_3\text{-N}$  is 0.9950 for non-Linear models, and 0.9988 for Linear models, demonstrating that PSO fits more to the experimental findings than PFO. The  $q_e$  value calculated by PFO is smaller than experimental results (0.60 mg/g) however, the  $q_e$  (mg/g) determined by PSO is identical to the experimental result. Based on the better fit by the PSO model, it can be deduced that rate controlling step is the chemical adsorption and there is no validation for chemisorption if the experimental data follow the PSO (Tran *et al.*, 2017). Further, the characterization of ATR-IR and EDX reveals that adsorption of  $\text{NH}_3\text{-N}$  is occur chemically because the interaction between oxygen functional groups as well as the value-added metals are involved in the adsorption process.

**Table 4.8.** Kinetic parameters for adsorption of NH<sub>3</sub>-N onto OPF biochar

<b>Model</b>	<b>Parameters</b>	<b>Linear model</b>	<b>Non-Linear model</b>
Pseudo first order	q <sub>e</sub> (mg/g)	0.24	0.57
	K <sub>1</sub> (1/min)	0.0168	0.086
	R <sup>2</sup>	0.9861	0.9843
	χ <sup>2</sup>	7.07	0.008
Pseudo second order	q <sub>e</sub> (mg/g)	0.63	0.63
	K <sub>2</sub> (g/mg.min)	0.196	0.222
	R <sup>2</sup>	0.9988	0.9950
	χ <sup>2</sup>	0.004	0.002
Intra-particle diffusion model	k <sub>p</sub> (mg/g × min <sup>0.5</sup> )	0.022	-
	C	0.70	-
	R <sub>i</sub>	0.47	-
	R <sup>2</sup>	0.9767	-

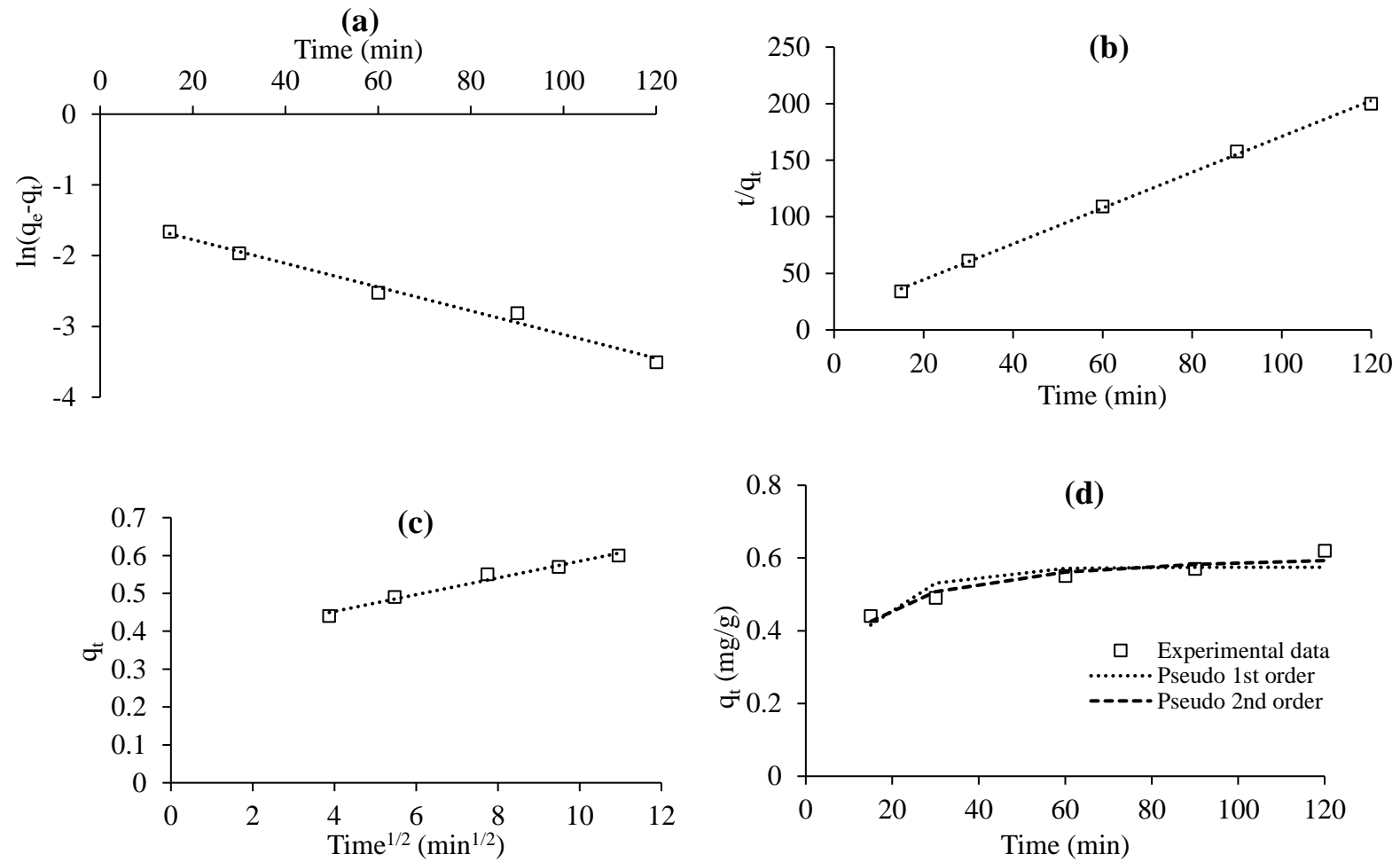


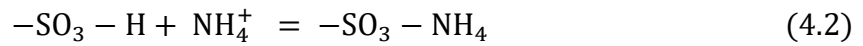
**Figure 4.24:** Plot for (a) Linear model of pseudo first order model (b) Linear model of pseudo second order (c) Linear model of intra-particle diffusion model (d) Non-linear kinetics models

The effectiveness of the models (non-Linear and Linear) could be examined by observing  $\chi^2$  and comparing the estimated  $q_e$  values with to the experimental  $q_e$  values. The  $q_e$  value ( $q_e = 0.63$  mg/g) of non-Linear PSO is nearly identical to the experimental result. In addition to this, the non-Linear PFO also has a similar  $q_e$  value to the experimental value but the  $R^2$  value is slightly lower than the non-Linear PSO. In Table 4.8 the non-Linear and Linear kinetic models the error analysis is demonstrated. Error analysis of the kinetic models (non-Linear and Linear) are shown in the **Table 4.8**. The non-Linear PSO model represent smaller  $\chi^2$ , which means the model agrees well to the experimental results.

**Figure 4.24 (c)** represent the intra-particle diffusion model's plot. The analysis of experimental results using the intra-particle diffusion model, it was found that the plot did not pass through the origin but with a significant intercept, indicating that intraparticle diffusion was not the rate-limiting step. **Table 4.8** contains the parameters determined using intra-particle diffusion model. Where the value of the initial characteristic curve ( $R_i$ ) shows strong initial adsorption because  $R_i = 0.47$  is between  $0.5 > R_i > 0.1$ . The  $R_i$  value has been divided into four zones:  $1 > R_i > 0.9$  is called weakly adsorption (zone 1);  $0.9 > R_i > 0.5$ , intermediate initial adsorption (zone 2);  $0.5 > R_i > 0.1$ , strong initial adsorption (zone 3); and  $R_i < 0.1$ , approaching completely initial adsorption (zone 4). For example,  $R_i = 0.1$  means that the initial adsorption has already reached 90 %, and later on the adsorption proceeds following the intraparticle diffusion. Also, when  $R_i = 0.5$  i.e., the other 50 %

of the adsorption governed by intraparticle diffusion (Wu, Tseng and Juang, 2009).

In addition to this, it has been reported that the various functional groups ((carboxylic, hydroxylic, and phenolic hydroxyl group) on the surface of biochar (Li *et al.*, 2013, 2018) are account for the ion exchange (between the  $\text{NH}_4^+$  and the functional groups) in adsorption of nitrogen compounds (Liu *et al.*, 2010; Yin *et al.*, 2017; Dai *et al.*, 2020). The mechanism of hydroxylic, carboxylic and sulfonic acid groups and  $\text{NH}_4^+$  on the biochar surface is expected as follows:



#### 4.8. Nutrient recovery from actual AQW

To investigate the adsorbent performance for other pollutants in the actual AQW, the optimized process parameters were used for OPF biochar. The optimized parameters are temperature 25 °C, contact time 3 hr, shaking speed (150 rpm), and dosage 2 g. **Table 4.9** details the quality of the AQW before and after being treated with OPF biochar.

**Table 4.9:** Composition of aquaculture wastewater before and after treatment

Parameters	Characteristics of AQW (average)		Removal efficiency (%)	Malaysian Standard
	Initial	Treated		
pH	8.5 ± 0.12	8.6 ± 0.02	-	6-9
NH <sub>3</sub> -N	5.3 ± 0.26 ppm	1.45 ± 0.07 ppm	72.64 ± 1.33	10
NO <sub>2</sub> <sup>-</sup> -N	0.03 ± 0.001 ppm	0.03 ± 0.001 ppm	-	-
NO <sub>3</sub> <sup>-</sup> -N	0.8 ± 0.10 ppm	0.8 ± 0.07 ppm	-	-
PO <sub>4</sub> <sup>3-</sup> -P	1.06 ± 0.04 ppm	1.09 ± 0.01 ppm	-3.15 ± 1.33	-
TP	1.23 ± 0.18 ppm	1.29 ± 0.02 ppm	-5.71 ± 1.73	-
COD	45.2 ± 3.89 ppm	48 ± 3.54 ppm	-6.13 ± 0.65	80
Turbidity	3.2 ± 0.10 NTU	1.5 ± 0.042 NTU	54.06 ± 1.32	-
Salinity	0.09 ± 0.00 ‰	0.09 ± 0.00 ‰	-	-



The pH of AQW is similar before and after treatment, because the OPF biochar has not been modified and is alkaline in nature. There were no obvious changes in the pH. Thus, addition of OPF biochar does not change the pH of water to be discharged and no pH adjustment is required. The  $\text{NH}_3\text{-N}$  recovery from actual AQW was 72.6 %. The recovery of  $\text{NH}_3\text{-N}$  is lower compared to the one reported for synthetic wastewater (79.8 %) in Section 4.3. This could be due to the existence of other pollutants in the actual AQW. The pollutants could have caused competitive adsorption. The concentration of  $\text{NO}_2^- \text{-N}$  and  $\text{NO}_3^- \text{-N}$  is lower than 1 ppm, making it difficult to adsorb onto biochar because the interaction of the adsorbate molecule and adsorbent is very low. It has been reported that biochar contains acid surface functional groups and can repulse the negative charge  $\text{NO}_2^- \text{-N}$  and  $\text{NO}_3^- \text{-N}$  molecule (J. Yang *et al.*, 2017). The concentration of  $\text{PO}_4^{3-} \text{-P}$  is slightly increased after treatment with OPF biochar. The increase in  $\text{PO}_4^{3-} \text{-P}$  occurs because our OPF biochar leaches  $\text{PO}_4^{3-} \text{-P}$  even when tested in synthetic wastewater. A similar behavior of  $\text{PO}_4^{3-} \text{-P}$  leaching was reported when synthetic wastewater was treated with various biochar (Yao *et al.*, 2012). A small increase in chemical oxygen demand (COD) was noticed because biochar is an organic material and some organic compounds leached into the water after treatment. It has been found that various light aromatic compounds leached from biochar using ultrapure water (Lievens *et al.*, 2015). But still the COD is lower than the effluent standard and can be disposed to the water body without further treatment. The OPF biochar reduced the turbidity by 54.1 %. The reduction in turbidity may be due to adsorption (electrostatic interaction and Brownian motion between the

surface of the pore and the particles), straining/size exclusion (due to size difference between the pore opening and the particle), and/or sedimentation/gravity settling (due to density difference between the carrying effluent and the particles) (Khiari *et al.*, 2020). In Brownian motion the random motion of suspended particle during this motion the smaller particle enter to porous structure of the biochar and adsorbed. In straining/size exclusion the particles are stuck inside the pores and depends on the size of the particle or molecule and the opening of the pores in the OPF biochar. The salinity of AQW did not change after treatment with OPF biochar. It could be the lower presence of the  $\text{Na}^+$ ,  $\text{K}^+$ ,  $\text{Ca}^{2+}$  in the wastewater (Yang *et al.*, 2019). Also, lower salinity of the treated wastewater is better for the growth of aquatic organism and can be released to the water bodies (Velasco *et al.*, 2019). Without major change in salinity, pH and other components, this makes the treated water safe for fish and can be even recycled back to the pond for reutilization. Moreover, it will be much healthier as the  $\text{NH}_3\text{-N}$  content has been reduced drastically. For selective recovery of  $\text{NH}_3\text{-N}$  in real AQW the OPF biochar will be a suitable adsorbent. The spent OPF biochar (nutrient rich) can be further tested for its feasibility to be used as fertilizer or soil conditioner. In addition, OPF biochar is an environmentally friendly and biodegradable sorbent (Shang *et al.*, 2018) . For the spent adsorbent, there is no requirement for a separate treatment process and can be simply disposed of. This directly decreases the overall recovery process of the cost. After the recovery of the nutrient, the addition of OPF biochar to the AQW did not alter any of the AQW's fundamental properties, such as pH and salinity.

A comparison was also made with the Malaysian standards as shown in **Table 4.9** (DOE Malaysia, 2009). The industrial effluent should meet the requirement before discharge. After treatment of the AQW with OPF biochar, pH, NH<sub>3</sub>-N, and COD are within the standard limits. As a result, it is safe to release the treated AQW to water bodies or recycle the treated water back to the pond or fish tank.

#### **4.9. Comparison of OPF biochar with different adsorbents**

In **Table 4.10**, a comparison of the OPF biochar with the adsorbents used in actual AQW is given. The adsorption performance of the carbon-based adsorbent is lower than the OPF biochar. Among the carbon-based adsorbent, commercial activated carbon shows the highest adsorption efficiency of 58.82 % NH<sub>3</sub>-N at a dosage of 75 g/L adsorbent and contact time of 3 days (Karia *et al.*, 2022). In our study, the OPF biochar removed 72.64 % of NH<sub>3</sub>-N within 3 hr with very lower dosage of 10 g/L.

Other adsorbents such as Clay 1 and aged refused have slightly higher performance than OPF biochar because of higher adsorbent dosage. Further coal cinder zeolite ball were chemically modified with polyvinyl alcohol and succinic acid (Tian *et al.*, 2016) and mordenite impregnated with magnesium (Yao *et al.*, 2022) did not performed well for removal of NH<sub>3</sub>-N. Among all the adsorbents, the bentonite-hydrochar (composite material) completely removed the NH<sub>3</sub> in a continuous study with in 7.5 min (Ismadji *et al.*, 2016).

Except the composite material, the adsorption efficiency of OPF-based biochar for  $\text{NH}_3\text{-N}$  at low concentration was found to be comparable with other adsorbents and activated carbon, indicating that this developed OPF-based adsorbent can be used on any scale of wastewater treatment processes.

**Table 4.10:** Comparison of different adsorbents with OPF biochar for NH<sub>3</sub>-N in AQW

<b>Adsorbent</b>	<b>Contact time (hr)</b>	<b>Dosage (g/L)</b>	<b>Removal efficiency (%)</b>	<b>Ref.</b>
Clay 1	3	75	~ 75	Zadinelo <i>et al.</i> , 2015
Bentonite-hydrochar	0.125	-	100	Ismadji <i>et al.</i> , 2016
Coal cinder zeolite ball	-	-	15.7 – 49.9	Tian <i>et al.</i> , 2016
Zeolite	7 days	1×10 <sup>-11</sup>	61.27	Aly <i>et al.</i> , 2017
Q2	5	10	55.08	Bernardi <i>et al.</i> , 2018
Aged refuse	1	20	88	Anijiofor <i>et al.</i> , 2018
Sawdust	Overnight	10	44.4	El-sherbiny, El-chaghaby and El-Shafea, 2019
Mg-mordenite	0.17	9	0	Yao <i>et al.</i> , 2022
Activated carbon filter	0.9 – 1.8	-	17.78	Jegatheesan <i>et al.</i> , 2007
Activated carbon	3	0.33	38.77	Sichula <i>et al.</i> , 2011
Pyrolyzed chicken feather fiber	0.5	3.3	40.47	Moon <i>et al.</i> , 2017
Commercial activated carbon	3 days	75	58.82	Karia <i>et al.</i> , 2022
OPF biochar	3	10	72.64	Present study

#### **4.10. OPF biochar production cost analysis**

The results and discussion sections have shown that OPF-based biochar is effective in adsorbing  $\text{NH}_3\text{-N}$  from AQW. Waste-based carbons were found to be as good as or better than commercially available activated carbon in the adsorption of  $\text{NH}_3\text{-N}$ . As a result, if the product is expected to be commercialized, the following process scale-up to produce biochar can be considered. The potential will aid in determining the biochar's ultimate marketability. The process flow diagrams for OPF-based biochar production, as well as their economic evaluation, were discussed in this section.

##### **4.10.1. Process flow design**

The process flow for the industrial scale-up was designed based on the lab setup tested. Each process of the lab test was scaled up. Different types of equipment were chosen and designed to suit the lab setup. **Figure 4.25** indicates the overall process flow design. First the raw sample was picked up in the truck from oil palm mill and brought to the pilot plant site and put in the storage place. Then the raw OPF from storage is transferred to the shredder via conveyor belt to be converted into small pieces and further carried (using conveyor) to the rotary kiln for carbonization process. After carbonization process, the biochar is directly shifted to the rotary cooler to cool down the samples. In lab scale the amount is small so no need of the cooler but in actual pilot plant design cooler is necessary because of the continuous process and high amount of the product. After, the rotary cooler the prepared

biochar was further gone to packaging process and stored in the storage room. In this design, during the rotary kiln, the prepared biochar converted into powder form, so there is no need for a grinder after the cooling process. Some design ideas were adapted from Ng *et al.*, (2003), who has designed a similar system for the preparation of activated carbon. Based on market demand, a rotary kiln is selected to produce around 1500 kg of biochar on a daily basis.

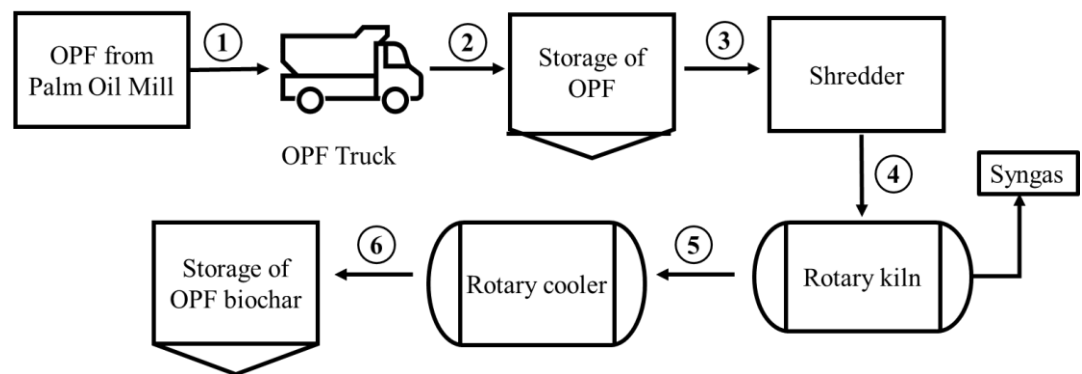


**Figure 4.25:** Process flow diagram to produce OPF biochar

The scale-up production cost study was performed using equipment design, sizing, and capital cost estimates (Ng *et al.*, 2003). A comparable production system for activated carbon from pecan shell was reported by Ng *et al.* (2003). The palm industry produces EFB and mesocarp fiber approximately 15.8 and 9.6 million tons annually (Marsin *et al.*, 2018). Converting the annual to daily production of EFB and mesocarp fiber to 43,267 and 26,301 kg/day. So, it is easy to get 5,000 kg of OPF on a daily basis from the palm industry. The projected cost of electricity usage for OPF

biochar preparation based on 5,000 kg/day of OPF feed is shown in **Table 4.11**. The estimated cost of each equipment in the pilot plant scale is calculated using Equation given in section 3.9. The electric tariff 1-200 kWh is RM 0.38 in Malaysia and RM 0.44 higher than 200 kWh. The operation time and power of each equipment are given in **Table 4.11**. The capacity of conveyor belt is 250 kg/min, and it took 0.33 hr to transport 5000 kg of the material. The shredding process takes 10 hr as the crusher has a capacity of 500 – 800 kg. The carbonization kiln has an effective volume of 4-8 m<sup>3</sup> that will take 5 hr to prepare around 1500 kg of biochar in two batches. The rotary cooler has capacity > 1.2 ton and took 2 hr to cool down the biochar to room temperature. Similar time has been reported for rotary cooler for decreasing temperature from 750 °C to less than 100 °C (Lai and Ngu, 2020). The equipment details are given in the Appendix. The total operation cost per day and per annual (320 days operation per year) for the OPF biochar at 300 °C is mentioned in **Table 4.11**.



**Table 4.11.** Electricity consumption for OPF biochar

Items	Purpose	Power (kW)	Time (hour)	Total (kWh)	Cost (RM)	
					1-200 kWh	Total
<b>Conveyor</b>	Transport OPF from Storage to crusher	1.5	0.33	0.5	0.19	0.19
<b>Shredder</b>	Cut the OPF into smaller pieces	7.5	10	75	28.5	28.5
<b>Conveyor</b>	Transport OPF from crusher to Rotary kiln	1.5	0.33	0.5	0.19	0.19
<b>Rotary kiln</b>	Carbonization of OPF at 300 °C	22	5	110	41.8	41.8
<b>Rotary cooler</b>	Cool down the biochar 300 °C prior grinding process	7.5	2	15	5.7	5.7
<b>Conveyor</b>	Transport biochar 300 °C from rotary cooler to storage tank	1.5	0.33	0.5	0.19	0.19
<b>Total cost per day</b>						<b>76.564</b>
<b>Total cost per annual (320 operation day)</b>						<b>24,500.58</b>

\*Electric Tarrif (TNB., 2014)

#### **4.10.2. Manufacturing of OPF biochar at 300 °C**

Palm oil mills with a daily supply capacity of 5,000 kg of OPF per day was chosen for this study. OPF biochar from OPF is a straightforward procedure that requires very little capital equipment. Sample preparation, crushing, and post treatment / sample collection are the unit processes. **Figure 4.25** shows the general design of the procedure and the conversion of OPF to biochar involves six processing steps. Initially, the OPF was delivered to the production side by OPF truck (step 1) and kept in the OPF storage tank (step 2) while waiting for the shredding process (step 3). 2500 kg of OPF per batch shall be added to the crusher machine through a conveyor, with a power of 1.5 kWh and a maximum capacity of 250 kg/min. The shredded OPF was then added to the rotary kiln (step 4) for pyrolysis. The OPF biochar was cooled down in a rotary cooler (step 5). Finally, it is stored in preparation for packaging (step 6). Long-term OPF storage was not included in this design since it was believed that the 5,000 kg/day of OPF would be processed on the same day.

The received dried OPF were fed into a 7.5 kW of commercial biomass crusher and shredded the OPF to 1 – 2 cm particle size. The larger particle size was recycled back to the crusher. Fine particle can be disposed or used other purposes. The process stream, with an 95% or 4,750 kg/day recovery, was directed to a rotary kiln.

Upon crushing, OPF was added to the rotary kiln and the temperature of the rotary kiln was increased to 300 °C to pyrolyze the OPF to become biochar under limited air injection for 2.5 hours. The yield of OPF biochar is approximately 30 % on dry basis. Based on the daily input of 4,750 kg of OPF, it is estimated 1,425 kg of OPF biochar will be produced respectively.

Once the pyrolysis process is completed, the OPF biochar shall be transported to a rotary cooler to cool down the biochar sample to room temperature. The rotary cooler is driven by a 7.5 Kw motor with a maximum capacity of 1.2 ton/hour. After being cooled, the OPF biochar will be stored for future packaging.

#### **4.10.3. Cost analysis**

The scale-up production cost study was performed using Ng et al. (2003) equipment design, sizing, and capital cost estimates. A comparable production system for producing activated carbon from a pecan shell was reported by (Ng *et al.*, 2003). The estimated cost of electricity consumption for OPF biochar preparation based on 5,000 kg/day OPF feed is shown in **Table 4.11** and discussed in Section 4.9.1. The estimated capital cost to produce biochar was calculated, in **Table 4.12**, according to the design flow diagram and the method discussed in Section 3.9. For the pilot plant, the price of the equipment (asset cost) and capital cost such as land, installation, building construction, engineering supervision, electrical installation etc. are given in detail in the **Table 4.12**, which shows that the estimated capital cost

of the pilot plant is RM 0.46 million. For the operation cost of 1,425 kg/day of biochar, the assumptions are discussed in Section 3.9. Therefore, 456,000 kg/year will be produced from 320 working days. **Table 4.13** shows the total operating cost of the OPF biochar. The total annual operating cost is RM 0.53 million to produced 456,000 kg/year.

**Table 4.12.** Estimated equipment capital cost for OPF biochar

<b>Equipment</b>	<b>Cost RM</b>
Shredder	5,947.89
Conveyor (3 units)	6,869.70
Rotary kiln	89,044.56
Rotary cooler	41,218.20
<b>Total equipment cost (a)</b>	<b>143,080.35</b>
Equipment installation	35,770.09
instrumentation	8,584.82
Piping and material transport (augers)	114,464.28
Electrical installation	14,308.04
Building	18,543.21
Yard improvement	14,308.08
Service facilities	42,924.11
Land	11,446.43
Engineering and supervision	42,924.11
Construction expense	2,317.90
Contractor's fee	2,317.90
Contingency	7,154.02
<b>Capital cost (b)</b>	<b>315,062.93</b>
<b>Total capital cost (c) = (a) + (b)</b>	<b>458,153.28</b>

**Table 4.13.** Estimated annual operating cost for OPF biochar

<b>Item</b>	<b>Annual operating cost (RM)</b>
<b>Raw materials</b>	
OPF	0.00
<b>Utilities</b>	
Electricity	24,500.58
<b>Labour</b>	
Operating labour	276,480.00
Maintenance labour	41,472.00
Supervision	41,472.00
Fringe benefits	44,236.8
<b>Supplies</b>	
Operating supplies	429.24
Maintenance supplies	2,861.61
<b>General works</b>	
General and administrative	55,296.00
Property insurance and tax	30,905.36
Depreciation	14,864.33
<b>Total annual operating cost</b>	<b>532,517.91</b>

The cost of the pilot plant is summarized in **Table 4.14**. The estimated OPF biochar cost is RM 2.17/kg. This study demonstrates that OPF-based biochar is simple to make and does not need tedious operations.

**Table 4.14.** Summary of the cost

<b>Items</b>	<b>Summary of costs (RM)</b>
Total equipment cost <b>(a)</b>	143,080.35
Capital cost <b>(b)</b>	315,062.93
Total fixed capital investment <b>(c) = (a) + (b)</b>	458,153.28
Total annual operating cost <b>(d)</b>	532,517.91
<b>Estimated total production cost = (c) + (d)</b>	<b>990,671.19</b>
<b>Estimated annual production of biochar (kg)</b>	<b>456,000.00</b>
<b>Estimated cost (RM/kg)</b>	<b>2.17</b>

**Table 4.15** shows the comparable price in US dollars (\$=USD) for the biochar and activated carbon production and the details of the commercial online markets is given in Appendix. Compared to activated carbon, the biochar is cheaper. If the current study is compared to commercial prices of the activated carbon/biochar and to the literature activated carbon/biochar as well the cost of our biochar is comparable to that of the literature. While much lower than commercial prices. Among the biochar cost according to literature, the biochar prepared from rice husk is the lowest (0.52 \$/kg) however, the lowest commercial price (0.77 \$/Kg) for biochar was found on online commercial selling website Lazada Malaysia. The price of OPF biochar is 0.49\$/kg (based on USD 4.4). In addition to this, the remaining cost/prices reported in literature or commercial selling website is higher.

**Table 4.15.** Comparative cost of biochar and activated carbon production

<b>Raw material</b>	<b>Material</b>	<b>Region</b>	<b>Cost/kg USD</b>	<b>Ref.</b>
Rice straw	Biochar	India	0.55	Sakhiya, Vijay and Kaushal, 2022
Rice husk	Biochar	India	0.52	Praveen <i>et al.</i> , 2021
Fruit peel	Biochar	China	4.96	Hu <i>et al.</i> , 2020
-	Commercial activated carbon	China	45.71	
Coal	Activated carbon	China	1.9	Alibaba ( <a href="https://www.alibaba.com/">https://www.alibaba.com/</a> )
Palm kernel shell	Activated carbon	China	1.19	
Orchard biomass	Biochar	USA	0.45-1.85	Nematian, Keske and Ng'ombe, 2021
Biomass from black spruce forest	Biochar	Canada	0.74	Keske <i>et al.</i> , 2020
-	Commercial Humichar	Singapore	25.62	Amazon ( <a href="https://www.amazon.sg/">https://www.amazon.sg/</a> )
-	Commercial activated carbon	Singapore	30.94	

**Table 4.15.** Continued.

<b>Raw material</b>	<b>Material</b>	<b>Region</b>	<b>Cost/kg USD</b>	<b>Ref.</b>
Oil palm wastes	Activated carbon (chemically activated)	Malaysia	2.93 -3.24	Lai and Ngu, 2020
Coconut shell	Activated carbon (physically activated)		2.73	
-	Commercial activated carbon		6.6	Shopee
-	Commercial biochar	Malaysia	1.02	( <a href="https://shopee.com.my/">https://shopee.com.my/</a> )
-	Commercial activated carbon		1.78 – 2.22	
-	Activated carbon	Malaysia	1.33	Lazada
-	Biochar		0.77	( <a href="https://www.lazada.com.my/">https://www.lazada.com.my/</a> )
Oil palm fiber	Biochar	Malaysia	0.49	This study



Based on our calculation and flow diagram, the process is very simple, and few equipment's are required for biochar production compared to literature. The raw material (OPF) used in our study is abundantly available and free of cost in Malaysia which directly affects the operating cost. Also, in our study no chemicals have been used for the activation process which makes the OPF biochar cheaper and cost effective as well as environmentally friendly.

## CHAPTER 5

### CONCLUSION AND RECOMMENDATION

#### 5.1. Conclusion

In this work, OPF biochar was tested as an adsorbent for  $\text{NH}_3\text{-N}$  recovery from AQW. Based on the experimental results, the following conclusion are made:

Physical and chemical activation of OPF biochar did not improve the adsorption efficiency of  $\text{NH}_3\text{-N}$ . Air injected OPF biochar shows better adsorption performance of  $\text{NH}_3\text{-N}$  compared to  $\text{N}_2$  biochar, due to addition of oxygen functional groups.

Upon preliminary study, air was used to prepare OPF biochar (partial oxidation). The preparation was optimized using RSM and synthetic AQW. Parameters such as carbonization temperature, holding time, and air flow were varied for biochar preparation. Biochar prepared at carbonization temperature of  $300\text{ }^\circ\text{C}$ , holding time of 2.5 hr and air flow rate of 100 ml/min shows the best recovery of  $\text{NH}_3\text{-N}$ . The adsorption efficiency and capacity were deduced as 71.6 % and 1.6 mg/g respectively at 10 ppm of synthetic  $\text{NH}_3\text{-N}$ .

ANOVA analysis presented the model for air OPF biochar preparation in line with NH<sub>3</sub>-N removal. Among the variables the carbonization temperature was the most significant. The coefficient of the determination (R<sup>2</sup>) of NH<sub>3</sub>-N is 0.98. The error between the experimental and predicted value was less than 3 % and further confirmed the validity of the model.

The adsorption process parameters have been evaluated on the OPF biochar in actual AQW. The initial concentration of the actual AQW studied was  $5.3 \pm 0.26$  ppm. The optimum adsorption efficiency of 72.6 % and capacity of 0.4 mg/g for NH<sub>3</sub>-N was achieved at conditions; contact time (3 hr), dosage (2 g), and temperature (25 °C). The removal efficiency of the OPF biochar is the same to synthetic wastewater but the capacity reduces because higher dosage was needed to recover more NH<sub>3</sub>-N from the actual AQW, due to the presence of other pollutants which hinder the performance of the OPF biochar.

The non-Linear and Linear adsorption isotherms and kinetic models represent that the non-Linear model agrees well with the experimental data. The experimental data best fit to Freundlich model compared to Langmuir model. Therefore, the adsorption is multilayer and heterogeneous onto OPF biochar. The kinetic model reveals that PSO represent the experimental data well, which means that the adsorption process is chemisorption. The non-Linear PSO represents better performance compared to the Linear model. The intraparticle diffusion model indicates strong initial adsorption, and the

intraparticle diffusion is not the rate-limiting step because the plot did not pass through the origin but with a significant intercept. The thermodynamic parameters express that the adsorption process is endothermic and spontaneous. The entropy value suggests that the randomness increases on the interface of OPF biochar during the adsorption process. In addition to this, the surface functional groups such as hydroxyl, carboxyl, and sulfonic acid on the surface of biochar adsorbed  $\text{NH}_3\text{-N}$  in which the hydrogen atom of the surface functional groups is replaced by  $\text{NH}_4^+$ .

The characterization reveals different properties of the adsorbent. The FESEM represent that the OPF biochar has well developed honeycomb like structure. The EDX result shows that various value-added metals in spent biochar are significantly reduced, which confirms the adsorption process through the ion exchange process. The BET surface area of the OPF biochar did not increase and has no correlation with the adsorption efficiency of  $\text{NH}_3\text{-N}$ . The CEC and zeta potential of biochar samples decrease with increasing carbonization temperature and exhibits direct correlation with the adsorption of  $\text{NH}_3\text{-N}$ . Furthermore, the ultimate analysis shows significant increase in weight percent of the nitrogen content which can be as a fertilizer or soil conditioner.

The cost of the OPF biochar using pilot plant scale is RM 2.17 (\$0.49). The cost analysis work suggests that production of OPF biochar is cost effective, and the price value is comparable to the biochar prepared in the literature. Further, the price of our biochar lower than the commercial

activated and can be commercialized for the treatment of the treatment of  $\text{NH}_3\text{-N}$  in low concentration as well as the OPF biochar can be used for other type of wastewater containing  $\text{NH}_3\text{-N}$  such as domestic wastewater, urban drainage wastewater, landfill leachate etc.

## 5.2. Future recommendation

The following recommendation can be made to further improve the performance of OPF based sorbent for removal of  $\text{NH}_3\text{-N}$ :

- The biochar preparation can be tested using hydrothermal carbonization. This method is expected to increase the oxygen functional groups on the surface of biochar and improve the  $\text{NH}_3\text{-N}$  adsorption.
- Biochar can be modified with different metals such as Fe, Ca, Na, Zn etc. to enhance the adsorption efficiency and simultaneously remove other pollutants.
- The column study is needed to be investigated for the removal of  $\text{NH}_3\text{-N}$  and further will extend to the treatment of the large volume of wastewater.
- More kinetics and isotherms models will be evaluated for the detail adsorption mechanism of the  $\text{NH}_3\text{-N}$  onto OPF biochar.

- The effect of co-existing ion such as  $\text{Na}^+$ ,  $\text{Ca}^{2+}$ , etc on the adsorption efficiency of  $\text{NH}_3\text{-N}$  will be evaluated.
- Test the spent biochar on plant germination study to prove the spent biochar can be applied as a plant fertilizer. The spent biochar contains adsorbed  $\text{NH}_3\text{-N}$ , thus making the spent OPF biochar a nutrient rich biochar for soil fertility.

## List of References

Abreu, M. H. *et al.* (2011) 'IMTA with *Gracilaria vermiculophylla* : Productivity and nutrient removal performance of the seaweed in a land-based pilot scale system', *Aquaculture*, 312, pp. 77–87. doi: 10.1016/j.aquaculture.2010.12.036.

Aghoghovwia, M. P., Hardie, A. G. and Rozanov, A. B. (2020) 'Characterisation, adsorption and desorption of ammonium and nitrate of biochar derived from different feedstocks', *Environmental Technology (United Kingdom)*, 43, pp. 774–787. doi: 10.1080/09593330.2020.1804466.

Ahmad, A. L. *et al.* (2022) 'Environmental impacts and imperative technologies towards sustainable treatment of aquaculture wastewater: A review', *Journal of Water Process Engineering*, 46, p. 102553. doi: 10.1016/j.jwpe.2021.102553.

Ahmad, T. *et al.* (2021) 'Evaluation of various preparation methods of oil palm fiber (OPF) biochar for ammonia-nitrogen (NH<sub>3</sub>-N) removal', in *IOP Conference Series: Earth and Environmental Science*, p. 012020. doi: 10.1088/1755-1315/945/1/012020.

Ahmad, W. *et al.* (2019) 'A review on the removal of hydrogen sulfide from biogas by adsorption using sorbents derived from waste', *Reviews in Chemical Engineering*. doi: <https://doi.org/10.1515/revce-2018-0048>.

Ahmadiannamini, P. *et al.* (2017) 'Mixed-matrix membranes for efficient ammonium removal from wastewaters', *Journal of Membrane Science*, 526, pp. 147–155. doi: 10.1016/j.memsci.2016.12.032.

Ahmed, M. B. *et al.* (2016) 'Insight into biochar properties and its cost analysis', *Biomass and Bioenergy*, 84, pp. 76–86. doi: 10.1016/j.biombioe.2015.11.002.

Akinwale, A. O., Dauda, A. B. and Ololade, O. A. (2016) 'Haematological Response of *Clarias gariepinus* Juveniles Reared in Treated Wastewater after Waste Solids Removal using Alum or *Moringa oleifera* Seed Powder', *International Journal of Aquaculture*, 6, pp. 1–8. doi: 10.5376/ija.2016.06.0011.

Ali, S. A. (2013) 'Design and evaluate a drum screen filter driven by undershot waterwheel for aquaculture recirculating systems', *Aquacultural Engineering*, 54, pp. 38–44. doi: 10.1016/j.aquaeng.2012.10.006.

Alibaba (2022) *Price for equipments*. Available at: <https://www.alibaba.com/>.

Aller, M. F. (2016) 'Biochar properties: Transport, fate, and impact', *Critical Reviews in Environmental Science and Technology*, 46, pp. 1183–1296. doi: 10.1080/10643389.2016.1212368.



Aly, H. A. *et al.* (2017) ‘The Applicability of Activated Carbon, Natural Zeolites, and Probiotics (EM®) and Its Effects on Ammonia Removal Efficiency and Fry Performance of European Seabass *Dicentrarchus labrax*’, *Journal of Aquaculture Research and Development*, 7, pp. 1–8. doi: 10.4172/2155-9546.1000459.

Amer, M. and Elwardany, A. (2020) ‘Biomass carbonization’, in Qubeissi, M. Al, El-Kharouf, A., and Soyhan, H. S. (eds) *Renewable Energy - Resources, Challenges and Applications*. Intech Publication, pp. 225–240. doi: 10.5772/intechopen.81765.

Amiri, M., Shahhosseini, S. and Ghaemi, A. (2017) ‘Optimization of CO<sub>2</sub> Capture Process from Simulated Flue Gas by Dry Regenerable Alkali Metal Carbonate Based Adsorbent Using Response Surface Methodology’, *Energy and Fuels*, 31, pp. 5286–5296. doi: 10.1021/acs.energyfuels.6b03303.

An, Q. *et al.* (2021) ‘Ammonium removal from groundwater using peanut shell based modified biochar: Mechanism analysis and column experiments’, *Journal of Water Process Engineering*, 43, p. 102219. doi: 10.1016/j.jwpe.2021.102219.

Anijiofor, S. C. *et al.* (2018) ‘Recycling of fishpond wastewater by adsorption of pollutants using aged refuse as an alternative low-cost adsorbent’, *Sustainable Environment Research*, 28, pp. 315–321. doi: 10.1016/j.serj.2018.05.005.

Barquilha, C. E. R. and Braga, M. C. B. (2021) 'Adsorption of organic and inorganic pollutants onto biochars: Challenges, operating conditions, and mechanisms', *Bioresource Technology Reports*, 15, p. 100728. doi: 10.1016/j.biteb.2021.100728.

Beckinghausen, A., Odlare, M., *et al.* (2020) 'From removal to recovery: An evaluation of nitrogen recovery techniques from wastewater', *Applied Energy*, 263, p. 114616. doi: 10.1016/j.apenergy.2020.114616.

Beckinghausen, A., Reynders, J., *et al.* (2020) 'Post-pyrolysis treatments of biochars from sewage sludge and *A. mearnsii* for ammonia (NH<sub>4</sub>-n) recovery', *Applied Energy*, 271, p. 115212. doi: 10.1016/j.apenergy.2020.115212.

Begum, S. A. *et al.* (2021) 'Adsorption characteristics of ammonium onto biochar from an aqueous solution', *Journal of Water Supply: Research and Technology - AQUA*, 70, pp. 113–122. doi: 10.2166/aqua.2020.062.

Bernal, M. P. and Lopez-Real, J. M. (1993) 'Natural zeolites and sepiolite as ammonium and ammonia adsorbent materials', *Bioresource Technology*, 43, pp. 27–33.

Bernardi, F. *et al.* (2018) 'Chitins and chitosans for the removal of total ammonia of aquaculture effluents', *Aquaculture*, 483, pp. 203–212. doi: 10.1016/j.aquaculture.2017.10.027.

Bossier, P. and Ekasari, J. (2017) 'Bio flocculation technology application in aquaculture to support sustainable development goals', *Microbial biotechnology*, 10, pp. 1012–1016. doi: 10.1111/1751-7915.12836.

Boyd, C. E. *et al.* (2000) 'Environmental Assessment of Channel Catfish *Ictalurus punctatus* Farming in Alabama', *Journal of the World Aquaculture Society*, 31(4), pp. 511–544. doi: 10.1111/j.1749-7345.2000.tb00903.x.

Boyd, C. E. and Massaut, L. (1999) 'Risks associated with the use of chemicals in pond aquaculture', *Aquacultural Engineering*, 20(2), pp. 113–132. doi: 10.1016/S0144-8609(99)00010-2.

Bratby, J. (2006) *Coagulation and Flocculation in Water and Wastewater Treatment Second Edition*.

Brownsort, P. A. (2009) *Biomass pyrolysis processes: performance parameters and their influence on biochar system benefits*. University of Edinburgh.

Brune, D. E. *et al.* (2003) 'Intensification of pond aquaculture and high rate photosynthetic systems', *Aquacultural Engineering*, 28, pp. 65–86. doi: 10.1016/S0144-8609(03)00025-6.

Buck, B. H. *et al.* (2018) 'State of the Art and Challenges for Offshore Integrated Multi-Trophic Aquaculture ( IMTA )', *Frontiers in Marine Science*, 5, pp. 1–21. doi: 10.3389/fmars.2018.00165.

Cai, Y. *et al.* (2016) 'Sorption/Desorption Behavior and Mechanism of NH<sub>4</sub><sup>+</sup> by Biochar as a Nitrogen Fertilizer Sustained-Release Material', *Journal of Agricultural and Food Chemistry*, 64, pp. 4958–4964. doi: 10.1021/acs.jafc.6b00109.

Chen, D. *et al.* (2022) 'Insight into biomass pyrolysis mechanism based on cellulose, hemicellulose, and lignin: Evolution of volatiles and kinetics, elucidation of reaction pathways, and characterization of gas, biochar and bio-oil', *Combustion and Flame*, 242, p. 112142. doi: 10.1016/j.combustflame.2022.112142.

Chen, L. *et al.* (2017) 'Environmental-friendly montmorillonite-biochar composites: Facile production and tunable adsorption-release of ammonium and phosphate', *Journal of Cleaner Production*, 156, pp. 648–659. doi: 10.1016/j.jclepro.2017.04.050.

Chen, S. *et al.* (2015) ‘A pilot-scale coupling catalytic ozonation – membrane filtration system for recirculating aquaculture wastewater treatment’, *Desalination*, 363, pp. 37–43. doi: 10.1016/j.desal.2014.09.006.

Chopin, T. *et al.* (2001) ‘Integrating seaweeds into marine aquaculture systems: a key toward sustainability’, *Journal of Phycology*, 37, pp. 975–986.

Chung, Y. C. (2006) *Improvement of aquaculture wastewater using chitosan of different degrees of deacetylation*, *Environmental Technology*. doi: 10.1080/09593332708618734.

Chung, Y. C., Li, Y. H. and Chen, C. C. (2005) *Pollutant removal from aquaculture wastewater using the biopolymer chitosan at different molecular weights*, *Journal of Environmental Science and Health*. doi: 10.1081/ESE-200068058.

Crab, R., Avnimelech, Y. and Defoirdt, T. (2007) ‘Nitrogen removal techniques in aquaculture for a sustainable production’, *Aquaculture*, 270, pp. 1–14. doi: 10.1016/j.aquaculture.2007.05.006.

Crini, G. and Lichtfouse, E. (2019) ‘Advantages and disadvantages of techniques used for wastewater treatment’, *Environmental Chemistry Letters*, 17, pp. 145–

155. doi: 10.1007/s10311-018-0785-9.

Cripps, S. J. and Bergheim, A. (2000) 'Solids management and removal for intensive land-based aquaculture production systems', *Aquacultural Engineering*, 22, pp. 33–56. doi: 10.1016/S0144-8609(00)00031-5.

Crittenden, J. C., Trussell, R. R. and Hand, D. W. (2012) *Water treatment principle and design*.

Czernik, S. and Bridgwater, A. V (2004) 'Overview of applications of biomass fast pyrolysis oil', *Energy and Fuels*, 18, pp. 590–598. doi: 10.1021/ef034067u.

Dai, Y. *et al.* (2020) 'Utilization of biochar for the removal of nitrogen and phosphorus', *Journal of Cleaner Production*, 257, p. 120573. doi: 10.1016/j.jclepro.2020.120573.

Daneshfozoun, S., Abdullah, B. and Abdullah, M. A. (2016) 'The Effects of Oil Palm Empty Fruit Bunch Sorbent Sizes on Plumbum (II) Ion Sorption', *Advanced Materials Research*, 1133, pp. 542–546. doi: 10.4028/www.scientific.net/amr.1133.542.

Daneshfozoun, S., Abdullah, M. A. and Abdullah, B. (2017) 'Preparation and characterization of magnetic biosorbent based on oil palm empty fruit bunch fibers, cellulose and Ceiba pentandra for heavy metal ions removal', *Industrial Crops and Products*, 105, pp. 93–103. doi: 10.1016/j.indcrop.2017.05.011.

Dauda, A. B. *et al.* (2018) 'Influence of carbon/nitrogen ratios on biofloc production and biochemical composition and subsequent effects on the growth, physiological status and disease resistance of African catfish (*Clarias gariepinus*) cultured in glycerol- based biofloc systems', *Aquaculture*, 483, pp. 120–130. doi: 10.1016/j.aquaculture.2017.10.016.

Dauda, A. B. *et al.* (2019) 'Waste production in aquaculture: Sources, components and managements in different culture systems', *Aquaculture and Fisheries*, 4, pp. 81–88. doi: 10.1016/j.aaf.2018.10.002.

Dauda, A. B. and Akinwale, A. O. (2014) 'Interrelationships among Water Quality Parameters in Recirculating Aquaculture System', *Nigerian Journal of Rural Extension and Development*, 8, pp. 20–25.

Dauda, A. B. and Akinwale, A. O. (2015) 'Evaluation of Polypropylene and Palm Kernel Shell As Biofilter Media for Denitrification of Fish Culture Wastewater', *NSUK journal of Science & Technology*, 5(December), pp. 1597–5527.

Dauda, A. B., Akinwale, A. O. and Olatinwo, L. K. (2014) 'Biodenitrification of Aquaculture Wastewater at Different Drying Times in Water Reuse System', *J. Agric. Food. Tech*, 4(2), pp. 6–12.

Davidson, J. and Summerfelt, S. T. (2005) *Solids removal from a coldwater recirculating system - Comparison of a swirl separator and a radial-flow settler*, *Aquacultural Engineering*. Elsevier B.V. doi: 10.1016/j.aquaeng.2004.11.002.

Davis, M. L. (2010) *Water and Wastewater Engineering*. McGraw Hill Professional.

Deng, Q., Elbeshbishy, E. and Lee, H. S. (2016) 'Simultaneous regeneration of exhausted zeolite and nitrogen recovery using an air stripping method at alkaline pH', *Water Quality Research Journal of Canada*, 51, pp. 321–330. doi: 10.2166/wqrjc.2016.007.

Deng, Y., Zhang, T. and Wang, Q. (2017) 'Biochar Adsorption Treatment for Typical Pollutants Removal in Livestock Wastewater: A Review', in *Engineering Applications of Biochar*, pp. 71–82. Available at: <http://dx.doi.org/10.1039/C7RA00172J><https://www.intechopen.com/books/advanced-biometric-technologies/liveness-detection-in-biometrics><http://dx.doi.org/10.1016/j.colsurfa.2011.12.014>.



Department of Statistics Malaysia (2020) *Selected Agricultural Indicators, Malaysia*.

DOE Malaysia (2009) *Environmental Quality Industrial Effluent Regulations 2009*.

DOF (2020) *Department of Fishery Malaysia*.

Dolan, E., Murphy, N. and Hehir, M. O. (2013) 'Aquacultural Engineering Factors influencing optimal micro-screen drum filter selection for recirculating aquaculture systems', *Aquacultural Engineering*, 56, pp. 42–50. doi: 10.1016/j.aquaeng.2013.04.005.

Ebelegi, A. N., Ayawei, N. and Wankasi, D. (2020) 'Interpretation of Adsorption Thermodynamics and Kinetics', *Open Journal of Physical Chemistry*, 10, pp. 166–182. doi: 10.4236/ojpc.2020.103010.

Ebeling, J. M., Rishel, K. L. and Sibrell, P. L. (2005) 'Screening and evaluation of polymers as flocculation aids for the treatment of aquacultural effluents', *Aquacultural Engineering*, 33, pp. 235–249. doi: 10.1016/j.aquaeng.2005.02.001.

Ebeling, J. M. and Timmons, M. B. (2012) 'Recirculating Aquaculture Systems', in *Aquaculture production system*. A publication of World Aquaculture Society. John Willey & Sons, Inc, pp. 245–277.

Ebeling, J. M., Welsh, C. F. and Rishel, K. L. (2006) 'Performance evaluation of an inclined belt filter using coagulation/flocculation aids for the removal of suspended solids and phosphorus from microscreen backwash effluent', *Aquacultural Engineering*, 35, pp. 61–77. doi: 10.1016/j.aquaeng.2005.08.006.

Ekasari, J., Crab, R. and Verstraete, W. (2010) 'Primary Nutritional Content of Bio-Flocs Cultured with Different Organic Carbon Sources and Salinity', *HAYATI Journal of Biosciences*, 17(3), pp. 125–130. doi: 10.4308/hjb.17.3.125.

El-sherbiny, M. A., El-chaghaby, G. A. and El-Shafea, Y. M. A. (2019) 'Treatment of aquaculture waste effluent to be reused in fish culture in Egypt', *Egyptian Journal of Aquatic Biology & Fisheries*, 23, pp. 233–243.

Ellersdorfer, M. (2018) 'The ion-exchanger-loop-stripping process: Ammonium recovery from sludge liquor using NaCl-treated clinoptilolite and simultaneous air stripping', *Water Science and Technology*, 77, pp. 695–705. doi: 10.2166/wst.2017.561.

Fang, C. *et al.* (2015) 'Phosphorus recovery from biogas fermentation liquid by Ca-Mg loaded biochar', *Journal of Environmental Sciences*, 29, pp. 106–114. doi: 10.1016/j.jes.2014.08.019.

FAO (2018) *Food and agriculture data*.

FAO (2020) *The State of World Fisheries and Aquaculture Sustainability in Action*.

FAO (2021) *National Aquaculture Sector Overview Malaysia*.

Fatimah, N. *et al.* (2019) 'The role of microbial quorum sensing on the characteristics and functionality of bioflocs in aquaculture systems', *Aquaculture*, 504, pp. 420–426. doi: 10.1016/j.aquaculture.2019.02.022.

Gai, X. *et al.* (2014) 'Effects of feedstock and pyrolysis temperature on biochar adsorption of ammonium and nitrate', *PLOS ONE*, 9, pp. 1–19. doi: 10.1371/journal.pone.0113888.

Gao, F. *et al.* (2015) 'Removal of aqueous ammonium by biochars derived from agricultural residuals at different pyrolysis temperatures', *Chemical Speciation and Bioavailability*, 27(2), pp. 92–97. doi: 10.1080/09542299.2015.1087162.

Godini, H. *et al.* (2017) 'Efficiency of Powdery Activated carbon in Ammonia-Nitrogen Removal from Aqueous Environments (Response Surface Methodology)', *Archives of Hygiene Sciences*, 6, pp. 111–120. doi: 10.29252/archhygsci.6.2.111.

Goh, C. L. *et al.* (2019) 'Adsorptive behaviour of palm oil mill sludge biochar pyrolyzed at low temperature for copper and cadmium removal', *Journal of Environmental Management*, 237, pp. 281–288. doi: 10.1016/j.jenvman.2018.12.103.

Gong, H. *et al.* (2019) 'Preparation of biochar with high absorbability and its nutrient adsorption–desorption behaviour', *Science of the Total Environment*, 694, p. 133728. doi: 10.1016/j.scitotenv.2019.133728.

Hafshejani, L. D. *et al.* (2016) 'Removal of nitrate from aqueous solution by modified sugarcane bagasse biochar', *Ecological Engineering*, 95, pp. 101–111. doi: 10.1016/j.ecoleng.2016.06.035.

Hailegnaw, N. S. *et al.* (2019) 'High temperature-produced biochar can be efficient in nitrate loss prevention and carbon sequestration', *Geoderma*, 338, pp. 48–55. doi: 10.1016/j.geoderma.2018.11.006.

Hale, S. E. *et al.* (2013) 'The sorption and desorption of phosphate-P, ammonium-N and nitrate-N in cacao shell and corn cob biochars', *Chemosphere*, 91(11), pp. 1612–1619. doi: 10.1016/j.chemosphere.2012.12.057.

Hall, K. R. *et al.* (1966) 'Pore-and solid-diffusion kinetics in fixed-bed adsorption under constant-pattern conditions', *Industrial and Engineering Chemistry Fundamentals*, 5, pp. 212–223. doi: 10.1021/i160018a011.

Hargreaves, J. A. and Tucker, C. S. (2004) 'Managing Ammonia in Fish Ponds', *Southern Regional Aquaculture Centre (SRAC) Publication*, (4603), pp. 1–8.

Hsu, D. *et al.* (2019) 'Adsorption of ammonium nitrogen from aqueous solution on chemically activated biochar prepared from sorghum distillers grain', *Applied Sciences*, 9, p. 5249. doi: 10.3390/app9235249.

Hu, X. *et al.* (2020) 'Comparison study on the ammonium adsorption of the biochars derived from different kinds of fruit peel', *Science of the Total Environment*, 707, p. 135544. doi: 10.1016/j.scitotenv.2019.135544.

Huff, M. D. and Lee, J. W. (2016) 'Biochar-surface oxygenation with hydrogen peroxide', *Journal of Environmental Management*, 165, pp. 17–21. doi: 10.1016/j.jenvman.2015.08.046.

Hussain, S. *et al.* (2007) ‘Physico-chemical method for ammonia removal from synthetic wastewater using limestone and GAC in batch and column studies’, *Bioresource Technology*, 98, pp. 874–880. doi: 10.1016/j.biortech.2006.03.003.

Iber, B. T. and Kasan, N. A. (2021) ‘Recent advances in Shrimp aquaculture wastewater management’, *Heliyon*, 7, p. e08283. doi: 10.1016/j.heliyon.2021.e08283.

Iberahim, N. *et al.* (2019) ‘Optimization of activated palm oil sludge biochar preparation for sulphur dioxide adsorption’, *Journal of Environmental Management*, 248, p. 109302. doi: 10.1016/j.jenvman.2019.109302.

Iberahim, N. *et al.* (2022) ‘Evaluation of oil palm fiber biochar and activated biochar for sulphur dioxide adsorption’, *Science of the Total Environment*, 805, p. 150421. doi: 10.1016/j.scitotenv.2021.150421.

Ibrahim, I. *et al.* (2021) ‘Surface Functionalization of Biochar from Oil Palm Empty Fruit Bunch through Hydrothermal Process’, *Processes*, 9, pp. 1–14.

Ismadji, S. *et al.* (2016) ‘Bentonite hydrochar composite for removal of ammonium from Koi fish tank’, *Applied Clay Science*, 119, pp. 146–154. doi: 10.1016/j.clay.2015.08.022.

Ismail, Y. M. N. S. *et al.* (2018) 'Preparation of activated carbon from oil palm empty fruit bunch by physical activation for treatment of landfill leachate', in *IOP Conference Series: Materials Science and Engineering*, p. 012036. doi: 10.1088/1757-899X/458/1/012036.

Israel, D., Lupatsch, I. and Angel, D. L. (2019) 'Testing the digestibility of seabream wastes in three candidates for integrated multi-trophic aquaculture : Grey mullet , sea urchin and sea cucumber', *Aquaculture*, 510, pp. 364–370. doi: 10.1016/j.aquaculture.2019.06.003.

Jafri, N. H. S. *et al.* (2021) 'The potential of biomass waste in Malaysian palm oil industry: A case study of Boustead Plantation Berhad', *IOP Conference Series: Materials Science and Engineering*, 1192, p. 012028. doi: 10.1088/1757-899x/1192/1/012028.

Jamil, N. *et al.* (2014) 'Removal of direct red 16 (Textile Dye) from industrial effluent by using feldspar', *Journal of the Chemical Society of Pakistan*, 36, pp. 191–197.

Jegatheesan, V. *et al.* (2007) 'Technological advances in aquaculture farms for minimal effluent discharge to oceans', *Journal of Cleaner Production*, 15, pp. 1535–1544. doi: 10.1016/j.jclepro.2006.07.043.

Jeyasubramanian, K. *et al.* (2021) ‘A complete review on biochar: Production, property, multifaceted applications, interaction mechanism and computational approach’, *Fuel*, 292, p. 120243. doi: 10.1016/j.fuel.2021.120243.

John, E. M., Krishnapriya, K. and Sankar, T. V (2020) ‘Treatment of ammonia and nitrite in aquaculture wastewater by an assembled bacterial consortium’, *Aquaculture*, 526, p. 735390. doi: 10.1016/j.aquaculture.2020.735390.

Jones, E. R. *et al.* (2021) ‘Country-level and gridded estimates of wastewater production, collection, treatment and reuse’, *Earth System Science Data*, 13(2), pp. 237–254. doi: 10.5194/essd-13-237-2021.

Joseph, S. *et al.* (2013) ‘Shifting paradigms: Development of high-efficiency biochar fertilizers based on nano-structures and soluble components’, *Carbon Management*, 4, pp. 323–343. doi: 10.4155/cmt.13.23.

Kambo, H. S. and Dutta, A. (2015) ‘A comparative review of biochar and hydrochar in terms of production, physico-chemical properties and applications’, *Renewable and Sustainable Energy Reviews*, 45, pp. 359–378. doi: 10.1016/j.rser.2015.01.050.



Kaniapan, S. *et al.* (2021) 'The utilisation of palm oil and oil palm residues and the related challenges as a sustainable alternative in biofuel, bioenergy, and transportation sector: A review', *Sustainability*, 13, pp. 1–25. doi: 10.3390/su13063110.

Karia, M. T. *et al.* (2022) 'Remediation of aquaculture effluents using physical treatment', *Materials Today: Proceedings*, 57, pp. 1196–1201. doi: 10.1016/j.matpr.2021.10.386.

Karunanithi, R. *et al.* (2017) 'Sorption, kinetics and thermodynamics of phosphate sorption onto soybean stover derived biochar', *Environmental Technology and Innovation*, 8, pp. 113–125. doi: 10.1016/j.eti.2017.06.002.

Keske, C. *et al.* (2020) 'Economic feasibility of biochar and agriculture coproduction from Canadian black spruce forest', *Food and Energy Security*, 9, pp. 1–11. doi: 10.1002/fes3.188.

Khalil, A., Sergeevich, N. and Borisova, V. (2018) 'Removal of ammonium from fish farms by biochar obtained from rice straw: Isotherm and kinetic studies for ammonium adsorption', *Adsorption Science & Technology*, 36, pp. 1294–1309. doi: 10.1177/0263617418768944.

Khatun, R. *et al.* (2017) 'Sustainable oil palm industry: The possibilities', *Renewable and Sustainable Energy Reviews*, 76(December 2016), pp. 608–619. doi: 10.1016/j.rser.2017.03.077.

Khiari, Z. *et al.* (2020) 'Integration of Biochar Filtration into Aquaponics: Effects on Particle Size Distribution and Turbidity Removal', *Agricultural Water Management*, 229, p. 105874. doi: 10.1016/j.agwat.2019.105874.

Kim, D. W. *et al.* (2020) 'Efficient removals of Hg and Cd in aqueous solution through NaOH-modified activated carbon fiber', *Chemical Engineering Journal*, 392, p. 123768. doi: 10.1016/j.cej.2019.123768.

Kioussis, D. R., Wheaton, F. W. and Kofinas, P. (2000) 'Reactive nitrogen and phosphorus removal from aquaculture wastewater effluents using polymer hydrogels', *Aquacultural Engineering*, 23, pp. 315–332.

Kizito, S. *et al.* (2015) 'Evaluation of slow pyrolyzed wood and rice husks biochar for adsorption of ammonium nitrogen from piggery manure anaerobic digestate slurry', *Science of the Total Environment*, 505, pp. 102–112. doi: 10.1016/j.scitotenv.2014.09.096.

Kizito, S. *et al.* (2017) 'Phosphate recovery from liquid fraction of anaerobic digestate using four slow pyrolyzed biochars: Dynamics of adsorption, desorption and regeneration', *Journal of Environmental Management*, 201, pp. 260–267. doi: 10.1016/j.jenvman.2017.06.057.

Kong, S. *et al.* (2014) 'Biochar from oil palm biomass: A review of its potential and challenges', *Renewable and Sustainable Energy Reviews*, 39, pp. 729–739. doi: 10.1016/j.rser.2014.07.107.

Kurniawan, S. B. *et al.* (2021) 'Potential of valuable materials recovery from aquaculture wastewater: An introduction to resource reclamation', *Aquaculture Research*, 52(7), pp. 2954–2962. doi: 10.1111/are.15180.

Kurniawan, S. B. *et al.* (2022) 'Treatment of real aquaculture effluent using bacteria-based bioflocculant produced by *Serratia marcescens*', *Journal of Water Process Engineering*, 47, p. 102708. doi: 10.1016/j.jwpe.2022.102708.

Lai, J. Y. and Ngu, L. H. (2020) 'The production cost analysis of oil palm waste activated carbon: a pilot-scale evaluation', *Greenhouse Gases Science and Technology*, 10, pp. 999–1026. doi: 10.1002/ghg.2020.

Lazzari, R. and Baldisserotto, B. (2008) 'Nitrogen and Phosphorus Waste in Fish Farming', *Boletim do Instituto de Pesca*, 34(4), pp. 591–600.

Lee, J. (2014) 'Aquacultural Engineering Separation of fine organic particles by a low-pressure hydrocyclone (LPH)', *Aquacultural Engineering*, 63, pp. 32–38. doi: 10.1016/j.aquaeng.2014.07.002.

Lee, J. (2015) 'Aquacultural Engineering Practical applications of low-pressure hydrocyclone ( LPH ) for feed waste and fecal solid removal in a recirculating aquaculture system', *Aquacultural Engineering*, 69, pp. 37–42. doi: 10.1016/j.aquaeng.2015.08.003.

Lehr, J. H. and Keeley, J. (2005) *Domestic, Municipal, and Industrial Water Supply and Waste Disposal*. Hoboken, New Jersey: John Wiley & Sons, Inc.  
Available at:  
[http://www.eng.auth.gr/~pmavros/pubs/pdf\\_books/2005\\_mavros\\_book\\_mixing\\_water\\_encyclopedia.pdf](http://www.eng.auth.gr/~pmavros/pubs/pdf_books/2005_mavros_book_mixing_water_encyclopedia.pdf).

Lekang, O. (2007) *Aquaculture Engineering*.

Lepine, C. *et al.* (2018) 'Woodchip bioreactors as treatment for recirculating aquaculture systems ' wastewater : A cost assessment of nitrogen removal', *Aquacultural Engineering*, 83, pp. 85–92. doi: 10.1016/j.aquaeng.2018.09.001.

Li, B. *et al.* (2021) 'Simultaneous recovery of nitrogen and phosphorus from biogas slurry by Fe-modified biochar', *Journal of Saudi Chemical Society*, 25, p. 101213. doi: 10.1016/j.jscs.2021.101213.

Li, Changwei *et al.* (2019) 'Bioresource Technology Performance and microbial community analysis of Combined Denitrification and Biofloc Technology ( CDBFT ) system treating nitrogen-rich aquaculture wastewater', *Bioresource Technology*, 288, p. 121582. doi: 10.1016/j.biortech.2019.121582.

Li, Chunjie *et al.* (2019) 'Performance of a pilot-scale aquaponics system using hydroponics and immobilized biofilm treatment for water quality control', *Journal of Cleaner Production*, 208, pp. 274–284. doi: 10.1016/j.jclepro.2018.10.170.

Li, L. *et al.* (2019) 'Biochar as a sorbent for emerging contaminants enables improvements in waste management and sustainable resource use', *Journal of Cleaner Production*, 210, pp. 1324–1342. doi: 10.1016/j.jclepro.2018.11.087.

Li, R. *et al.* (2017) 'Simultaneous capture removal of phosphate, ammonium and organic substances by MgO impregnated biochar and its potential use in swine wastewater treatment', *Journal of Cleaner Production*, 147, pp. 96–107. doi: 10.1016/j.jclepro.2017.01.069.

Li, S. *et al.* (2018) 'Nitrogen retention of biochar derived from different feedstocks at variable pyrolysis temperatures', *Journal of Analytical and Applied Pyrolysis*, 133, pp. 136–146. doi: 10.1016/j.jaap.2018.04.010.

Li, X. *et al.* (2013) 'Functional Groups Determine Biochar Properties (pH and EC) as Studied by Two-Dimensional <sup>13</sup>C NMR Correlation Spectroscopy', *Plos One*, 8, p. e65949. doi: 10.1371/journal.pone.0065949.

Lievens, C. *et al.* (2015) 'Organic compounds leached from fast pyrolysis mallee leaf and bark biochars', *Chemosphere*, 139, pp. 659–664. doi: 10.1016/j.chemosphere.2014.11.009.

Liltved, H. and Landfald, B. (1995) 'Use of alternative disinfectants, individually and in combination, in aquacultural wastewater treatment', *Aquaculture research*, 26, pp. 567–576.

Ling, C. and Weimin, W. (2010) 'Wastewater Management in Freshwater Pond Aquaculture in China', in *Sustainability in Food and Water An Asian Perspective*, pp. 181–190. doi: 10.1007/978-90-481-9914-3.

Liu, H. *et al.* (2010) 'Ammonium adsorption from aqueous solutions by strawberry leaf powder: Equilibrium, kinetics and effects of coexisting ions', *Desalination*, 263, pp. 70–75. doi: 10.1016/j.desal.2010.06.040.

Liu, H. *et al.* (2019) 'Biofloc formation improves water quality and fish yield in a freshwater pond aquaculture system', *Aquaculture*, 506, pp. 256–269. doi: 10.1016/j.aquaculture.2019.03.031.

Liu, P. *et al.* (2022) 'Adsorption Mechanism of High-Concentration of Ammonium onto Chinese Natural Zeolite by Experimental Optimization and Theoretical Computation', *Water*, 14, p. 2413.

Liu, W. *et al.* (2019) 'Pilot study on water quality regulation in a recirculating aquaculture system with suspended growth bioreactors', *Aquaculture*, 504, pp. 396–403. doi: 10.1016/j.aquaculture.2019.01.057.

Liu, X., Shen, F. and Qi, X. (2019) 'Adsorption recovery of phosphate from aqueous solution by CaO-biochar composites prepared from eggshell and rice straw', *Science of the Total Environment*, 666, pp. 694–702. doi: 10.1016/j.scitotenv.2019.02.227.

Long, X.-L. *et al.* (2008) 'Adsorption of Ammonia on Activated Carbon from Aqueous Solutions', *Environmental Progress*, 27, pp. 225–233. doi: 10.1002/ep.

Lubensky, J. and Ellersdorfer, M. (2021) 'Pilot scale experiments for ammonium recovery from sludge liquor at a municipal waste water treatment plant', *Journal of Sustainable Development of Energy, Water and Environment Systems*, 9, p. 1080349. doi: 10.13044/j.sdewes.d8.0349.

Luo, G. *et al.* (2014) 'Growth, digestive activity, welfare , and partial cost-effectiveness of genetically improved farmed tilapia (*Oreochromis niloticus* ) cultured in a recirculating aquaculture system and an indoor bio floc system', *Aquaculture*, 423, pp. 1–7. doi: 10.1016/j.aquaculture.2013.11.023.

Lv, R. *et al.* (2021) 'Adsorption and leaching characteristics of ammonium and nitrate from paddy soil as affected by biochar amendment', *Plant, Soil and Environment*, 67, pp. 8–17. doi: 10.17221/276/2020-PSE.



Malone, R. F. and Beecher, L. E. (2000) 'Use of floating bead filters to recondition recirculating waters in warmwater aquaculture production systems', *Aquacultural Engineering*, 22, pp. 57–73.

Malone, R. F. and Pfeiffer, T. J. (2006) 'Rating fixed film nitrifying biofilters used in recirculating aquaculture systems', *Aquacultural Engineering*, 34, pp. 389–402. doi: 10.1016/j.aquaeng.2005.08.007.

Marcińczyk, M., Ok, Y. S. and Oleszczuk, P. (2022) 'From waste to fertilizer: Nutrient recovery from wastewater by pristine and engineered biochars', *Chemosphere*, 306, p. 135310. doi: 10.1016/j.chemosphere.2022.135310.

Marsin, F. M. *et al.* (2018) 'Recent advances in the preparation of oil palm waste-based adsorbents for removal of environmental pollutants-A review', *Malaysian Journal of Analytical Sciences*, 22, pp. 175–184.

Martan, E. (2008) 'Polyculture of Fishes in Aquaponics and Recirculating Aquaculture', *Acquaphonics Journal*, (48), pp. 28–33.

Martins, C. I. M. *et al.* (2010) 'New developments in recirculating aquaculture systems in Europe: A perspective on environmental sustainability', *Aquacultural Engineering*, 43(3), pp. 83–93. doi:

10.1016/j.aquaeng.2010.09.002.

Meng, F. *et al.* (2019) 'Assessment of nutrient removal and microbial population dynamics in a non-aerated vertical baffled flow constructed wetland for contaminated water treatment with composite biochar addition', *Journal of Environmental Management*, 246, pp. 355–361. doi: 10.1016/j.jenvman.2019.06.011.

Metcalf and Eddy (2003) *Wastewater Engineering - Treatment and Reuse*. 4th edn. McGraw-Hill.

Michels, M. H. A. *et al.* (2014) 'Growth of *Tetraselmis suecica* in a tubular photobioreactor on wastewater from a fish farm', *Water research*, 65, pp. 290–296. doi: 10.1016/j.watres.2014.07.017.

Min, H., Ahmad, T. and Lee, S.-S. (2017) 'Mercury adsorption characteristics as dependent upon the physical properties of activated carbon', *Energy and Fuels*, 31, pp. 724–729. doi: 10.1021/acs.energyfuels.6b02246.

Mohan, D., Pittman, C. U. J. and Steele, P. H. (2006) 'Pyrolysis of wood/biomass for bio-oil: A critical review', *Energy and Fuels*, 20, pp. 848–889. doi: 10.1021/ef0502397.

Moon, W. C. *et al.* (2017) 'Shrimp Pond Wastewater Treatment Using Pyrolyzed Chicken Feather as Adsorbent', in *AIP Conference Proceedings*, pp. 1–8. doi: 10.1063/1.5005702.

Mukherjee, A., Zimmerman, A. R. and Harris, W. (2011) 'Surface chemistry variations among a series of laboratory-produced biochars', *Geoderma*, 163, pp. 247–255. doi: 10.1016/j.geoderma.2011.04.021.

Mumme, J. *et al.* (2011) 'Hydrothermal carbonization of anaerobically digested maize silage', *Bioresource Technology*, 102, pp. 9255–9260. doi: 10.1016/j.biortech.2011.06.099.

Murithi, G., Onindo, C. O. and Muthakia, G. K. (2012) 'Kinetic and equilibrium study for the sorption of Pb(II) ions from aqueous phase by water hyacinth (*Eichhornia crassipes*)', *Bulletin of the Chemical Society of Ethiopia*, 26, pp. 181–193. doi: 10.4314/bcse.v26i2.3.

Nasir, N. *et al.* (2018) 'Utilization of empty fruit bunch fibre as potential adsorbent for ammonia nitrogen removal in natural rubber wastewater', *International Journal of Integrated Engineering*, 10(8), pp. 27–32. doi: 10.30880/ijie.2018.10.08.009.

Ndubuisi, U. C. *et al.* (2015) 'Effect of pH on the growth performance and survival rate of *Clarias gariepinus* fry', *International Journal of Research in Biosciences*, 4, pp. 14–20.

Nematian, M., Keske, C. and Ng'ombe, J. N. (2021) 'A techno-economic analysis of biochar production and the bioeconomy for orchard biomass', *Waste Management*, 135, pp. 467–477. doi: 10.1016/j.wasman.2021.09.014.

Neori, A. *et al.* (2004) 'Integrated aquaculture : rationale , evolution and state of the art emphasizing seaweed biofiltration in modern mariculture', *Aquaculture*, 231, pp. 361–391. doi: 10.1016/j.aquaculture.2003.11.015.

Nezhadheydari, H. *et al.* (2019) 'Effects of different concentrations of Fe<sub>3</sub>O<sub>4</sub>@ZnO and Fe<sub>3</sub>O<sub>4</sub>@CNT magnetic nanoparticles separately and in combination on aquaculture wastewater treatment', *Environmental Technology & Innovation*, 15, p. 100414. doi: 10.1016/j.eti.2019.100414.

Ng, C. *et al.* (2003) 'Activated carbon from pecan shell: Process description and economic analysis', *Industrial Crops and Products*, 17, pp. 209–217. doi: 10.1016/S0926-6690(03)00002-5.

Ng, Y. S. and Chan, D. J. C. (2021) 'The enhancement of treatment capacity and the performance of phytoremediation system by fed batch and periodic harvesting', *RSC Advances*, 11, pp. 6049–6059. doi: 10.1039/d0ra08088h.

Niyousha, K. M. *et al.* (2020) 'Experimental investigation and modeling of CO<sub>2</sub> adsorption using modified activated carbon', *Iranian Journal of Chemistry and Chemical Engineering*, 39, pp. 177–192. doi: 10.30492/IJCCE.2020.37648.

Onay, O. and Kockar, O. M. (2003) 'Slow, fast and flash pyrolysis of rapeseed', *Renewable Energy*, 28, pp. 2417–2433. doi: 10.1016/S0960-1481(03)00137-X.

Otieno, A. O. *et al.* (2021) 'Pineapple peel biochar and lateritic soil as adsorbents for recovery of ammonium nitrogen from human urine', *Journal of Environmental Management*, 293, p. 112794. doi: 10.1016/j.jenvman.2021.112794.

Park, J. H. *et al.* (2018) 'Effect of pyrolysis temperature on phosphate adsorption characteristics and mechanisms of crawfish char', *Journal of Colloid and Interface Science*, 525, pp. 143–151. doi: 10.1016/j.jcis.2018.04.078.

Peters, M. S. and Timmerhaus, K. D. (1991) *Plant design and economics for chemical engineers, Plant design and economics for chemical engineers*. New York: McGraw-Hill.

Pfeiffer, T. J., Osborn, A. and Davis, M. (2008) 'Particle sieve analysis for determining solids removal efficiency of water treatment components in a recirculating aquaculture system', *Aquacultural Engineering*, 39(1), pp. 24–29. doi: 10.1016/j.aquaeng.2008.05.003.

Pholosi, A., Naidoo, E. B. and Ofomaja, A. E. (2020) 'Intraparticle diffusion of Cr(VI) through biomass and magnetite coated biomass: A comparative kinetic and diffusion study', *South African Journal of Chemical Engineering*, 32, pp. 39–55. doi: 10.1016/j.sajce.2020.01.005.

Poli, M. A. *et al.* (2019) 'Integrated multitrophic aquaculture applied to shrimp rearing in a bio floc system', *Aquacultural Engineering*, 511, pp. 1–6. doi: 10.1016/j.aquaculture.2019.734274.

Praveen, S. *et al.* (2021) 'Techno-economic feasibility of biochar as biosorbent for basic dye sequestration', *Journal of the Indian Chemical Society*, 98, p. 100107. doi: 10.1016/j.jics.2021.100107.

Pungrasmi, W., Phinitthanaphak, P. and Powtongsook, S. (2016) 'Nitrogen removal from a recirculating aquaculture system using a pumice bottom substrate nitrification-denitrification tank', *Ecological Engineering*, 95, pp. 357–363. doi: 10.1016/j.ecoleng.2016.06.094.

Qiu, G. *et al.* (2019) 'Biochar synthesized via pyrolysis of *Broussonetia papyrifera* leaves: mechanisms and potential applications for phosphate removal', *Environmental Science and Pollution Research*, 26, pp. 6565–6575. doi: 10.1007/s11356-018-04095-w.

Raghav, S. and Kumar, D. (2018) 'Adsorption Equilibrium, Kinetics, and Thermodynamic Studies of Fluoride Adsorbed by Tetrametallic Oxide Adsorbent', *Journal of Chemical and Engineering Data*, 63, pp. 1682–1697. doi: 10.1021/acs.jced.8b00024.

Rahman, M. Y. A., Nachabe, M. H. and Ergas, S. J. (2020) 'Biochar amendment of stormwater bioretention systems for nitrogen and *Escherichia coli* removal: Effect of hydraulic loading rates and antecedent dry periods', *Bioresource Technology*, 310, p. 123428. doi: 10.1016/j.biortech.2020.123428.

Rajasulochana, P. and Preethy, V. (2016) 'Comparison on efficiency of various techniques in treatment of waste and sewage water – A comprehensive review', *Resource-Efficient Technologies*, 2, pp. 175–184. doi:

10.1016/j.refit.2016.09.004.

Rashed, M. N. (2013) 'Adsorption Technique for the Removal of Organic Pollutants from Water and Wastewater', in *Organic pollutants-Monitoring, Risk and Treatment*, pp. 167–194. Available at: <https://www.intechopen.com/books/advanced-biometric-technologies/liveness-detection-in-biometrics>.

Rashidi, N. A. and Yusup, S. (2020) 'A Mini Review of Biochar Synthesis, Characterization, and Related Standardization and Legislation', in Ahmed, A. and Mohamed, A. (eds) *Applications of Biochar for Environmental Safety*, pp. 1–276. doi: 10.5772/intechopen.87828.

Ricky, L. N. S. *et al.* (2016) 'Ammonia-nitrogen removal from urban drainage using modified fresh empty fruit bunches: A case study in Kota Kinabalu, Sabah', in *IOP Conference Series: Earth and Environmental Science*, p. 012055. doi: 10.1088/1755-1315/36/1/012055.

Rippy, J. F. M. and Nelson, P. V. (2007) 'Cation exchange capacity and base saturation variation among Alberta, Canada, moss peats', *HortScience*, 42(2), pp. 349–352. doi: 10.21273/hortsci.42.2.349.



Rishel, K. L. and Ebeling, J. M. (2006) 'Screening and Evaluation of Alum and Polymer Combinations as Coagulation/Flocculation Aids to Treat Effluents from Intensive Aquaculture Systems', *Journal Of The World Aquaculture Society*, 37(2), pp. 191–199.

Rogers, G. L. (1989) 'Short Communication Aeration and Circulation for Effective Aquaculture Pond Management', *Aquacultural Engineering*, pp. 349–355.

Romano, N. and Zeng, C. (2013) 'Toxic Effects of Ammonia, Nitrite, and Nitrate to Decapod Crustaceans: A Review on Factors Influencing their Toxicity, Physiological Consequences, and Coping Mechanisms', *Reviews in Fisheries Science*, 21, pp. 1–21. doi: 10.1080/10641262.2012.753404.

Roy, K., Kar, S. and Das, R. N. (2015) 'Background of QSAR and Historical Developments', in *Understanding the Basics of QSAR for Applications in Pharmaceutical Sciences and Risk Assessment*. Elsevier, pp. 1–46. doi: 10.1016/b978-0-12-801505-6.00001-6.

Şahin, D. *et al.* (2018) 'Evaluation of Natural Minerals (Zeolite and Bentonite) for Nitrogen Compounds Adsorption in Different Water Temperatures Suitable for Aquaculture', *International Letters of Natural Sciences*, 71, pp. 34–42. doi: 10.18052/www.scipress.com/ILNS.71.34.

Sakhiya, A. K., Vijay, V. K. and Kaushal, P. (2022) 'Efficacy of rice straw derived biochar for removal of Pb<sup>+2</sup> and Zn<sup>+2</sup> from aqueous: Adsorption, thermodynamic and cost analysis', *Bioresource Technology Reports*, 17, p. 100920. doi: 10.1016/j.biteb.2021.100920.

Saletnik, B. *et al.* (2019) 'Biochar as a multifunctional component of the environment-a review', *Applied Sciences (Switzerland)*, 9, p. 1139. doi: 10.3390/app9061139.

Saliu, T. D. *et al.* (2019) 'Expounding the role of interference on the recovery of nutrient fractions from aqua matrix using calcined gastropod shell', *Journal of Water Process Engineering journal homepage*, 27, pp. 152–161. doi: 10.1016/j.jwpe.2018.12.004.

Saxena, A. *et al.* (2022) 'Growth of marine diatoms on aquaculture wastewater supplemented with nanosilica', *Bioresource Technology*, 344, p. 126210. doi: 10.1016/j.biortech.2021.126210.

SEAFDEC (2018) *Fishery Statistical Bulletin of Southeast Asia*.

Sgnaulin, T. *et al.* (2018) 'Bio flocculation technology ( BFT ): An alternative aquaculture system for piracanjuba *Brycon orbignyanus*?' , *Aquaculture*, 485(May 2017), pp. 119–123. doi: 10.1016/j.aquaculture.2017.11.043.

Shaaban, A. *et al.* (2014) 'Influence of heating temperature and holding time on biochars derived from rubber wood sawdust via slow pyrolysis', *Journal of Analytical and Applied Pyrolysis*, 107, pp. 31–39. doi: 10.1016/j.jaap.2014.01.021.

Shakoor, M. B. *et al.* (2020) 'A review of biochar-based sorbents for separation of heavy metals from water', *International Journal of Phytoremediation*, 22, pp. 111–126. doi: 10.1080/15226514.2019.1647405.

Shang, L. *et al.* (2018) 'Adsorption of Ammonium in Aqueous Solutions by the Modified Biochar and its Application as an Effective N-Fertilizer', *Water, Air, & Soil Pollution*, 229, p. 320.

Sharrer, M. J., Rishel, K. and Summerfelt, S. (2009) 'Evaluation of geotextile filtration applying coagulant and flocculant amendments for aquaculture biosolids dewatering and phosphorus removal', *Aquacultural Engineering*, 40, pp. 1–10. doi: 10.1016/j.aquaeng.2008.10.001.

Shi, M., Wang, Z. and Zheng, Z. (2013) 'Effect of Na<sup>+</sup> impregnated activated carbon on the adsorption of NH<sub>4</sub><sup>+</sup>-N from aqueous solution', *Journal of Environmental Sciences*, 25, pp. 1501–1510. doi: 10.1016/S1001-0742(8)60227-7.

Shim, J. W., Park, S. J. and Ryu, S. K. (2001) 'Effect of modification with HNO<sub>3</sub> and NaOH on metal adsorption by pitch-based activated carbon fibers', *Carbon*, 39, pp. 1635–1642. doi: 10.1016/S0008-6223(00)00290-6.

Shpigel, M. *et al.* (2016) 'Nutrient recovery and sludge management in seabream and grey mullet co-culture in Integrated Multi-Trophic Aquaculture ( IMTA )', *Aquaculture*, 464, pp. 316–322. doi: 10.1016/j.aquaculture.2016.07.007.

Sichula, J. *et al.* (2011) 'Removal of ammonia from aquaculture water using maize cob activated carbon', *Malawi j. aquac. fish*, 1, pp. 10–15.

Song, H. *et al.* (2019) 'Potential of novel biochars produced from invasive aquatic species outside food chain in removing ammonium nitrogen: Comparison with conventional biochars and clinoptilolite', *Sustainability*, 11, p. 7136. doi: 10.3390/su11247136.

Souza, J. *et al.* (2019) ‘Does the biofloc size matter to the nitrification process in Biofloc Technology ( BFT ) systems ?’, *Aquaculture*, 500, pp. 443–450. doi: 10.1016/j.aquaculture.2018.10.051.

Stamenković, M., Steinwall, E. and Wulff, A. (2021) ‘Cultivation and Photophysiological Characteristics of Desmids in Moderately Saline Aquaculture Wastewater’, *Journal of Phycology*, 57, pp. 726–741. doi: 10.1111/jpy.13150.

Stávková, J. and Maroušek, J. (2021) ‘Novel sorbent shows promising financial results on P recovery from sludge water’, *Chemosphere*, 276, p. 130097. doi: 10.1016/j.chemosphere.2021.130097.

Stechemesser, H. and Dobiás, B. (2005) *Coagulation and Flocculation*.

Steicke, C., Jegatheesan, V. and Zeng, C. (2007) ‘Mechanical mode floating medium filters for recirculating systems in aquaculture for higher solids retention and lower freshwater usage’, *Bioresource Technology*, 98, pp. 3375–3383. doi: 10.1016/j.biortech.2006.10.042.

Stickney, R. R. (2000) *Encyclopedia of Aquaculture*.

Sugiura, S. H. *et al.* (1999) 'Availability of phosphorus and trace elements in low-phytate varieties of barley and corn for rainbow trout (*Oncorhynchus mykiss*)', *Aquaculture*, 170(3–4), pp. 285–296. doi: 10.1016/S0044-8486(98)00414-1.

Sukmana, H. *et al.* (2021) 'Adsorption and coagulation in wastewater treatment - Review', *Progress in Agricultural Engineering Sciences*, 17, pp. 49–68. doi: 10.1556/446.2021.00029.

Summerfelt, S. T. *et al.* (2009) 'Process requirements for achieving full-flow disinfection of recirculating water using ozonation and UV irradiation', *Aquacultural Engineering*, 40(1), pp. 17–27. doi: 10.1016/j.aquaeng.2008.10.002.

Taghizadeh-Toosi, A. *et al.* (2012) 'Biochar adsorbed ammonia is bioavailable', *Plant and Soil*, 350, pp. 57–69. doi: 10.1007/s11104-011-0870-3.

Tal, Y. *et al.* (2009) 'Environmentally sustainable land-based marine aquaculture', *Aquaculture*, 286, pp. 28–35. doi: 10.1016/j.aquaculture.2008.08.043.

Tan, Y. L. *et al.* (2014) ‘Adsorption of carbon dioxide by sodium hydroxide-modified granular coconut shell activated carbon in a fixed bed’, *Energy*, 77, pp. 926–931. doi: 10.1016/j.energy.2014.09.079.

Tejido-nuñez, Y. *et al.* (2019) ‘Treatment of aquaculture effluent with *Chlorella vulgaris* and *Tetrademus obliquus* : The effect of pretreatment on microalgae growth and nutrient removal efficiency’, *Ecological Engineering*, 136, pp. 1–9. doi: 10.1016/j.ecoleng.2019.05.021.

Tenaga, N. (2022) *Electricity Tariffs*. Available at: <https://www.tnb.com.my/>.

Thao, V. T. M. *et al.* (2021) ‘Adsorption of ammonium, nitrite, and nitrate onto rice husk biochar for nitrogen removal’, *Engineering and Technology*, 11, pp. 30–44. doi: 10.46223/hcmcoujs.tech.en.11.1.1622.2021.

Tian, W. *et al.* (2016) ‘Remediation of aquaculture water in the estuarine wetlands using coal cinder-zeolite balls/reed wetland combination strategy’, *Journal of Environmental Management*, 181, pp. 261–268. doi: 10.1016/j.jenvman.2016.06.040.

Tran, H. N. *et al.* (2017) ‘Mistakes and inconsistencies regarding adsorption of contaminants from aqueous solutions: A critical review’, *Water Research*, 120, pp. 88–116. doi: 10.1016/j.watres.2017.04.014.

Troell, M. *et al.* (2003) ‘Integrated mariculture : asking the right questions’, *Aquaculture*, 226, pp. 69–90. doi: 10.1016/S0044-8486(03)00469-1.

Turcios, A. E. and Papenbrock, J. (2014) ‘Sustainable treatment of aquaculture effluents-What can we learn from the past for the future?’, *Sustainability*, 6, pp. 836–856. doi: 10.3390/su6020836.

Velasco, J. *et al.* (2019) ‘Effects of salinity changes on aquatic organisms in a multiple stressor context’, *Philosophical Transactions of the Royal Society B: Biological Sciences*, 374(1764), pp. 1–9. doi: 10.1098/rstb.2018.0011.

Viglašová, E. *et al.* (2018) ‘Production, characterization and adsorption studies of bamboo-based biochar/montmorillonite composite for nitrate removal’, *Waste Management*, 79, pp. 385–394. doi: 10.1016/j.wasman.2018.08.005.

Vijayaraghavan, K. and Balasubramanian, R. (2021) ‘Application of pinewood waste-derived biochar for the removal of nitrate and phosphate from single and binary solutions’, *Chemosphere*, 278, p. 130361. doi:



10.1016/j.chemosphere.2021.130361.

Villabona-Ortíz, Á., Figueroa-Lopez, K. J. and Ortega-Toro, R. (2022) 'Kinetics and Adsorption Equilibrium in the Removal of Azo-Anionic Dyes by Modified Cellulose', *Sustainability (Switzerland)*, 14, p. 3640. doi: 10.3390/su14063640.

Vinatea, L. *et al.* (2018) 'Short communication A comparison of recirculation aquaculture systems versus bio flocc technology culture system for on-growing of fry of Tinca tinca ( Cyprinidae ) and fry of grey Mugil cephalus ( Mugilidae )', *Aquaculture*, 482(September 2017), pp. 155–161. doi: 10.1016/j.aquaculture.2017.09.041.

Vu, N. T. and Do, K. U. (2021) 'Insights into adsorption of ammonium by biochar derived from low temperature pyrolysis of coffee husk', *Biomass Conversion and Biorefinery*. doi: 10.1007/s13399-021-01337-9.

Wafti, N. S. A. *et al.* (2017) 'Activated Carbon from Oil Palm Biomass as Potential Adsorbent for Palm Oil Effluent Treatment', *Journal of oil palm research*, 29, pp. 278–290.

Wang, Z. *et al.* (2015) 'Biochar produced from oak sawdust by Lanthanum (La)-involved pyrolysis for adsorption of ammonium (NH<sub>4</sub><sup>+</sup>), nitrate (NO<sub>3</sub><sup>-</sup>), and

phosphate (PO<sub>4</sub><sup>3-</sup>), *Chemosphere*, 119, pp. 646–653. doi: 10.1016/j.chemosphere.2014.07.084.

Weber, W. J. and Morris, C. j (1963) ‘Kinetics of Adsorption on Carbon from Solution’, *Journal of the Sanitary Engineering Division*, 89(2), pp. 31–60.

Wedemeyer, G. A. (1996) *Physiology of Fish Intensive Culture System*.

Wu, F. C., Tseng, R. L. and Juang, R. S. (2009) ‘Initial behavior of intraparticle diffusion model used in the description of adsorption kinetics’, *Chemical Engineering Journal*, 153, pp. 1–8. doi: 10.1016/j.cej.2009.04.042.

Wu, H. and Vaneeckhaute, C. (2022) ‘Nutrient recovery from wastewater: A review on the integrated Physicochemical technologies of ammonia stripping, adsorption and struvite precipitation’, *Chemical Engineering Journal*, 433, p. 133664. doi: 10.1016/j.cej.2021.133664.

Wurts, W. A. and Masser, M. P. (2013) ‘Liming Ponds for Aquaculture’, *Southern Regional Aquaculture Centre (SRAC) Publication*, (4100).

Xiao, F. *et al.* (2018) ‘Thermal air oxidation changes surface and adsorptive properties of black carbon (char/biochar)’, *Science of the Total Environment*,

618, pp. 276–283. doi: 10.1016/j.scitotenv.2017.11.008.

Xu, G., Zhang, Z. and Deng, L. (2018) ‘Adsorption behaviors and removal efficiencies of inorganic, polymeric and organic phosphates from aqueous solution on biochar derived from sewage sludge of chemically enhanced primary treatment process’, *Water*, 10, p. 869. doi: 10.3390/w10070869.

Xu, H. *et al.* (2022) ‘Adsorption behavior and performance of ammonium onto sorghum straw biochar from water’, *Scientific Reports*, 12, p. 5358. doi: 10.1038/s41598-022-08591-5.

Xu, K. *et al.* (2018) ‘Recovery of ammonium and phosphate from urine as value-added fertilizer using wood waste biochar loaded with magnesium oxides’, *Journal of Cleaner Production*, 187, pp. 205–214. doi: 10.1016/j.jclepro.2018.03.206.

Xue, S. *et al.* (2019) ‘Food waste based biochars for ammonia nitrogen removal from aqueous solutions’, *Bioresource Technology*, 292, p. 121927. doi: 10.1016/j.biortech.2019.121927.

Yan, W. *et al.* (2010) ‘Mass and energy balances of wet torrefaction of lignocellulosic biomass’, *Energy and Fuels*, 24, pp. 4738–4742. doi:

10.1021/ef901273n.

Yang, B. *et al.* (2017) 'Using desulfurization slag as the aquacultural amendment for fish pond water quality improvement: Mechanisms and effectiveness studies', *Journal of Cleaner Production*, 143, pp. 1313–1326. doi: 10.1016/j.jclepro.2016.11.105.

Yang, H. I. *et al.* (2018) 'Adsorption of ammonium in aqueous solutions by pine sawdust and wheat straw biochars', *Environmental Science and Pollution Research*, 25, pp. 25638–25647. doi: 10.1007/s11356-017-8551-2.

Yang, J. *et al.* (2017) 'Limited role of biochars in nitrogen fixation through nitrate adsorption', *Science of the Total Environment*, 592, pp. 758–765. doi: 10.1016/j.scitotenv.2016.10.182.

Yang, W. *et al.* (2019) 'Adsorption of copper(II) and lead(II) from seawater using hydrothermal biochar derived from Enteromorpha', *Marine Pollution Bulletin*, 149, p. 110586. doi: 10.1016/j.marpolbul.2019.110586.

Yao, A. K. Z. *et al.* (2022) 'Ammonium sorption and regeneration using Mg-modified zeolites: A study on the interferences of competing ions from aquaculture effluent', *Journal of Water Process Engineering*, 48, p. 102909. doi:

10.1016/j.jwpe.2022.102909.

Yao, Y. *et al.* (2012) 'Effect of biochar amendment on sorption and leaching of nitrate, ammonium, and phosphate in a sandy soil', *Chemosphere*, 89, pp. 1467–1471. doi: 10.1016/j.chemosphere.2012.06.002.

Yavari, Saba *et al.* (2017) 'Sorption properties optimization of agricultural wastes-derived biochars using response surface methodology', *Process Safety and Environmental Protection*, 109, pp. 509–519. doi: 10.1016/j.psep.2017.05.002.

Yin, H. *et al.* (2018) 'Dual removal of phosphate and ammonium from high concentrations of aquaculture wastewaters using an efficient two-stage infiltration system', *Science of the Total Environment*, 635, pp. 936–946. doi: 10.1016/j.scitotenv.2018.04.218.

Yin, Q. *et al.* (2017) 'Biochar as an adsorbent for inorganic nitrogen and phosphorus removal from water: a review', *Environmental Science and Pollution Research*, 24, pp. 26297–26309. doi: 10.1007/s11356-017-0338-y.

Yin, Q. *et al.* (2018) 'Phosphate and ammonium adsorption of sesame straw biochars produced at different pyrolysis temperatures', *Environmental Science*

*and Pollution Research*, 25, pp. 4320–4329. doi: 10.1007/s11356-017-0778-4.

Yin, Q., Liu, M. and Ren, H. (2019) ‘Biochar produced from the co-pyrolysis of sewage sludge and walnut shell for ammonium and phosphate adsorption from water’, *Journal of Environmental Management*, 249, p. 109410. doi: 10.1016/j.jenvman.2019.109410.

Yin, Q., Wang, R. and Zhao, Z. (2018) ‘Application of Mg–Al-modified biochar for simultaneous removal of ammonium, nitrate, and phosphate from eutrophic water’, *Journal of Cleaner Production*, 176, pp. 230–240. doi: 10.1016/j.jclepro.2017.12.117.

Yogev, U. *et al.* (2020) ‘Phosphorous recovery from a novel recirculating aquaculture system followed by its sustainable reuse as a fertilizer’, *Science of the Total Environment*, 722, p. 137949. doi: 10.1016/j.scitotenv.2020.137949.

Yu, Q. *et al.* (2016) ‘Effectiveness and mechanisms of ammonium adsorption on biochars derived from biogas residues’, *RSC Advances*, 6, pp. 88373–88381. doi: 10.1039/c6ra16913a.

Yuan, J.-H., Xu, R.-K. and Zhang, H. (2011) ‘The forms of alkalis in the biochar produced from crop residues at different temperatures’, *Bioresource*

*Technology*, 102, pp. 3488–3497. doi: 10.1016/j.biortech.2010.11.018.

Zadinelo, I. V. *et al.* (2015) ‘Influence of the chemical composition of smectites on the removal of ammonium ions from aquaculture effluents’, *J Mater Sci*, 50, pp. 1865–1875. doi: 10.1007/s10853-014-8749-3.

Zadinelo, I. V. *et al.* (2018) ‘Adsorption of aquaculture pollutants using a sustainable biopolymer’, *Environmental Science and Pollution Research*, 25, pp. 4361–4370.

Zahrim, A. Y. *et al.* (2017) ‘Ammonia-Nitrogen Recovery from Synthetic Solution using Agricultural Waste Fibers’, *Indian Journal of Science and Technology*, 10, pp. 1–5. doi: 10.17485/ijst/2017/v10i6/111221.

Zhang, X. *et al.* (2014) ‘Aquacultural Engineering Performance of inorganic coagulants in treatment of backwash waters from a brackish aquaculture recirculation system and digestibility of salty sludge’, *Aquacultural Engineering*, 61, pp. 9–16. doi: 10.1016/j.aquaeng.2014.05.005.

Zhao, H. *et al.* (2018) ‘Adsorption of nitrate onto biochar derived from agricultural residuals’, *Water Science and Technology*, 77, pp. 548–554. doi:

10.2166/wst.2017.568.

Zheng, H. *et al.* (2008) 'Adsorption characteristics of ammonium ion by zeolite 13X', *Journal of Hazardous Materials*, 158, pp. 577–584. doi: 10.1016/j.jhazmat.2008.01.115.

Zheng, Y. *et al.* (2019) 'Reclaiming phosphorus from secondary treated municipal wastewater with engineered biochar', *Chemical Engineering Journal*, 362, pp. 460–468. doi: 10.1016/j.cej.2019.01.036.

Zhou, L. *et al.* (2019) 'Phosphorus and nitrogen adsorption capacities of biochars derived from feedstocks at different pyrolysis temperatures', *Water (Switzerland)*, 11(8), pp. 1–16. doi: 10.3390/w11081559.

Zhou, L. and Boyd, C. E. (2014) 'Total ammonia nitrogen removal from aqueous solutions by the natural zeolite, mordenite: A laboratory test and experimental study', *Aquaculture*, 432, pp. 252–257. doi: 10.1016/j.aquaculture.2014.05.019.

Zhou, X. (2017) 'Minor correction to the thermodynamic calculation using the distribution constant by Shan *et al.* and Rahmani-Sani *et al.*', *Journal of Hazardous Materials*, 323, pp. 735–736. doi: 10.1016/j.jhazmat.2016.05.073.



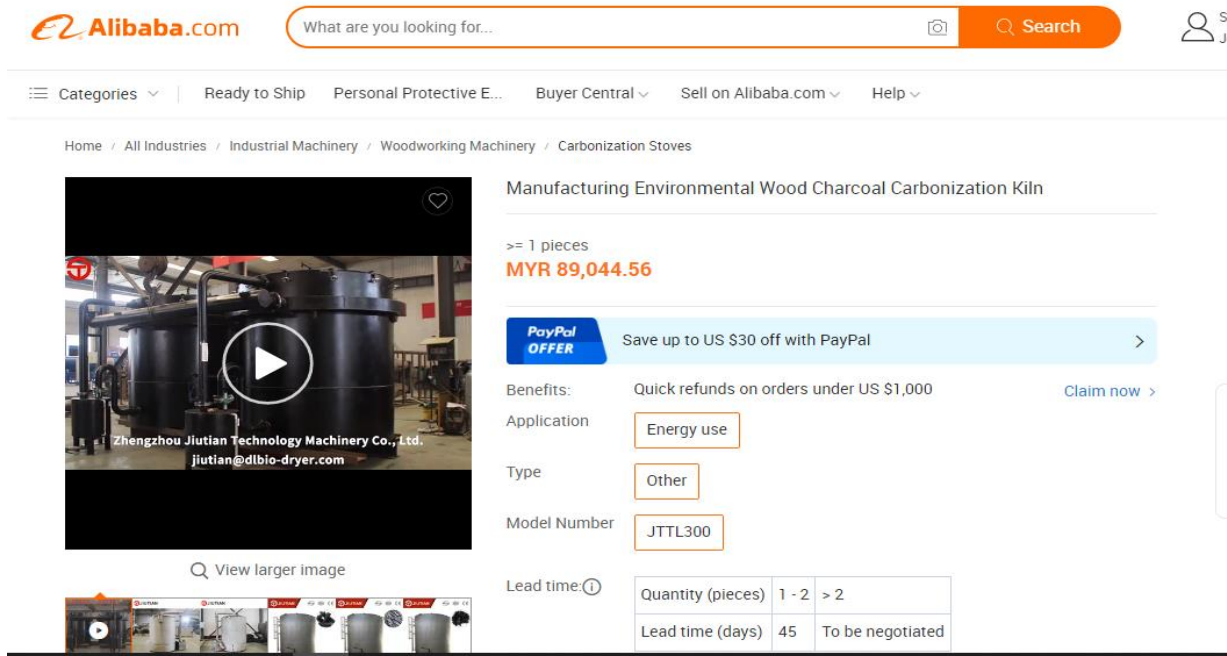
Zou, S. *et al.* (2018) 'Nitrogen removal from water of recirculating aquaculture system by a microbial fuel cell', *Aquaculture*, 497, pp. 74–81. doi: 10.1016/j.aquaculture.2018.07.036.

## List of Publications

1. Tanveer Ahmad, Sumathi Sethupathi, Mohammed J.K Bashir, Sin Ying Tan “Appraising the Performance of Oil Palm Fiber Biochar for Low Concentration Ammoniacal Nitrogen Recovery from Aquaculture Wastewater”. *Environmental Technology*, Accepted 2022. doi.org/10.1080/09593330.2022.2152735.
2. Tanveer Ahmad, Sumathi Sethupathi, Mohammed J.K Bashir, Sin Ying Tan “Evaluation of various preparation methods of oil palm fiber (OPF) biochar for ammonia-nitrogen (NH<sub>3</sub>-N) removal” in *IOP Conference Series: Earth and Environmental Science*, p. 012020. doi: 10.1088/1755-1315/945/1/012020.
3. Tanveer Ahmad, Sumathi Sethupathi, Mohammed J.K Bashir, Sin Ying Tan “Optimization and economic analysis of oil palm fiber biochar for ammoniacal nitrogen recovery from Aquaculture wastewater” *Environmental Science and Pollution Research*, Under Review.

## Appendix

Pricing data for cost analysis from commercial websites.

Item	Website Link	Screenshot
Rotary kiln	https://www.alibaba.com/	 <p>The screenshot displays the Alibaba.com product page for a 'Manufacturing Environmental Wood Charcoal Carbonization Kiln'. The page features a video player showing the kiln in operation, with a play button overlay. Below the video, there is a 'View larger image' link and a gallery of smaller images. The product title is 'Manufacturing Environmental Wood Charcoal Carbonization Kiln'. The price is listed as 'MYR 89,044.56' for quantities of '&gt;= 1 pieces'. A 'PayPal OFFER' banner indicates a 'Save up to US \$30 off with PayPal'. The 'Benefits' section mentions 'Quick refunds on orders under US \$1,000' with a 'Claim now &gt;' link. The 'Application' is 'Energy use', 'Type' is 'Other', and 'Model Number' is 'JTTL300'. The 'Lead time' table shows '45' days for '1 - 2' pieces and 'To be negotiated' for '&gt; 2' pieces.</p>

Product details
Company profile
Report Suspi

Product Description
Working Principle
Application
Product Paramenters
Successful Case
Company Introduction

**Essential details**

Place of Origin:	Henan, China	Condition:	New
Video outgoing-inspection:	Provided	Machinery Test Report:	Provided
Marketing Type:	New Product 2020	Warranty of core components:	1 Year
Core Components:	Motor	Brand Name:	Jiutian
Effective Volume:	4-8 m3	Dimension(L*W*H):	Customized
Voltage:	220V-10KV	Power:	15-22kw
Warranty:	1 Year	Key Selling Points:	Energy saving
Applicable Industries:	Manufacturing Plant	Showroom Location:	None
Weight (KG):	8000	Product name:	Carbonization Kiln
Capacity:	300kg/4-6h	Diameter:	1.45-2.15m
Height:	1.85-2.2m	Heating source:	Biomass, natural gas, diesel, coal
Application material:	Wood chips, rice husks, peanut shells, plant stalks, bark	Material:	Carbon Steel, Refractory
Weight:	Customized	Feature:	Continuous Machine
		Certification:	ISO:9001

Product details
Company profile
Report Suspicious Activity!

Product Description
Working Principle
Application
Product Paramenters
Successful Case
Company Introduction

**Product Paramenters**

Model	CAPACITY	DIAMETER	HEIGHT	Material
JTTL-300	300kg/4-6h	1.45m	1.85m	Carbon steel, refractory
JTTL-500	500kg/4-8h	1.8m	1.9m	Carbon steel, refractory
JTTL-1000	1000kg/5-8h	2.15m	2.2m	Carbon steel, refractory

Biomass  
crusher


<https://www.alibaba.com/>

What are you looking for... Sign In  
Join for free

Home / All Industries / Machinery / Woodworking Machinery / Wood Crushers [Subscribe to Trade Alert](#)

**Super** Commercial Equipment Biomass Straw Waste Wood Shaving Sawdust  
Crusher Crushing Machine

>= 1 sets  
**MYR 5,947.89**



Benefits: US \$10 off with a new supplier [Claim now >](#)

Model Number

Lead Time: ⓘ

Quantity(sets)	1 - 1	> 1
Est. Time(days)	20	To Be Negotiated

Customization: Customized logo (Min. Order 5 sets)

Shipping:  Sea freight  Land freight

Protection:  Trade Assurance Protects your Alibaba.com orders

On-time Dispatch Guarantee  
 Refund Policy

[View larger image](#)

Add to Compare  Share

## Overview

---

### Quick Details

Place of Origin: Henan, China  
Condition: New

Machinery Test Report: Provided

Core Components: Motor  
Power: 7.5 kw  
Warranty: 1 Year

Applicable Industries: Manufacturing Plant, Energy & Mining

Weight (KG): 400

Usage: crushing waste wood

Material: Carbon Steel

After-sales Service Provided: Online support

Brand Name: SUNRISE

Video outgoing-inspection: Provided

Marketing Type: Ordinary Product

Warranty of core components: 1 Year

Voltage: 220/380 V

Dimension(L\*W\*H): 1.25\*0.7\*0.9 m

Key Selling Points: Long Service Life

Showroom Location: None

Item: Wood crusher

Raw material: waste wood

Spare parts: blade and sieve

Weight: 400 kg

Certification: CE ISO

---

Rotary cooler

<https://www.alibaba.com/>


What are you looking for.. Sign In  
Join for free

Home > All Industries > Machinery > Chemical & Pharmaceutical Machinery > Chemical Machinery & Equipment > Drying Equipment [Subscribe to Trade Alert](#)

**Hot Sale Horizontal Rotary Cooler For Calcined Kiln**  
 FOB Reference Price: [Get Latest Price](#)

**MYR 41,218.20 - MYR 457,980.00/ set | 1 set/sets(Min. Order)**

Benefits: Quick refunds on orders under US \$1,000 [Claim now >](#)  
 Shipping: Support Sea freight  
[Alibaba.com Freight](#) | [Compare Rates](#) | [Learn more](#)



**Product Details** **Company Profile** Report Suspicious Activity

Company Information Company Information Our Services

**Overview**

**Quick Details**


Type:	cooling machine	Model Number:	pls reference to the form
Condition:	New	Place of Origin:	Henan, China
Brand Name:	ZK Brand	Voltage:	220v/380v
Power:	7.5-75KW	Dimension(L*W*H):	3*30m
Warranty:	1 year	Weight:	as the model
After-sales Service Provided:	Engineers available to service machinery overseas	Certification:	ISO9001:14000, ISO9001:14000
Installation:	under our engineer's guide	Product Name:	Hot Sale Horizontal Rotary Cooler For Calcined Kiln
warranty:	12 months	after sale service:	for the whole using life
experiences:	more than 50 years	training:	on site for free
length:	Can Be Designed	diameter(m):	1-4.5m
		power:	7.5-80kw

Conveyor  
belt


<https://www.alibaba.com/>

What are you looking for... Sign In  
Join for free Messa

Home > All Industries > Material Handling > Transporting > Conveyors [Subscribe to Trade Alert](#)



Click here to expended view



**Low noise automatic scanning weighing and sorting aluminum profile PVC PU belt flat conveyor belting**

FOB Reference Price: [Get Latest Price](#)

---

**MYR 2,289.90 - MYR 11,449.50** / set | 1 set/sets(Min. Order)

Benefits: Quick refunds on orders under US \$1,000 [Claim now >](#)

Type: Other

Load Capacity: 250kg/m

Model Number: BC-FL-MD

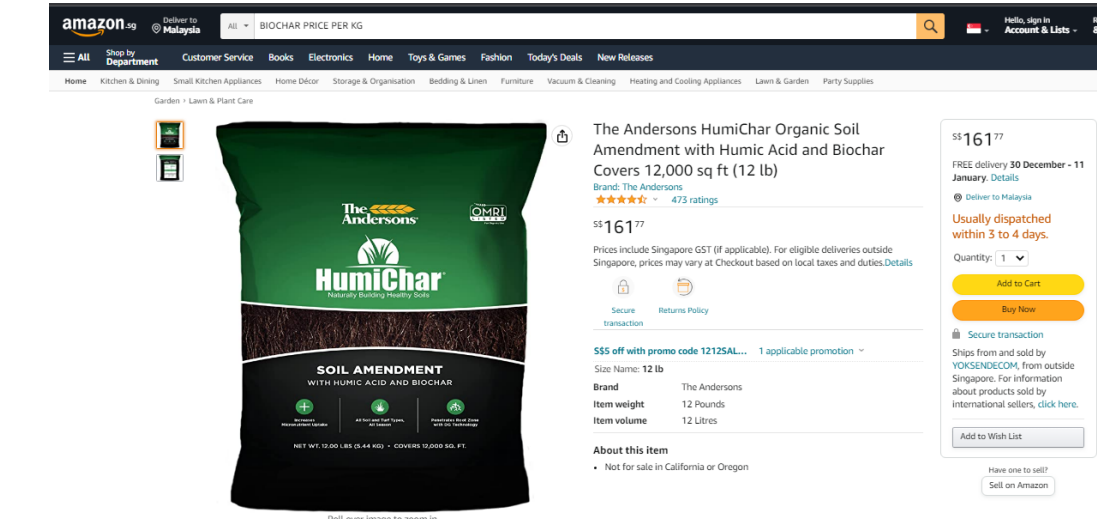
Lead TimeⓄ:

Quantity(sets)	1 - 50	>50
Est. Time(days)	21	To be negotiated

Condition: <b>New</b>	Material: <b>Aluminium</b>
Material Feature: <b>Oil Resistant</b>	Structure: <b>Belt conveyer</b>
Place of Origin: <b>Zhejiang, China</b>	Brand Name: <b>AILONG</b>
Voltage: <b>110V/220V/380V</b>	Power: <b>1.5 KW</b>
Dimension(L*W*H): <b>L3000*W800*H800</b>	Warranty: <b>1 Year</b>
Width or Diameter: <b>800mm</b>	Machinery Test Report: <b>Provided</b>
Video outgoing-inspection: <b>Provided</b>	Marketing Type: <b>Ordinary Product</b>
Core Components: <b>Motor, Bearing, Gearbox, Sprocket, Roller</b>	Warranty of core components: <b>1 Year</b>
Application: <b>Material Handling</b>	Weight (KG): <b>200 kg</b>
Function: <b>Screening\separation\sorting\sieving</b>	Feature: <b>High Transmission Efficiency</b>
Advantage: <b>Clean, low-noise, economical</b>	Frame Material: <b>Aluminium profile</b>
Motor: <b>Gear Motor</b>	Belt material: <b>PVC/PU/Rubber/Polyester/PE/PVK/etc.</b>
Installation: <b>Vedio Easy Installation</b>	Speed: <b>Variable speed 0-1.2m/s</b>
	Packing: <b>Wooden Case</b>



Prices of biochar and activated carbon from commercial websites

Items	Website link	Screen shot												
Biochar	<a href="https://www.amazon.sg">https://www.amazon.sg</a>	 <p><b>Product information</b></p> <table border="1"> <thead> <tr> <th colspan="2">Technical Details</th> </tr> </thead> <tbody> <tr> <td>Manufacturer</td> <td>The Andersons</td> </tr> <tr> <td>Item model number</td> <td>12</td> </tr> <tr> <td>Product Dimensions</td> <td>38.1 x 35.56 x 10.16 cm; 5.44 Kilograms</td> </tr> <tr> <td>ASIN</td> <td>B08ZBGQNJ7</td> </tr> </tbody> </table> <p><b>Additional Information</b></p> <table border="1"> <tr> <td>Best Sellers Rank</td> <td>8,839 in Garden (See Top 100 in Garden) 1,381 in Lawn &amp; Plant Care Products</td> </tr> </table> <p><b>Feedback</b></p> <p>Would you like to <a href="#">tell us about a lower price?</a></p>	Technical Details		Manufacturer	The Andersons	Item model number	12	Product Dimensions	38.1 x 35.56 x 10.16 cm; 5.44 Kilograms	ASIN	B08ZBGQNJ7	Best Sellers Rank	8,839 in Garden (See Top 100 in Garden) 1,381 in Lawn & Plant Care Products
Technical Details														
Manufacturer	The Andersons													
Item model number	12													
Product Dimensions	38.1 x 35.56 x 10.16 cm; 5.44 Kilograms													
ASIN	B08ZBGQNJ7													
Best Sellers Rank	8,839 in Garden (See Top 100 in Garden) 1,381 in Lawn & Plant Care Products													

Activated carbon

<https://www.amazon.sg>

The screenshot shows the Amazon Singapore product page for 'CNZ Media Filter Bags Activated Carbon Charcoal Aquarium Fish Tank Pond Canister Filter, 4 lb, Black C4PK'. The page features a search bar at the top with the text 'ACTIVATED CARBON PRICE PER KG'. The product is displayed with four black filter bags in a 2x2 grid. The price is listed as S\$75.06 (S\$75.06 / count). The product has a 4.5-star rating from 305 reviews. The page includes a 'Special offers and product promotions' section with two offers: a 12.12 Sale and a 1% off with PayNow. Below the main product image are sections for 'Product information' (Technical Details) and 'Additional Information' (Best Sellers Rank, Feedback). The right sidebar contains a 'Quantity' selector set to 1, 'Add to Cart' and 'Buy Now' buttons, and a 'Secure transaction' badge. The bottom right corner has a 'Have one to sell? Sell on Amazon' button.

**Product information**

**Technical Details**

Manufacturer	activated charcoal
Item model number	CNZ_C4PK
Product Dimensions	20.32 x 10.16 x 5.08 cm; 1.79 Kilograms
ASIN	B00WFLNOV8

**Additional Information**

Best Sellers Rank	23,164 in Pet Supplies (See Top 100 in Pet Supplies) 400 in Aquarium Filter Accessories
-------------------	--

**Feedback**

Would you like to [tell us about a lower price?](#)

Activated carbon

<https://www.alibaba.com/>

The screenshot shows the Alibaba.com product page for '3Mm 4Mm Factory Price Columnar Active Charcoal Bulk Coal Pellet Activated Carbon For Air Treatment'. The page includes a search bar, navigation menu, and product details. A video player shows a close-up of the charcoal pellets with a play button and a 'CONTACTS US NOW!' banner. The price is listed as MYR 8.55 for 1-999 kilograms, MYR 6.75 for 1000-9999 kilograms, and MYR 2.70 for 10000 kilograms and above. A PayPal offer is also visible.

**Product details**

**Company profile**

Product Description | Products Raw Material | Products Application | Our Company and Lab | Packing And Delivery | Certifica

### Overview

**Essential details**

Classification:	Chemical Auxiliary Agent	CAS No.:	7440-44-0
Other Names:	Activated Charcoal	MF:	C
EINECS No.:	231-545-4	Purity:	99%
Place of Origin:	Henan, China	Type:	Adsorbent
Adsorbent Variety:	Activated Carbon	Usage:	Petroleum Additives, Textile Auxiliary Agents, Water T...
Brand Name:	Yihang	Model Number:	YH - CY02
Product name:	Bulk column pellets coal based activated carbon for a...	Application:	Water Purification,Gas Purification
Material:	Coal Based	Color:	Black
Shape:	Columnar	Iodine Value (mg/g):	500-1100
PH:	8-11	Ash(%):	<15
Keywords:	Columnar Activated Carbon	MOQ:	25kilograms

Activated carbon

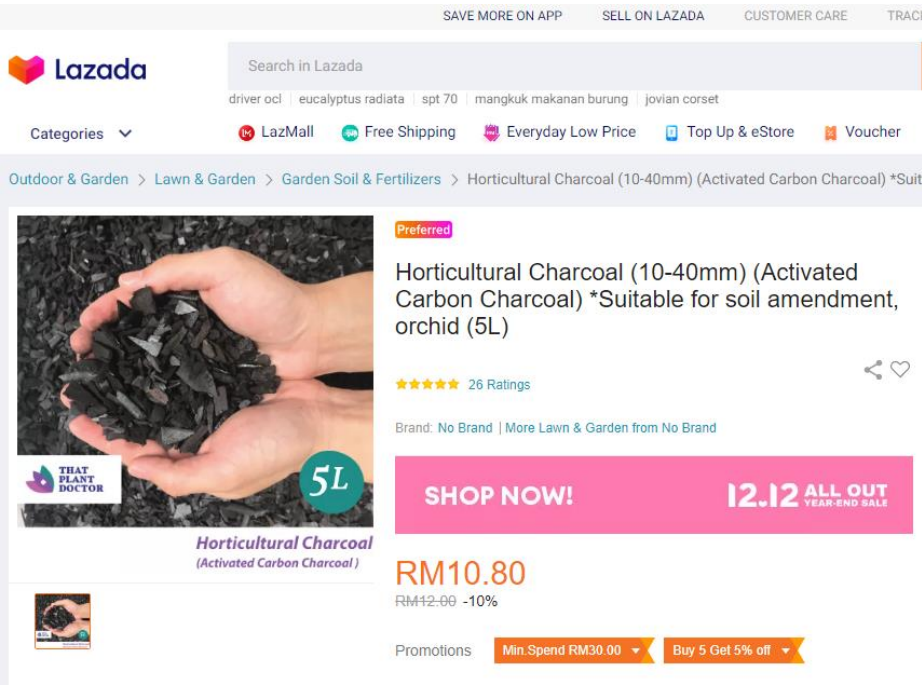
<https://www.alibaba.com/>

The screenshot shows the Alibaba.com product page for "Palm kernel shell granular activated carbon for water treatment". The page features a search bar at the top with the text "What are you looking for...". Below the search bar, there are navigation links for "Categories", "Ready to Ship", "Personal Protective E...", "Trade Shows", "Buyer Central", "Sell on Alibaba.com", and "Help". The breadcrumb trail indicates the product is in "Home / All Industries / Chemicals / Catalysts & Chemical Auxiliary Agents / Chemical Auxiliary Agent".

The product title is "Palm kernel shell granular activated carbon for water treatment". Below the title, there is a video player showing a bowl of dark granules. To the right of the video, the price is listed as "MYR 5,374.16" for 1-4 tons and "MYR 4,025.00" for quantities greater than or equal to 5 tons. A "PayPal OFFER" banner indicates a "Save up to US \$30 off with PayPal". Below this, there are details for "Benefits", "Quantity" (set to 1 tons), "Samples" (MYR 5,374.16/ton, Min. order: 1 ton, Get samples), and "Lead time" (7 days for 1-10 tons, 10 days for 11-15 tons, and To be negotiated for > 15 tons).

The screenshot shows the "Product details" section of the Alibaba.com product page. It includes tabs for "Product details" and "Company profile", with a "Report Suspicious Activity!" link. The "Product Description" tab is active, showing an "Overview" section with "Essential details".

Essential details	
Classification:	Chemical Auxiliary Agent
Other Names:	activated charcoal
EINECS No.:	264-846-4
Place of Origin:	Henan, China
Adsorbent Variety:	Activated Carbon
Brand Name:	ZHONGCHUANG
Application:	Water treatment, air purifying
Appearance:	Black granule
Certification:	ISO9001 MSDS
Iodine value:	800 min
Moisture:	5% Max
CAS No.:	64365-11-3
MF:	C
Purity:	99.9%
Type:	Adsorbent
Usage:	Coating Auxiliary Agents, Electronics Chemicals, Leat...
Model Number:	ZC-08-30
Material:	high-quality coal
Keywords:	granular activated carbon
PH:	6-8
CAS:	64365-11-3
Ash:	5%

<p>Activated carbon</p>	<p><a href="https://www.lazada.com.my/">https://www.lazada.com.my/</a></p>	 <p><b>Product details of Horticultural Charcoal (10-40mm) (Activated Carbon Charcoal) *Suitable for soil amendment, orchid (5L)</b></p> <ul style="list-style-type: none"> <li>• Volume: 5L</li> <li>• Weight: Approx 1.8kg</li> <li>• Material : Activated Carbon Charcoal / Arang Orkid (RED)(10-40mm)</li> <li>• **** Horticultural Charcoal is a lightweight and mild soil additive that will assist in draining excess moisture from any container or potted plant. Charcoal prolongs the life of soil media by balancing pH levels and sweetening the soil of potted plants and terrariums..****</li> <li>• Very good drainage</li> <li>• Good amendment material for potting mix</li> <li>• Suitable for Orchid planting</li> <li>• Purify impurities in the soil</li> <li>• Neutralize the pH level of the soil</li> <li>• Poison Free &amp; Odorless, Clean, and easy to use.</li> </ul>
-------------------------	--	---

Biochar

<https://www.lazada.com.my/>

The screenshot shows the Lazada mobile app interface. At the top, there are navigation links: 'SAVE MORE ON APP', 'SELL ON LAZADA', 'CUSTOMER CARE', and 'TRACK MY'. The Lazada logo is on the left, and a search bar is in the center. Below the search bar, there are category filters: 'Categories', 'LazMall', 'Free Shipping', 'Everyday Low Price', 'Top Up & eStore', and 'Voucher'. The breadcrumb trail reads: 'Outdoor & Garden > Lawn & Garden > Garden Soil & Fertilizers > Pure Biochar Probiotic Natural Soil Amendment Bacillus subtilis 枯草桿菌'. The product title is 'Pure Biochar Probiotic Natural Soil Amendment Bacillus subtilis 枯草桿菌 SHS KEBUN'. It has a 'Preferred' badge, a 5-star rating with 17 reviews, and a price of RM5.20 (40% off from RM8.60). A 'SHOP NOW!' button is prominent, along with a '12.12 ALL OUT YEAR-END SALE' banner. Below the product image, there are smaller images of the product packaging and a 'Promotions' section with a 'Min. Spend RM30.00' filter and a 'Buy 2, Get 2% off; Buy 3, Get 3% off; Buy 4, Get 4% off' offer.

#### Product details of Pure Biochar Probiotic Natural Soil Amendment Bacillus subtilis 枯草桿菌 SHS KEBUN

- SHS KEBUN Biochar Probiotic 1.5kg
- A soil amendment with beneficial microbes (Bacillus sp.) 枯草桿菌
- Carbon-rich, high in Boron/Mineral ash
- Increases yield
- Improves soil structure
- Increases pH
- Retains water/releases it when plants need
- Enhances plant growth
- Better root development
- Prevents root rot and bacteria diseases
- Ready-stock and Shipped from Kulim
- SHS KEBUN/SHS Garden is the registered trademark of Grand SHS Resources (M) Sdn. Bhd. Beware of any fake listings using our trade name

Biochar

<https://shopee.com.my/>



Seller Centre | Download | Follow us on

Notifications Help English Sign Up | Login

Sign Up & Get RM18 Off Voucher!

Dress Kasut Perempuan Blouse Kasut Lelaki Powerbank Baju Kurung Smart Watch Jersey

Shopee > Home & Living > Home Improvement > Outdoor & Garden > Pure Biochar Probiotic Natural Soil Amendment Bacillus subtilis 枯草桿菌 1.5kg SHS KEBUN



**Biochar  
+  
Soil  
Probiotic**

**Dihantar  
Dari  
Kulim**

**Preferred+** Pure Biochar Probiotic Natural Soil Amendment Bacillus subtilis  
枯草桿菌 1.5kg SHS KEBUN

4.9 | 48 Ratings | 197 Sold

RM8.60 **RM6.88** **20% OFF**

**100% Authentic Guarantee**  
Guarantee Authentic or Money Back

Shop Vouchers **10% OFF** **15% OFF**

**Shop Vouchers**  
Save more by applying these Shop Vouchers to the items in your shopping cart.

**10% off**  
Min. Spend RM5 Capped at RM50 **Claim**  
85% used, Expiring: 12 hours left

**12.12 FREE SHIPPING MIN. SPEND 10**

Activated carbon

<https://shopee.com.my/>

The screenshot shows a product listing on the Shopee website. The product is '1KG High Quality Loose Form Granular Activated Carbon (GAC)/Charcoal for Water Filter and Air Purifier' by the brand 'ELECTRON WATER'. The price is RM30.00, marked down from RM35.00 (14% OFF). The product has a 4.9-star rating from 39 reviews and 125 units sold. Shipping is free to KL City, Kuala Lumpur. The quantity is set to 1, with 1028 pieces available. There are 'Add To Cart' and 'Buy Now' buttons. At the bottom of the screenshot, there are promotional banners for '12.12 FREE SHIPPING MIN. SPEND 10' and '15% CASHBACK'.

#### Product Description

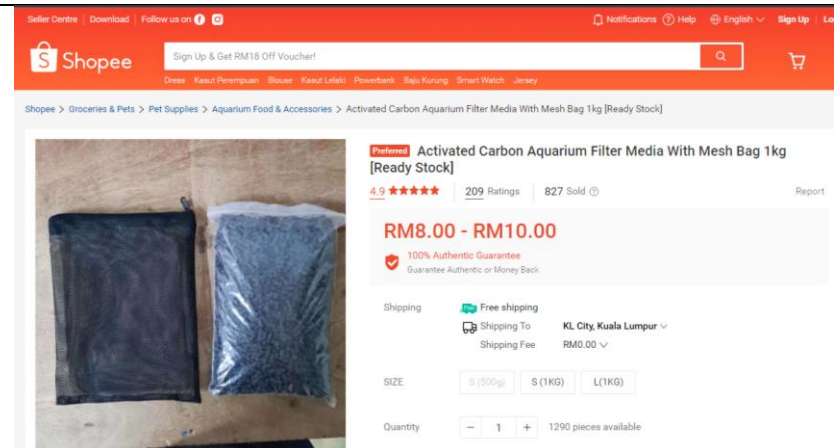
\*\*\*PM US IF YOU'RE LOOKING FOR LARGE QUANTITY\*\*\*

- Activated Carbon Specifications:
- Made from Coconut Shell
  - 8x30 MESH SIZE (0.6mm-1.7mm)
  - IODINE NUMBER: > 1100
  - ASH CONTENT: <3%
  - HALAL CERTIFIED



Activated carbon

<https://shopee.com.my/>



Activated Charcoal Filter Media 1kg x1 pcs

Product features:

- Perfect for biological and mechanical filtration.
- Activated Carbon are highly porous and create optimal living conditions for nitrifying bacteria and other microscopic organisms.
- Comes in handy net bag for use in your sump
- Can also be used in a reactor

Package incl.:

1KG x Aquarium Activated Carbon

\*comes with net